Illinois U Library

The American Mineralogist

Journal of the Mineralogical Society of America

Vol. 36 NOVEMBER-DECEMBER, 1951 Nos. 11 and 12

Contents

Thermal analysis and x-ray studies of sauconite and some zinc minerals of the same paragenetic association. George T. Faust 795

Notes on precision and accuracy of optic angle determination with the universal stage. . . . . .H. W. Fairbairn and T. Podolsky 823

The crystal structure of claudetite (monoclinic As_2O_3). . . . Alfred J. Frueh, Jr. 833

Structural transformations in amphiboles at elevated temperatures. . . . . .Mark Wittels 851

Chloritoid from Rawlinsville, Lancaster County, Pennsylvania. . . . . .Anna Hietanen 859

The geology and paragenesis of the Lord Hill pegmatite. . . . . .H. H. Woodard 869

Petrological studies on plagioclase twins. . . . . .Masao Gorai 884

Notes and news: Jarosite from the California Tertiary. . . .Louis I. Briggs, Jr. 902

Fluid inclusions in beryl and quartz from pegmatites of the Middletown District, Connecticut. . . . . .Eugene N. Cameron, Robert B. Rowe and Paul L. Weis 906

Apparatus for the separation of mineral grains. . . . . .F. E. Senftle 910

Unit cell of schairerite. . . . . .C. W. Wolfe and Alice Caras 912

A new dumortierite locality from Montana. . . . . .Charles E. Graham and Forbes Robertson 916

Unit cell and space group of glaucochroite. . . . . .J. H. O'Mara 918

Some measurements on minerals of the pyrite group. . .Robert B. Gordon 918

Book reviews. 921

New mineral names; Discredited minerals. 925

Index to volume 36; Title page; Table of contents. 929

EDITOR
WALTER F. HUNT
ASSOCIATE EDITORS
MICHAEL FLEISCHER, ESPER S. LARSEN,
AUSTIN F. ROGERS, M. N. SHORT AND GEORGE TUNELL

Published bi-monthly by the Society

Mineralogical Society of America

ASSOCIATED WITH THE GEOLOGICAL SOCIETY OF AMERICA

President: Adolf Pabst, University of California, Berkeley, California.
Vice President: Michael Fleischer, U. S. Geological Survey, Washington 25, D. C.
Secretary: C. S. Hurlbut, Jr., Harvard University, Cambridge, Massachusetts.
Treasurer: Earl Ingerson, U. S. Geological Survey, Washington 25, D.C.
Editor: Walter F. Hunt, University of Michigan, Ann Arbor, Michigan.
Councilors: Clifford Frondel, Harvard University, Cambridge, Massachusetts.
Lewis S. Ramsdell, University of Michigan, Ann Arbor, Michigan.
E. F. Osborn, School of Mineral Industries, Pennsylvania State College, Pennsylvania.
George T. Faust, U. S. Geological Survey, Washington 25, D. C.
George Tunell, University of California at Los Angeles, California.

The enlarged issues of this journal for 1951 are made possible by a grant from the Penrose Fund of the Geological Society of America.

The American Mineralogist—Journal of the Mineralogical Society of America

A journal containing articles on mineralogy, crystallography, petrography, and allied sciences, issued every two months. Contributions are invited from everyone.

Office of Publication, Mineralogical Laboratory, Ann Arbor, Mich.

The general conduct of the journal is in the hands of the Editor, Walter F. Hunt, Ann Arbor, Michigan. The council of the Mineralogical Society has appointed the following board of associate editors, to whom should be sent articles dealing with the special subjects indicated:

Michael Fleischer, U. S. Geological Survey, Washington, D.C., *New minerals.*
Esper S. Larsen, U. S. Geological Survey, Washington, D.C., *Optical crystallography.*
Austin F. Rogers, Stanford University, California, *Geometrical crystallography.*
M. N. Short, University of Arizona, Tucson, Arizona, *Mineralography.*
George Tunell, University of California at Los Angeles, *Structural crystallography.*

Contributors of leading articles are given without charge 100 reprints (without covers) of their article. If additional reprints are desired these can be purchased at the following rates:

Pages	*1–4*	*5–8*	*9–12*	*13–16*	*17–20*	*21–24*	*25–28*	*29–32*	*Covers*
Copies									
25	$3.50	$5.00	$ 8.00	$ 9.50	$11.00	$13.00	$15.00	$16.00	$4.90
50	3.80	5.55	8.80	10.40	12.10	14.20	16.40	17.50	5.50
75	4.10	6.10	9.60	11.30	13.20	15.40	17.80	19.00	6.10
100	4.40	6.65	10.40	12.20	14.30	16.60	19.20	20.50	6.70
Addl. C's	1.20	2.20	3.20	3.60	4.40	4.80	5.60	6.00	2.40

Cover Composition $1.55.

Sent to all members and fellows of the Mineralogical Society of America. Subscription price, $4.00 per year (single copies of normal issues, $1.00 plus postage).

Entered as second class matter at the post office at Menasha, Wis., under Act of March 3, 1879. Acceptance for mailing at the special rate of postage provided for in section 1103, Act of Oct. 3, 1917, paragraph 4 section 429 P. L. & R. authorized March 13, 1922.

Notices of change of address, orders, and remittances should be sent to Dr. Earl Ingerson, U.S. Geological Survey, Washington 25, D. C.

Printed by the George Banta Publishing Company, Menasha, Wisconsin

THE AMERICAN MINERALOGIST
JOURNAL OF THE MINERALOGICAL SOCIETY OF AMERICA

Vol. 36 NOVEMBER–DECEMBER, 1951 Nos. 11 and 12

THERMAL ANALYSIS AND X-RAY STUDIES OF SAUCONITE AND OF SOME ZINC MINERALS OF THE SAME PARAGENETIC ASSOCIATION*

GEORGE T. FAUST, *U. S. Geological Survey, Washington, D. C.**

TABLE OF CONTENTS

Abstract 795
Introduction 796
Descriptions and chemical analyses of the specimens studied 796
Thermal analysis
  (*a*) Differential thermal analysis of the sauconites 798
  (*b*) Differential thermal analysis of a base-exchanged sauconite 801
  (*c*) Differential thermal analysis of the discredited mixtures, moresnetite and vanuxemite 804
  (*d*) Differential thermal analysis of smithsonite and hemimorphite 805
  (*e*) Dehydration curves for a sauconite and a saponite 809
X-Ray studies
  (*a*) X-ray data for the sauconites dried at room temperature 810
  (*b*) X-ray data for the sauconites treated with ethylene glycol 811
  (*c*) Interpretation of the x-ray powder diffraction data of sauconite 812
  (*d*) Identification of the phases formed in the dissociated minerals 817
    (1) Phases present in sauconite heated to about 350° C 817
    (2) Phases present in sauconite heated to a temperature just above the dissociation point 817
    (3) Phases present in sauconite heated to about 1000° C 818
Acknowledgment 821

ABSTRACT

Sauconite is the name given to the zinc-rich members of the montmorillonite group. This paper presents the results of a differential thermal analysis study of these clays. In addition, differential thermal analysis studies are reported on a base-exchanged sauconite. Differential thermal analysis curves are given for the discredited mixtures vanuxemite and moresnetite.

X-ray powder data are given for the various specimens of sauconite. The products formed in the differential thermal analysis studies were identified by means of x-ray methods. Polymorphism was observed in zinc orthosilicate.

Differential thermal analysis of hemimorphite confirmed and extended the views of Zambonini.

---

* Publication authorized by the Director, Geological Survey.

INTRODUCTION

The name sauconite was given by Roepper to a clay mineral rich in zinc found at the Uberroth Mine, near Friedensville, in the Saucon Valley of Pennsylvania. The analyses of the mineral together with a mineralogical description appeared in Genth's (1875) Mineralogy of Pennsylvania. In 1946, C. S. Ross in connection with his studies of the clay minerals restudied the type sauconite of Roepper and proved the validity of the species and showed that this mineral is a member of the montmorillonite group and is particularly related to the saponites, the magnesium-rich member. In sauconite, zinc takes the place of magnesium in the octahedral positions in the crystal structure. This is illustrated by the formula of the saponite from Cathkin Hills, Scotland

$$(\mathrm{Mg}_{2.30}\mathrm{Fe}^{+3}{}_{.45}\mathrm{Fe}^{+2}{}_{.25})(\mathrm{Al}_{.80}\mathrm{Si}_{3.20})\mathrm{O}_{10}(\mathrm{OH})_2\left(\frac{\mathrm{Ca}}{2}\right)_{.24}$$

and the sauconite from the New Discovery Mine, Leadville, Colorado

$$(\mathrm{Zn}_{2.40}\mathrm{Mg}_{.18}\mathrm{Al}_{.22}\mathrm{Fe}^{+3}{}_{.17})(\mathrm{Al}_{.53}\mathrm{Si}_{3.47})\mathrm{O}_{10}(\mathrm{OH})_2\left(\frac{\mathrm{Ca}}{2}\right)_{.23}\mathrm{Na}_{.09}$$

This paper is an additional study of this group of minerals and contains some data on the minerals belonging to the same paragenetic associations.

DESCRIPTIONS AND CHEMICAL ANALYSES OF THE SPECIMENS STUDIED

The thermal analysis studies were made on fractions prepared by Dr. Ross in connection with the earlier study. The *x*-ray work was made on portions selected from the original samples. Sauconite no. 7 was selected from a sample submitted by Dr. A. C. Spencer of Washington, D. C.

The samples used were prepared by selecting pure fragments of the minerals, crushing them gently so as to produce a minimum of fines and selecting under a binocular microscope, so as to obtain only the purest grains. The samples thus obtained were then crushed to pass a 58 mesh cloth sieve and the resulting particles were re-examined for impurities.

Sauconite No. 1 Locality: Coon Hollow Mine, about three-fourths of a mile north of the village of Zinc, Boone County, Arkansas. White porous layers in reddish brown sauconite. Analysis 1, table 1.

Sauconite No. 2 Locality: Same as sauconite No. 1. Reddish brown masses. Analysis 2, table 1.

Sauconite No. 3 Locality: New Discovery Mine, Leadville, Colorado. Massive brown material. Analysis 3, table 1.

Sauconite No. 4 Locality: Yankee Doodle Mine, Leadville, Colorado. Mottled brownish yellow masses. Analysis 4, table 1.

Sauconite No. 5 Locality: Liberty Mine, near Meekers Grove, Plattesville District, Wisconsin. Brown masses. Analysis 5, table 1.

Sauconite No. 6 Locality: Uberroth Mine, one-half mile N.N.W. of Friedensville, Saucon

Valley, Northampton County, Pennsylvania. Pale brownish yellow masses. Roepper's original material. Analysis 6, table 1.

Sauconite No. 7 Locality: Same as sauconite No. 6. Yellowish white mass. Unanalyzed.

Sauconite No. 8 Locality: Liberty Mine, near Meekers Grove, Plattesville District, Wisconsin. Dark brown masses. Analysis 8, table 1.

Smithsonite Locality: Kelly Mine, Magdalena, Socorro County, New Mexico. Yellow botryoidal masses. Analyzed by W. T. Schaller and J. G. Fairchild (1938) and found to contain 0.57% Cd, 0.34% MnO, 1.56% FeO, tr. PbO, insol. in HCl=0.02%.

Hemimorphite Locality: Sterling Hill Mine, Ogdensburg, Sussex County, New Jersey. Crystals selected from a mass consisting of radiating crystals.

Saponite Locality: Cathkin, Carmunnock Parish, County Lanarkshire, Scotland. (Sometimes given as S.S.E. of Glasgow.) Greenish brown masses. Analysis 9, table 1.

Table 1 contains the chemical analyses reported by Ross (1946) which is included here for the convenience of the reader. The analyses of the sauconites and of the saponite from Scotland were made in the Geochemistry and Petrology Branch of the U. S. Geological Survey. The sauconite analyses are arranged according to decreasing zinc oxide content, sauconite No. 1 being richest in this constituent.

Sulfur was determined on sauconite No. 4, from the Yankee Doodle Mine, Colorado, and on sauconite No. 6, from Friedensville, Pennsyl-

TABLE 1. CHEMICAL ANALYSES OF THE SAUCONITES AND A SAPONITE

Number	1	2	3	4	5	6	8	9
Mineral	Sauconite #1	Sauconite #2	Sauconite #3	Sauconite #4	Sauconite #5	Sauconite #6	Sauconite #8	Saponite #9
Locality	Coon Hollow Mine, Ark. White	Coon Hollow Mine, Ark. Brown	New Discovery Mine, Leadville, Colo.	Yankee Doodle Mine, Leadville, Colo.	Liberty Mine, Meekers Grove, Plattesville district, Wis.	Uberroth Mine, Friedensville, Pa.	Liberty Mine, Meekers Grove, Plattesville district, Wis.	Cathkin, County Lanarkshire, Scotland
SiO_2	33.59	33.40	35.95	37.10	38.59	34.46	38.70	40.16
Al_2O_3	6.01	7.45	6.57	14.18	13.36	16.95	16.29	8.03
Fe_2O_3	.28	1.73	2.36	.30	3.41	6.21	3.91	8.50
FeO								3.83
MgO	.70	.78	1.26	1.10	1.18	1.11	1.62	19.40
MnO	.12	tr.	.04	.02			.06	
ZnO	39.33	36.73	33.70	28.19	23.50	23.10	22.48	
CaO	1.90	1.92	.62	1.22	.94		tr.	1.91
Na_2O	.13	.22	.44	.24	.01		.43	
K_2O	.07	.27	.10	.13	.18	.49	.32	
CuO	.10	.13		.02				
TiO_2	.03	.15	.07	tr.	.31	.24	.30	
H_2O-	10.68	9.78	11.34	8.82	10.39	6.72	7.50	11.15
H_2O+	6.98	7.14	7.24	8.90	8.05	10.67	8.38	7.60
Σ	99.92	99.70	99.69	100.22	99.92	99.95	99.99	100.58

Analysts: 1. M. K. Carron, 2. M. K. Carron, 3. J. G. Fairchild, 4. M. K. Carron, 5. M. K. Carron, 6. J. G. Fairchild, 8. S. H. Cress, 9. L. T. Richardson.

vania, by J. J. Fahey and found to be absent. These two samples were selected for this determination because their *x*-ray powder patterns contain the greatest number of lines.

All seven of the sauconites were *x*-rayed and the patterns were examined and the absence of sphalerite, wurtzite, smithsonite, and hemimorphite established.

Thermal Analysis

(*a*) *Differential thermal analysis of the sauconites*

The equipment and technique used in this laboratory in differential thermal analysis studies, together with pertinent references to the literature, are given by Faust (1948) and (1950). The samples were heated at the rate of approximately 10° to 12° C. per minute. The records were obtained as photographs.

The differential thermal analysis curves for a saponite from Scotland and for four sauconites are shown in Fig. 1 and the data, taken from these curves, are summarized in Table 2. These curves show that sauconite is closely related to saponite and all are members of the montmorillonite group. All of these curves exhibit the characteristic double breaks, in the temperature range of 150° to 290° C. of montmorillonite—Alexander, Hendricks and Nelson (1939); Grim and Rowland (1942). This double break is almost always present in the curves for the natural, untreated, members of the montmorillonite group. These breaks arise from the absorption of the heat necessary to expel the adsorbed and interlayer water (water between the basal planes in the montmorillonite structure). This interlayer water is associated with the swelling of the montmorillonite. The loss of essential, or hydroxyl, water is represented by the endothermic breaks taking place above 400° C. and its culmination is reached in the last endothermic break in the temperature range of 680°–735° C., where the sauconite structure is completely destroyed and new phases appear. The break in curve C-81 at 601° C. and the break in curve C-567 at 569° C. represent the decomposition of the halloysite, present as an admixture in the samples.

Some montmorillonites show an exothermic break above 900° C.—Alexander, Hendricks and Nelson (1939, p. 265). Grim and Rowland (1942, p. 757) have suggested that the exothermic reaction is closely related to the amount of iron present in the mineral. The greater the iron content the lower the temperature of the exothermic reaction. They associate this break with the formation of a spinel. The saponite from Scotland, shown in Fig. 1, does not show any high temperature exothermic reaction. It contains 8.50% Fe_2O_3 and 3.83% FeO. A possible explanation of its absence may be that the double endothermic breaks at

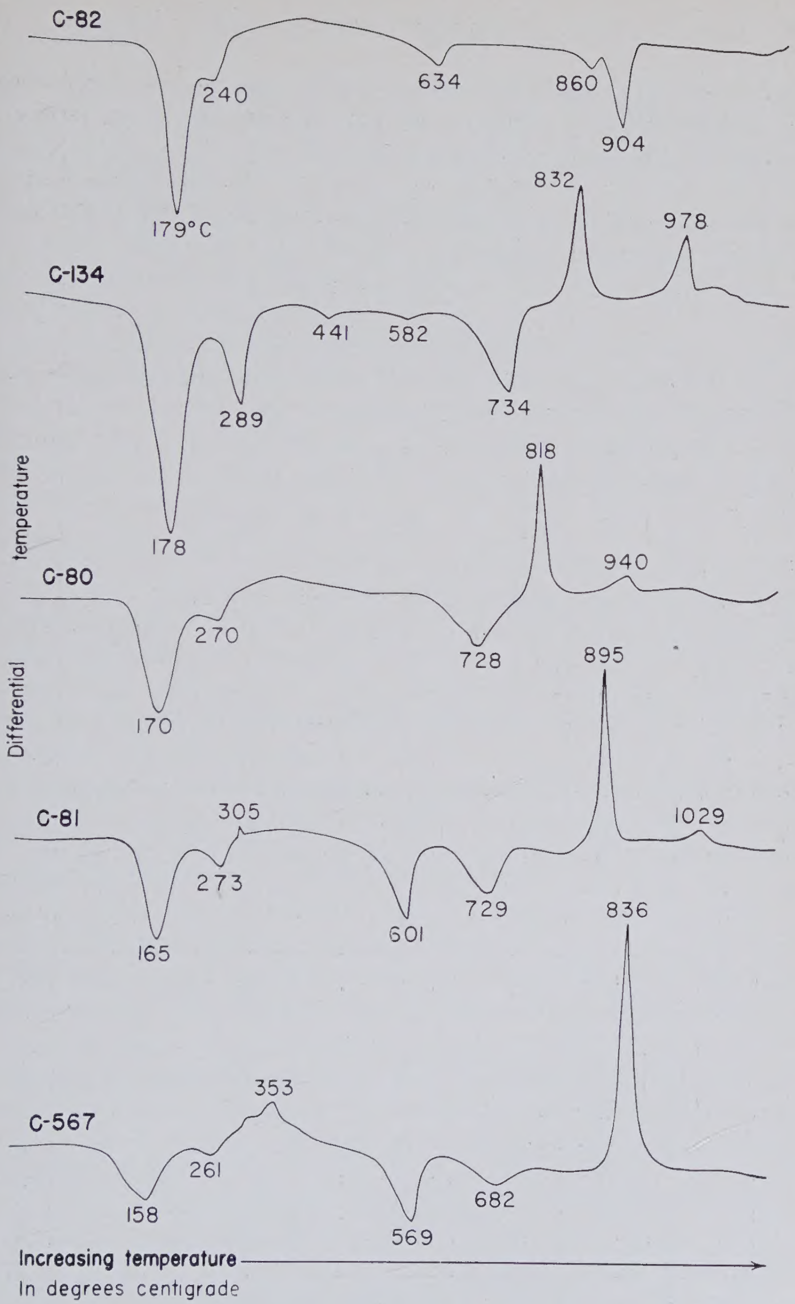

FIG. 1. Differential thermal analysis curves for sauconites and saponite. C-82 = saponite, C-134 = sauconite #2, C-80 = sauconite #3, C-81 = sauconite #4, C-567 = sauconite #6. The temperature where the curves begin, on the left, is about 25° C. the temperature of the termination of the curves, on the right, is about 1000° C.

TABLE 2. OBSERVATIONS ON THE THERMAL ANALYSIS CURVES[1] OF SAPONITE AND SAUCONITE

Mineral (ZnO content)	Record No.	Temperature of breaks in curves (Knickpunkt)										Locality	Weight of sample used
		Low Temperature			Intermediate Temp.			High Temperature					
		Endothermic		Exo-thermic	Endothermic			Endothermic		Exothermic			
		°C.	°C.	°C.	°C.	°C.	°C.	°C.	°C.	°C.	°C.		
Saponite	C-82	179	240	—	—	634	—	860	904	—	—	Cathkin, Carmunnock Parish, Lanarkshire County, Scotland (S.S.E. of Glasgow).	0.5290 grams
Sauconite #2 (ZnO=36.73)	C-154	178	289	—	441	582	734	—	—	832	978	Coon Hollow Mine, 0.75 mile north of Zinc, Boone County, Ark. (Brown variety).	0.5562
Sauconite #3 (ZnO=33.70)	C-80	170	270	—	—	Present	728	—	—	818	940	New Discovery Mine, Leadville, Colorado.	0.4951
Sauconite #4 (ZnO=28.19)	C-81	165	273	305	—	601	729	—	—	895	1029	Yankee Doodle Mine, Leadville, Colorado.	0.5082
Sauconite #6 (ZnO=23.10)	C-567	158	261	353	—	569	682	—	—	836	—	Uberroth Mine, Saucon Valley, 0.5 mile N.N.W. of Friedensville, Penna. (Roepper's material-Lehigh).	0.3343

---

[1] These curves were all obtained with a resistance of 600 ohms in the galvanometer circuit.

832°–978° C. represent an algebraic addition of the thermal effects accompanying the endothermic reaction associated with the breakdown of the saponite structure and the exothermic reactions involved in the crystallization of spinel.

All of the sauconites show a sharp exothermic break above 800° C. and some show a subsequent break of much lesser magnitude. The probable interpretation of these breaks will be considered in the discussion of the *x*-ray study of the decomposed materials.

The sauconites are arranged in Table 2 from top to bottom, in order of their decreasing content of ZnO. The data in this table suggest that the temperature at which the "low temperature" water is lost, is higher for the zinc-rich clays. Likewise the last well-defined endothermic break in the temperature range of 680°–735° C. takes place at higher temperatures for the zinc-rich sauconites.

(*b*) *Differential thermal analysis of a base-exchanged sauconite*

Hendricks, Nelson and Alexander (1940) studied the hydration mechanism of montmorillonite. In this research they showed that the character of the base-exchanged ions affected the shape of the double break which occurs at low temperatures, in the differential thermal analysis pattern. They investigated montmorillonites saturated with Li^+, Na^+, K^+, Cs^+, Mg^{++}, Ca^{++}, Sr^{++}, Ba^{++} and H^+.

Caillére and Henin (1944) also examined the differential thermal analysis curves of base-exchanged montmorillonites and made observations on the changes in the character of the three principal breaks. They noted the presence of an exothermic break above 850° C.

The modification of the double break of sauconite, associated with the loss of water at low temperatures, was investigated for H^+, Na^+ and Ca^{++} on the brown variety of sauconite from the Coon Hollow Mine, Arkansas. These results are shown in Fig. 2 and the data are summarized in Table 3.

TABLE 3. OBSERVATIONS ON THE THERMAL ANALYSIS CURVES[1] OF NATURAL AND BASE-EXCHANGED SAUCONITE FROM THE COON HOLLOW MINE, ARKANSAS (NO. 2)

Description of the material	Record No.	Temperature of breaks in curves (Knickpunkt)								Weight of sample used
		Low Temperature Endothermic		Intermediate Temperature Endothermic			High Temperature Exothermic			
		°C.	°C.	°C.	°C.	°C.	°C.	°C.	°C.	gms.
Natural, untreated mineral	C-134	178	289	441	582	734	832	978	—	0.5562
Ca-Na-Sauconite	C-211	170	271	437	573	719	807	949	—	0.5941
Na-Sauconite	C-222	162	210	459	—	724	—	—	985	0.6480
H-Sauconite	C-209	159	—	—	—	701	827	915	954	0.5024

[1] These curves were all obtained with a resistance of 600 ohms in the galvanometer circuit.

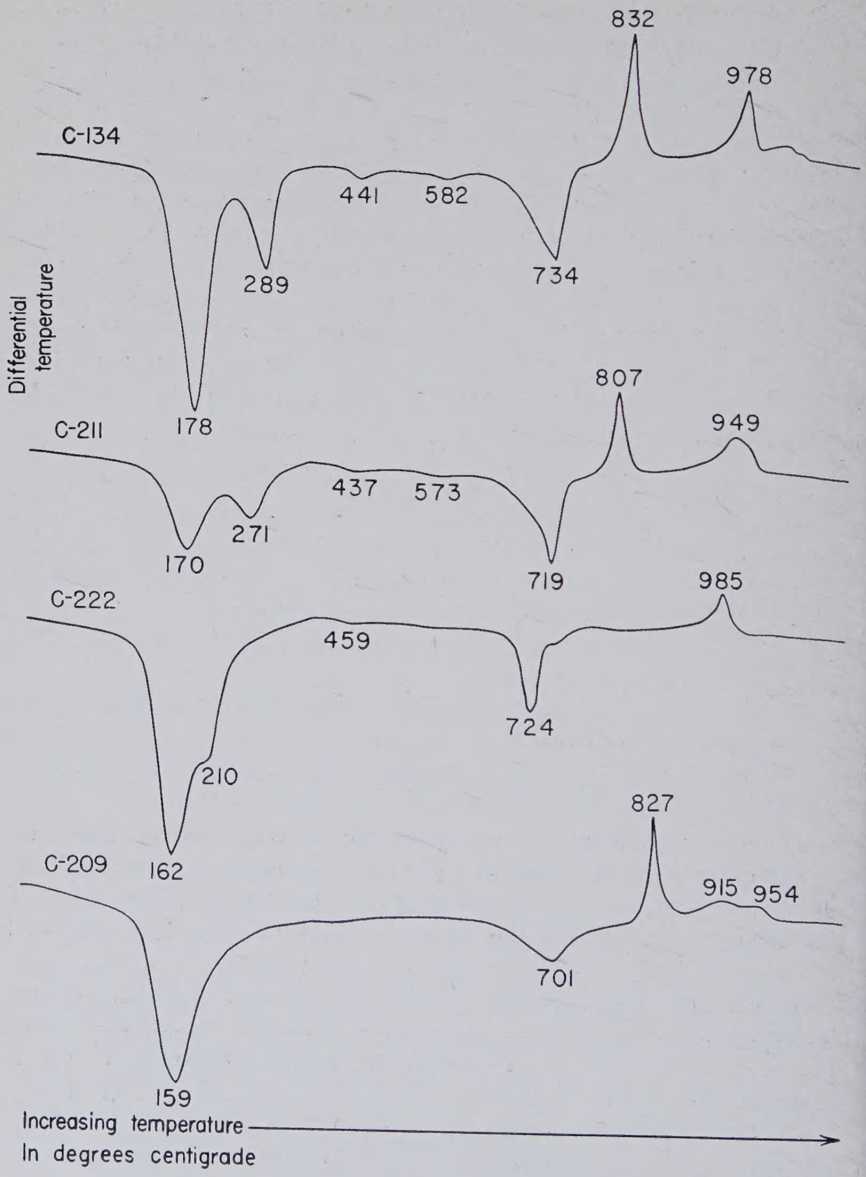

FIG. 2. Differential thermal analysis curves for sauconite #2, from Coon Hollow Mine, Arkansas. C-134=natural, untreated mineral; C-211=calcium-sodium sauconite; C-222=sodium sauconite; C-209=hydrogen sauconite.

The base-exchanged samples were analyzed for alkalies by W. W. Brannock using the flame photometer and his results are given in Table 4. These alkali determinations show that the small original quantity of K_2O has not been displaced by the base-exchange experiments; the value for all samples being about 0.18%. Apparently these potassium atoms are located in sites, in the sheets, where they are held more tenaciously than that portion of the potassium which may be base-exchanged. Another possible explanation is that there are some "mixed-layers" present in the sauconite structure, the non-base exchangeable K^+ ions being in mica sheets.

The sodium-exchanged sauconite was prepared by treating the natural zinc clay, which is calcium saturated, with a sodium chloride solution. The calcium-exchanged sauconite was prepared by treating the sodium-exchanged sauconite with a calcium chloride solution. The chemical data in Table 4 show that the latter exchange failed to go to completion due to some mechanical difficulty, as incomplete dispersion of the clay.

TABLE 4. PARTIAL CHEMICAL ANALYSIS OF THE BROWN SAUCONITE FROM THE COON HOLLOW MINE, BOONE COUNTY, ARKANSAS

Description of the material	K_2O[1]	Na_2O[2]	CaO
Natural Sauconite	0.18%	0.03%	1.92%[3]
Ca-Na-Sauconite	0.17	0.55	1.62.[4]
Na-Sauconite	0.16	1.99	
H-Sauconite	0.20	0.04	

[1,2] Analyst, W. W. Brannock.

[3] Analyst, M. K. Carron.

[4] Analyst, T. Woodward.

A study of the data in Table 3 and an examination of Fig. 2 show that this base-exchange treatment of the natural sauconite results in a modification of the double break occurring at low temperatures. The calcium-saturated sauconite shows two well-defined and clearly separate breaks. In the sodium-saturated clay the second break has lost its individual character and is represented by an inflection on the high-temperature side of the break. The hydrogen-exchanged sauconite has only one break. The low-temperature breaks, in the differential thermal curves, appear at lower temperatures for the base-exchanged sauconites than for the corresponding natural, untreated, sauconite.

These results may be explained as follows: when sauconite is dispersed in water and base-exchanged the crystal structure is so modified that the forces acting on the interlayer water are weakened resulting in the easier removal of the interlayer water at lower temperatures (Auflockern and Gitterlockern of some German authors).

(*c*) *Differential thermal analysis of the discredited mixtures, moresnetite and vanuxemite*

Moresnetite was described by Risse (1895) from the lead mines at Altenberg, near Moresnet, and Aachen in Germany. Kenngott (1868, p. 153) later claimed that moresnetite was a mixture of hemimorphite and clay. Ross (1946) re-examined moresnetite microscopically and found a light gray to dark blue-gray zinc mineral associated with a brown material made up of micas and chlorite, and with fine-grained masses of hemimorphite.

The differential thermal analysis curve of moresnetite shown in Fig. 3, Curve C-258, was made on 0.7397 gram of the material. The curve is obviously that of a mixture of minerals. The low-temperature double breaks suggest very strongly that sauconite is part of the mixture. The *x*-ray powder photograph of this material established the presence of sauconite in the mixture.

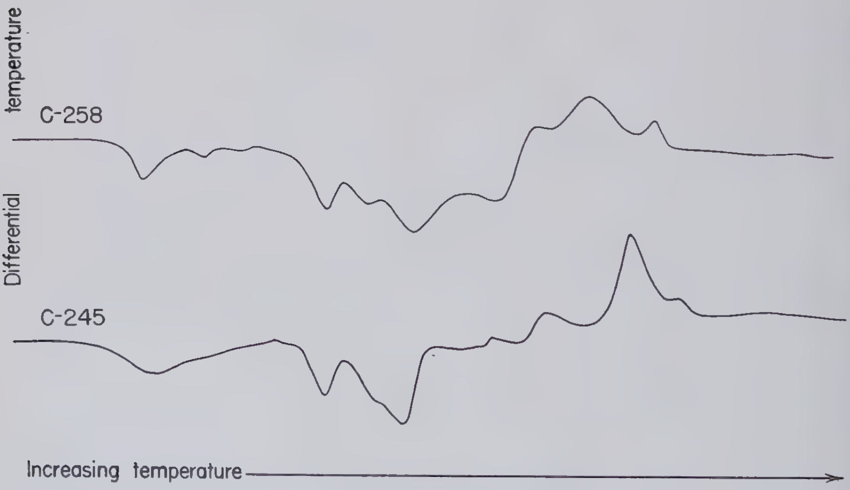

Fig. 3. Differential thermal analysis curves for the discredited mixtures moresnetite and vanuxemite Curve C-258 = Moresnetite, Altenberg, Aachen, Germany; C-245 = vanuxemite, Sterling Hill, Sussex County, New Jersey. Resistance in the galvanometer circuit is 600 ohms.

Vanuxemite was described by Shepard (1876) from Sterling Hill, Sussex County, New Jersey, as a new mineral. Cross (1877) claimed, on the basis of a chemical analysis, that vanuxemite was a mixture of equal parts of hemimorphite and halloysite. Ross (1946) on the basis of an optical study of the type material found it to be a mixture of several minerals.

The differential thermal analysis curve, C-245, Fig. 3, confirms the conclusion that this substance is a mixture of several minerals.

(*d*) *Differential thermal analysis of smithsonite and hemimorphite*

In the study of the various specimens of sauconite it was necessary to prove the absence of smithsonite and hemimorphite in the purified fractions. This was checked by differential thermal analysis and *x*-ray methods.

Smithsonite

A differential thermal analysis curve of a yellow smithsonite, $ZnCO_3$, containing 0.57% Cd, from the Kelly Mine, Magdalena district, New Mexico, is shown in Fig. 4. The curve, C-85, was obtained using 1.0113 grams of the mineral. The resistance in the galvanometer circuit was 999.9 ohms. The temperature of the break is 590° C. The dissociation of zinc carbonate yields zinc oxide as the solid phase and carbon dioxide is

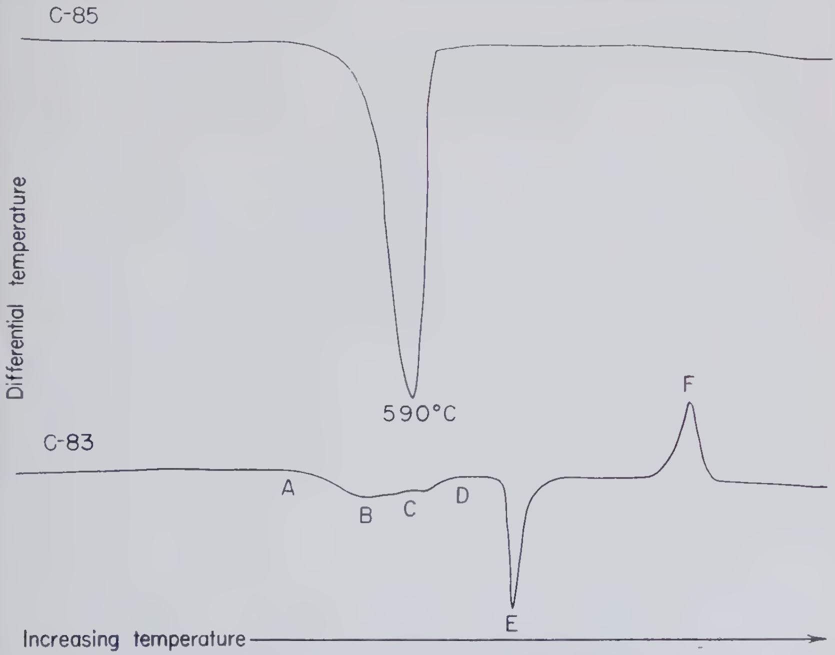

FIG. 4. Differential thermal analysis curve for smithsonite, Kelly Mine, New Mexico, C-85, and for hemimorphite, Sterling Hill, New Jersey, C-83.

lost to the atmosphere. X-ray examination shows the dissociated sample to consist of zincite (ZnO).

Hemimorphite

A differential thermal analysis study of hemimorphite is of considerable interest for it confirms and extends the earlier views of Zambonini (1908). Zambonini found that when hemimorphite was heated to 480° C. it lost one-half of its water and remained transparent. The remaining one-half of its water was lost at higher temperatures. A study of the crystal structure of hemimorphite by Ito and West (1932) confirmed this conclusion and they assigned the formula $(OH)_2Zn_4Si_2O_7 \cdot H_2O$.

The differential thermal analysis curve, C-83 in Fig. 4, furnishes a clear-cut demonstration of the process of dehydration of hemimorphite. The "low-temperature" water is lost more or less continuously over a span of temperatures (393°–657° C.). See Table 5. This water is represented by the H_2O molecules in the structure. According to Ito and West (1932) the water molecules are loosely held in the structure and are located on the digonal rotation axis. These water molecules can be removed without destroying the crystal structure.

Table 5. Observations on the Differential Thermal Curve of Hemimorphite

Letter on curve C-83, Fig. 4	Temperature	Observations
	°C.	
A	393	Beginning of loss of "low temperature" water
B	526	Temperature of first maximum on curve
C	612	Beginning of secondary shoulder
D	657	Completion of the loss of "low temperature" water
E	740	Loss of the "high temperature" water
F	971	Transformation into willemite

The "high-temperature" water is tied up in the hydroxyl groups and it is necessary to disrupt the crystal structure completely to free this water. Each hydroxyl group is shared by two zinc atoms and is firmly bound in the structure. The steepness of the break on the low-temperature side shows that the destruction of the crystal structure, with the expulsion of the hydroxyl, took place promptly. The break is narrow, and its maximum appears at 740° C. The high-temperature side of the break is spread out to about 790° C., and heat was being consumed in the process over this range of temperature. Thereafter, the curve is essentially flat until the appearance of the exothermic break at approximately 915° C., an interval of about 125°. The temperature of the maximum point on the exothermic break is 971° C. This exothermic break is spread out on both the low and high-temperature sides of the maximum.

In order to interpret the origin of the exothermic break at 971° C. it became necessary to study the polymorphism of Zn_2SiO_4. A brief review is given here of the polymorphism of Zn_2SiO_4, summarized from Ingerson, Morey and Tuttle (1948). Schleede and Gruhl (1923) observed that the rate of cooling of a melt of Mn-activated Zn_2SiO_4 determined the color of its fluorescence. Melts cooled slowly gave a green fluorescence, melts cooled rapidly gave a yellow fluorescence while melts that were suddenly chilled gave a red fluorescence. They also observed that the yellow and red-fluorescing polymorphs changed to the green-fluorescing willemite when heated to 900° C.

Leverenz and Seitz (1939) designated the green, yellow and red-fluorescing polymorphic forms as α-, β-, and γ-Zn_2SiO_4, respectively. They found that the β-form inverts to the α-form when heated at 900° C., and that the γ-form inverts to the α-form as low as 300°–400° C. The α-form of Zn_2SiO_4 corresponds to the mineral willemite.

Ingerson, Morey and Tuttle (1948) studied the transformation of the various polymorphic forms of Zn_2SiO_4. They state:

> When γ-Zn_2SiO_4 is heated it changes first to β-Zn_2SiO_4 and then to α-Zn_2SiO_4. Longer heating is required to effect complete transformation at lower temperatures. For example, at 900° C. the γ-form goes to β- in 5 minutes, but at 950° C. for the same time γ- goes to α-. If γ- is heated to 1000° C. for 1 minute it is transformed to β-. After 2 minutes both α- and β- are present, whereas in 3 minutes transformation to α- is complete. A cooling rate intermediate between the chilling to γ- and the slow cooling, which always produces alpha, sometimes gives rise directly to the β-form.

The study of the polymorphism of Zn_2SiO_4 required for this research was greatly facilitated by Dr. Ingerson who very kindly supplied me with several specimens of Zn_2SiO_4 which he had prepared in connection with the above-mentioned studies. These samples formed the standards adopted here. Dr. J. F. Schairer of the Geophysical Laboratory kindly inverted a sample of willemite into a mixture of the various polymorphs.

Powder diffraction data were obtained from a sample showing a strong yellow fluorescence, considered here to be the β-form, and from a substance witn yellowish-pink fluorescence, considered here to be the γ-form. One specimen with a reddish fluorescence gave an x-ray pattern having only a few diffuse lines.

A sample of hemimorphite was heated in the differential thermal analysis apparatus to a temperature of 761° C., the furnace was then pulled away from the sample support, and the dissociated material was allowed to cool down to room temperature. The record of the thermal behavior of this dissociated material is shown in Fig. 5. A fluorescent lamp

(Mineralight) was held above the cooling material to observe the character of the fluorescence. The results of the fluorescence test on the hot material were not convincing. The cold material exhibited a pale pinkish fluorescence. It should, however, be emphasized that this product was not activated by manganese.

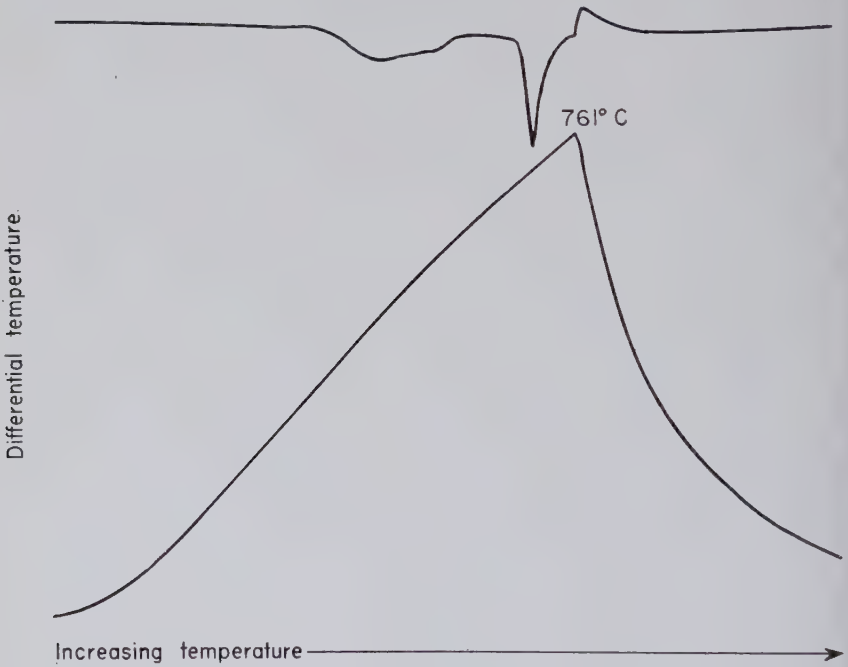

FIG. 5. Differential thermal analysis curve of a sample of hemimorphite from Sterling Hill, New Jersey, C-642, which was heated to 761° C. and then cooled down by removing the furnace.

The thermal behavior of the substance on cooling from 761° C. to nearly room temperature is shown in curve C-642, Fig. 5. A comparison of this figure with curve C-83 in Fig. 4 shows the appearance in curve C-642 of an exothermic reaction beginning at 761° C., which occurred as soon as the sample was cooled, whereas such a break in the curve does not appear in curve C-83. In addition curve C-642 does not show the exothermic break at 971° C. exhibited in curve C-83.

X-ray powder diffraction data obtained from these materials show that the hemimorphite heated to 761° C. consists of the β-form of zinc silicate, as defined by Ingerson, Morey and Tuttle (1948). The sample of hemimorphite heated to about 1100° C. consists of willemite, the α-form of zinc silicate. From these data we may conclude that the exothermic break at 971° C. represents the transformation of some polymorphic form of zinc silicate to the α-form, willemite.

The appearance of the exothermic reaction at 761° C. in curve C-642 suggests that the form of zinc silicate produced in the dissociation of hemimorphite at 740° C. is the γ-form and that the sudden cooling brought about the transformation of the γ-Zn_2SiO_4 to the β-Zn_2SiO_4. The area of this exothermic break thus is a measure of the heat of transformation of γ-Zn_2SiO_4 to β-Zn_2SiO_4.

These conclusions are in accord with the observations of Ingerson, Morey and Tuttle (1948) mentioned earlier in this discussion.

The *x*-ray powder diffraction data of the various polymorphic forms of zinc silicate and of the product, β-Zn_2SiO_4, produced in the differential analysis experiment C-642 will be published elsewhere.

(*e*) *Dehydration curves for a sauconite and a saponite*

The late Dr. Perley G. Nutting, formerly a member of this laboratory, obtained dehydration curves for a sauconite and a saponite. His records have been obtained for inclusion in this paper. The experimental data are given in Table 6 and the graphical plot of the data is presented in Fig. 6. The data in Table 6 are expressed first, as the actual loss in

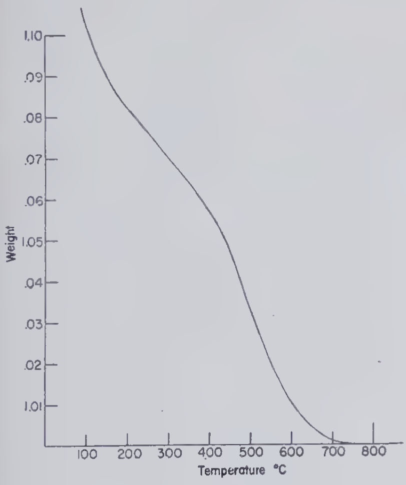

A

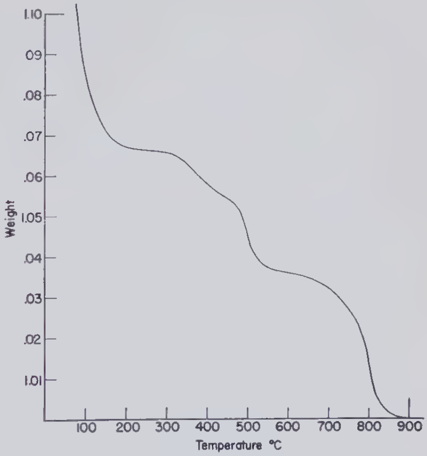

B

FIG. 6A. Dehydration curves for (A) sauconite #8, Liberty Mine, Meekers Grove, Plattesville District, Wisconsin, Record No. 358.

FIG. 6B. Dehydration curves for (B) saponite, Cathkin, Carmunnock Parish, County Lanarkshire, Scotland, Record No. 227. The ordinate is the weight of the sample at each temperature divided by the final weight at 960° C.

TABLE 6. THERMAL DEHYDRATION DATA FOR SAUCONITE AND SAPONITE

Sauconite #8			Saponite		
Liberty Mine, Meekers Grove, Plattesville District, Wisconsin			Cathkin, Carmunnock Parish, County Lanarkshire, Scotland		
Temperature	Loss in weight	Relative weight	Temperature	Loss in weight	Relative weight
°C.			°C.		
29	*	1.1531	27	*	1.2293
90	4.09%	1.1059	80	10.52%	1.1000
135	1.09	1.0933	170	2.55	1.0687
195	0.90	1.0829	215	0.15	1.0668
230	0.33	1.0791	285	0.09	1.0658
260	0.35	1.0750	325	0.10	1.0645
280	0.22	1.0725	395	0.50	1.0584
370	1.00	1.0610	428	0.22	1.0556
415	0.76	1.0522	475	0.23	1.0528
470	0.93	1.0414	530	1.12	1.0391
655	3.27	1.0037	560	0.19	1.0367
710	0.27	1.0007	646	0.17	1.0346
750	—	1.0000	720	0.33	1.0306
860	—	1.0000	780	0.65	1.0226
960	—	1.0000	895	1.81	1.0001
			960	0.03	1.0000
	13.21%			18.66%	

* Sample allowed to come to constant weight at room temperature.

weight of the sample at a given temperature, and secondly, as relative weight. These curves, according to Dr. Nutting, conform with those given by other members of the montmorillonite group. The oxidation of the ferrous iron to ferric iron in the saponite from Scotland results in an increase in weight of the sample. This reaction is indicated by a modification of the slope of the curve. The data suggest that this oxidation took place in the temperature range from 300°–400° C.

X-RAY STUDIES

(a) *X-ray data for the sauconites dried at room temperature*

The samples studied by the *x*-ray technique were prepared as spindles with "Duco cement" as the mounting medium. Patterns were obtained using filtered copper and iron radiation. The patterns obtained with copper radiation were very satisfactory for identification, and for the measurement of all but the (001) spacing. For most samples it was necessary to measure the (001) spacing on a pattern obtained using iron radiation. The poor quality of the (001) line, on the patterns obtained with copper radiation, arises from the inability of the cameras to record good lines at low angles of scattering. Samples containing a significant amount of iron produced some fluorescence with copper radiation.

The *x*-ray data for the various specimens of sauconite are given in Table 7. The data are arranged according to decreasing zinc oxide content; sauconite No. 1 being richest in this constituent. The lines were indexed on the basis of criteria established by Hofmann, Endell, and Wilm (1933); Gruner (1935); and Nagelschmidt (1938). This will be treated more fully at another place in this paper.

The *x*-ray data for the saponite (from Cathkin, Lanarkshire, Scotland, analysis No. 9, Table 1) are given in the last column for purposes of comparison.

(*b*) *X-ray data for the sauconites treated with ethylene glycol*

A portion of the sauconites, dried at room temperature, was ground, placed in a watch glass, covered with ethylene glycol, and allowed to stand over night. In the morning the excess liquid was decanted, and the sample was further dried by placing it on absorbent filter paper. The moist sample was mixed with "Duco cement" and formed into spindles. Patterns were obtained with copper and iron radiation. Treatment with ethylene glycol greatly improved the quality of the patterns and made it possible to measure lines which could not be clearly differentiated in the patterns of the untreated samples.

The data for the interplanar spacings of the samples treated with ethylene glycol, are given in Table 8.

A note of caution should be added here concerning the re-use of spindles containing a substance previously soaked in ethylene glycol. Samples of sauconite prepared in June and July of 1949 and stored in small cork-stoppered vials were re-used in powder cameras in May and June of 1950. It was found that the *d* spacings for the (001) line of several sauconites were smaller than those recorded for the same spindles the previous year. One of the spindles, showing this anomalous character, was soaked in ethylene glycol and re-examined by *x*-ray methods. The resulting powder pattern gave results comparable with those obtained from the freshly prepared spindle. The vapor pressure of ethylene glycol is apparently great enough to permit its loss from spindles stored over a period of a year. This behavior of stored spindles has been confirmed by J. M. Axelrod of this laboratory.

Table 7. *X*-ray Powder Data for Sauconites and a Saponite D

No. 1 Coon Hollow Mine, Ark. (White)				No. 2 Coon Hollow Mine, Ark. (Brown)				No. 3 New Discovery Mine, Leadville, Colo.				No. 4 Yankee Doodle Leadville, Colo.		
Miller Indices	*d*	*Notes*	*I*	*Miller Indices*	*d*	*Notes*	*I*	*Miller Indices*	*d*	*Notes*	*I*	*Miller Indices*	*d*	*Note*
(001)		3	s	(001)	15.4		s	(001)	15.3		s	(001)	15.4	
(002)	7.76		s	(002)	7.77		ms	(002)	7.92		ms	(002)	7.90	
Duco	5.51	b	w	Duco	5.58	b	w	Duco	5.47	b	w	Duco	5.48	b
(110)(020)	4.59		s	(110)(020)	4.60		ms	(110)(020)	4.60		ms	(110)(020)	4.55	
				(004)	3.87		w	(004)	3.92	b	w	(004)	3.94	
												Halloysite	3.59	
				(005)	3.09		w	(005)	3.14	b	m	(005)	3.16	
													2.83	(?)
(130)	2.68		s	(130)(200)	2.67	2	s	(130)(200)	2.67	d	ms	(130)	2.67	
(200)		1										(200)	2.590	
				(150)	1.748		vf	(150)	1.736	b	vvw			1
				(310)	1.718		vf							1
(060)(330)	1.542		vs	(060)(330)	1.544		s	(060)(330)	1.548		s	(060)	1.554	
												(330)	1.505	
(260)	1.329	b	w	(260)	1.334		m	(260)	1.332		w	(260)	1.334	
												(400)	1.293	
								(440)	1.133		vvvw	(440)	1.137	
(190)	1.003	b	w	(190)	1.005	b	w	(190)	1.007		vvw	(190)	1.015	
(550)(390)	0.890	b	w	(550)(390)	0.890	b	w	(550)(390)	0.898		vw	(550)(390)	0.894	b
													0.816	b

vs = very strong
s = strong
m = medium
wm = weak-medium
w = weak

vw = very weak
f = faint
vf = very faint
vvf = very, very faint
vvvf = very, very, very, faint

(*c*) *Interpretation of the x-ray powder diffraction data of sauconite*

The best powder pattern of the seven sauconites examined was found to be that of the sauconite from the Yankee Doodle Mine, Leadville, Colorado. Accordingly, this pattern was selected as the most suitable for indexing the lines and the other sauconite patterns were indexed on the basis of this as a standard.

Hofmann, Endell and Wilm (1933) proposed a structure for montmorillonite which is based on the structure of pyrophyllite. According to

TEMPERATURE (WITH INDICES ASSIGNED FROM TABLE 10)

Liberty Mine, ers Grove, Wis.			No. 6 Uberroth Mine, Friedensville, Pa. (Lehigh Univ.)				No. 7 Uberroth Mine, Friedensville, Pa. (Spencer)				No. 9 Saponite, Cathkin, near Glasgow, Scotland			
d	*Notes*	*I*	*Miller Indices*	*d*	*Notes*	*I*	*Miller Indices*	*d*	*Notes*	*I*	*Miller Indices*	*d*	*Notes*	*I*
15.5		vs	(001)	15.0		s	(001)	15.6		vs	(001)	14.8		vs
			(002)	7.44	b	m	(002)	7.80	b	m	(002)	7.71	b	m
5.54	b	s	Duco	5.37	b	m	Duco	5.47	b	m	(003)	5.14	b	vw
4.52		s	(110)(020)	4.51		s	(110)(020)	4.58		m	(110)(020)	4.59	b	ms
				4.21		s						4.34		vvf
							(004)	3.95		vw	(004)	3.79		vw
			Halloysite	3.60		m	Halloysite	3.59		vw				
								3.36		w				
3.3±	b	w					(005)	3.14		vw	(005)	3.09		m
								2.87		vw				
2.63	b, d	ms	(130)	2.68		m	(130)	2.67		m				
												2.613		m
			(200)	2.571		m	(200)	2.583		m	(200)	2.545	d	m
				2.455		m								
				2.344	Al	mw	(040)	2.360		vw				
				2.233		vw		2.138		vw				
								2.001		w				
								1.851		vw		1.852		vvf
							(150)	1.747		w	(150)	1.747		w
1.71±	b	vw	(310)	1.713		w					(310)	1.703		w
								1.640		vw				
1.545		ms	(060)	1.547		m	(060)	1.542		vs	(060)	1.543	b	s
1.51±		w	(330)	1.501		w	(330)	1.502		vw	(330)	1.495		vvvf
								1.459		vw		1.458		vvvf
								1.388		vw				
1.33±		vw	(260)	1.331		vw	(260)	1.329		m	(260)	1.327	b	m
											(400)	1.278	b	vvvf
				1.193	b	vvw								
1.137	b	vw		1.127	b	vvw								
1.077	b	vw		1.081	b	vvw	(190)	1.010		w		0.999	d	vvvf
0.870	b	m					(550)(390)	0.889		w	(550)(390)	0.890	b	vvvf
0.842	b	w												
0.818	b	w						0.818		vw				
0.793	b	w						0.798		vw				

ine appears here but it is too faint to measure
e dark edge of the band was measured
rong line present, but not measurable

Patterns for samples Nos. 1, 2, 5, 4, 7 corrected for film shrinkage.
Patterns for samples Nos. 5, 6 uncorrected for film shrinkage.
b = broad diffuse band
d = doublet, mean value used in table.

them montmorillonite is built up of units of three layers just as is pyrophyllite, but differs from pyrophyllite in that the three layer units are separated by interlayers of water. These investigators also found that the spacings of the basal reflections (00*l*) of montmorillonite vary with the water content while the other reflections are relatively unaffected. They indexed their patterns and found only lines corresponding to (00*l*) and (*hk*0) spacings. Gruner (1935) accepted most of their views but differed with them regarding the assignment of certain indices. Nagelschmidt (1938) followed Hofmann, Endell, and Wilm in the indexing of his

TABLE 8. *X*-RAY POWDER DATA FOR SAUCONITES TREAT

No. 1 Coon Hollow Mine, Arkansas (White)				No. 2 Coon Hollow Mine, Arkansas (Brown)				No. 3 New Discovery Mine, Leadville, Colorado				No. 4 Yankee Doodl Leadville, Color		
Miller Indices	*d*	*Notes*	*I*	*Miller Indices*	*d*	*Notes*	*I*	*Miller Indices*	*d*	*Notes*	*I*	*Miller Indices*	*d*	*N*
(001)	16.3		s	(001)	16.6		s	(001)		3	s	(001)	16.1	
	12.59	b	w											
(002)	8.50		s	(002)	8.33		s	(002)	8.49		s	(002)	8.40	
Duco	5.41		m	Duco	5.41	b	w	Duco	5.37		m	Duco	5.38	
(110)(020)	4.61		vf	(110)(020)	4.60		s	(110)(020)	4.59		ms	(020)	4.61	
												Halloysite in part (110)	4.45	
(004)	4.21		vvf											
												Halloysite	3.63	
(005)	3.39		s	(005)	3.34		m	(005)	3.40		m	(005)	3.37	
(006)	2.83	b	w									(006)	2.32	
(130)	2.69		m	(130)	2.62		s	(130)	2.68		ms	(130)	2.66	
(200)	2.478		m	(200)	2.473		m	(200)	2.601		m	(200)	2.579	
(150)	1.754		vvf	(150)	1.753		vvf	(150)	1.759		vvf	(150)	1.754	
(310)	1.706		vvvf	(310)	1.715		vvf					(310)	1.700	
(060)(330)	1.550	b	s	(060)(330)	1.550		s	(060)(330)	1.548		s	(060)	1.544	
												Halloysite in part (330)	1.491	
(260)	1.337	b	w	(260)	1.334		w	(260)	1.335		w	(260)(170)	1.327	
												(400)	1.285	
												(440)	1.134	
												(280)	1.067	
(190)	1.012	b	vw	(190)	1.010	b	vw	(190)	1.009	b	w	(190)	1.006	
(550)(390) (00.19)	0.895	b	w	(550)(390) (00.19)	0.894	b	vw	(550)(390) (00.19)	0.892	b	w	(550)(390) (00.19)	0.891	
												(620)	0.844	
													0.821	

vs = very strong
s = strong
m = medium
wm = weak-medium
w = weak

vw = very weak
f = faint
vf = very faint
vvf = very, very faint
vvvf = very, very, very faint

photographs. Maegdefrau and Hofmann (1937) proposed a modification of the structure of montmorillonite to account for the absence of (*hkl*) reflections. They postulated that the three-layer units of the structure were stacked upon one another in an irregular fashion.

Using the criteria proposed by the above-mentioned investigators the pattern of sauconite was indexed. Assuming the *d* values for (060) and for (200) the *d* values of the most probable (*hk*0) and (00*l*) planes were ne Glycol (with Indices Assigned from Table 10)

. 5 Liberty Mine, ers Grove, Wisconsin				No. 6 Uberroth Mine, Friedensville, Pa. (Lehigh University)				No. 7 Uberroth Mine, Friedensville, Pa. (Spencer)			
	d	*Notes*	*I*	*Miller Indices*	*d*	*Notes*	*I*	*Miller Indices*	*d*	*Notes*	*I*
11)	15.3		s	(001)		3	s	(001)	15.4		vs
								Halloysite	10.0		f
				(002)	8.39		m	(002)	8.20		m
				Halloysite	7.31		ms	Halloysite	7.30		w
	5.42	b	vs	Duco	5.48	b	ms	Duco	5.49		vs
				(110)(020)	4.50		ms	(110)(020)	4.58		s
				(004)	4.23		ms	(004)	4.09		w
				Halloysite	3.58		ms	Halloysite	3.62		m
5)	3.48	b	ms	(005)	3.39		ms	(005)	3.37		ms
								(006)?	2.90		w
0)	2.62		m	(130)	2.67		m	(130)	2.68		m
				(200)	2.585		m	(200)	2.603		m
					2.455		m		2.512		vw
					2.344	Al	f		2.144		w
					2.214		vvf	(008)?	2.063		w
					2.006	Al	vvf		2.007		w
									1.877		vw
								(150)	1.762		w
0)	1.71		vvvw	(310)	1.714		vf				
				(00.10)	1.678			(00.10)?	1.668		vw
0)	1.542	b	ms	(060)	1.534		s	(060)(330)	1.550		vs
				Halloysite in part (330)	1.497		w				
				(260)	1.326	b	vf	(260)	1.338		mw
0)	1.13	b	vw	(440)?	1.240	b	vvf				
	1.08	b	vw								
				(190)	1.007	b	vvvf	(190)	1.013	b	mw
0)	0.908	b	vw	(550)(390) (00.19)	0.891	b	vvvf	(550)(390) (00.19)	0.895	b	mw
	0.872	b	vw								
	0.846	b	vw								
	0.820	b	vw								
	0.791	b	vw								

line appears here but it is too faint to measure
he dark edge of the band was measured
trong line present, but not measurable
erns for samples Nos. 1, 2, 3, 4, 7 corrected for film shrinkage.
erns for samples Nos. 5, 6 uncorrected for film shrinkage.
road diffuse band
oublet, mean value used in table.

calculated using the monoclinic formula and the results are given in Table 9. In selecting the most probable indices the following were considered:

(1) The agreement between calculated and observed spacings.
(2) The quality of the line as indicated by the intensity and the width of the line.
(3) The specific effect of ethylene glycol upon the position of the (00*l*) spacings.

The powder diffraction data were also used to construct a diagram of the reciprocal lattice which afforded a check on the indexing of the data.

The presence of halloysite in some of the samples of sauconite was established by *x*-ray studies and confirmed by means of electron microscopy. The electron micrographs were made by Edward J. Dwornik.

TABLE 9. MOST PROBABLE INDICES OF THE LINES IN THE *X*-RAY DIFFRACTION PATTERN OF SAUCONITE NO. 4 FROM THE YANKEE DOODLE MINE, LEADVILLE, COLORADO

Most probable index	*d* (observed)	*d* (calculated) for possible spacings	Intensity	Width of line	Expansion of basal spacings	Error in line measurement ±0.2 mm.		Halloysite-Average pattern after G. Nagelschmidt
						(−)	(+)	
(001)	16.1	16.8 (001)	vs	0.7 mm.	0.7 Å			
(002)	8.4	Assumed (002)	s	0.5 mm.	0.5 Å			7.49 to 7.43 m to vw
(020)	4.61	4.63 (020)	m	0.4 mm.		4.66	4.56	
(110)	4.45	4.50 (110)*	ms	0.5 mm.		4.49	4.41	4.44 to 4.42 vs to s
	3.63	Halloysite	wm	0.6 mm.				3.72 to 3.60 s to w
(005)	3.37	3.36 (005)	m	0.7 mm.	0.21 Å	3.40	3.35	3.35 to 3.31 m to w
(006)	2.82	2.80 (006)	w	0.8 mm.	no data	2.836	2.801	
(130)	2.66	2.65 (130)	m	0.6 mm.		2.671	2.640	
(200)	2.579	Assumed (200)	wm	0.6 mm.				2.60 to 2.57 s
(150)	1.754	1.743 (150)	vw	broad, diffuse		1.760	1.747	2.36 to 2.33 s
		1.721 (240)						2.22 vw
(310)	1.700	1.687 (310)	vw	broad, diffuse		1.705	1.694	1.71 to 1.70 s to m
(060)	1.544	Assumed (060)	s	0.6 mm.				1.64 to 1.62 s to m
(330)	1.491	1.499 (330)*	w	0.8 mm.		1.495	1.486	1.491 to 1.486 vs to s
(260) (170)	1.327	1.324 (260) 1.324 (170)	wm	1.2 mm.		1.330	1.323	
(400)	1.285	1.289 (400)	vvw	broad, diffuse		1.288	1.282	1.291 to 1.289 m to w
		1.292 (00.13)						1.239 to 1.236 m to w
(440)	1.134	1.125 (440)	vvw	broad, diffuse		1.137	1.132	
(280)	1.067	1.056 (280)	vvvw	broad, diffuse		1.069	1.065	
		1.050 (00.16)						
(190)	1.006	1.004 (190)	vvw	broad, diffuse		1.0073	1.0043	
(550) (390) (00.19)	0.891	0.900 (550)	vvw	2.0 mm diffuse		0.8921	0.8903	
		0.890 (00.19) 0.883 (390)						
(620)	0.844	0.844 (620)	vvvw	broad, diffuse		0.8444	0.8431	
		0.840 (00.20)						
	0.821	0.826 (630)	vvw	broad, diffuse		0.8210	0.8200	

* Halloysite in part.

vs = very strong
s = strong
m = medium
ms = medium-strong
wm = weak-medium

w = weak
vw = very weak
vvw = very, very weak
vvvw = very, very, very weak

(*d*) *Identification of the phases formed in the dissociated minerals*

(1) *Phases present in sauconite heated to about 350° C.*

A sample of sauconite No. 2, the brown variety, from the Coon Hollow Mine, Arkansas, was heated in the differential thermal analysis apparatus to a temperature of 327° C. The heating was stopped after all the "low-temperature" water was expelled (see Fig. 7A). This "low-temperature" water represents the interlayer water and the very small amount of adsorbed water. An *x*-ray powder photograph was made of this heated material. Comparison of the powder patterns of the heated brown sauconite and of the natural sauconite shows that the basal spacings (00*l*) are smaller for the heated sauconite than for the unheated mineral, an observation that was expected. See Table 10. Otherwise, the patterns are almost identical. The background due to general scattering is much less for the heated sauconite and this decrease is chiefly due to the absence of the adsorbed water.

(2) *Phases present in sauconite heated to a temperature just above the dissociation point*

Zinc orthosilicate (Zn_2SiO_4) is one of the products formed when sauconite is dissociated. In order to determine the sequence in the polymorphic transformations of Zn_2SiO_4 in the differential thermal analysis, a sample of sauconite no. 2, from Boone County, Arkansas, was heated to a temperature of 866° C. and then suddenly cooled by pulling the furnace away from the sample. The record of this heating and quenching experiment is shown as curve C-643 in Figure 7B. A comparison of this curve C-134 in Fig. 1, shows that up to a temperature of about 840° C. the curves are essentially the same. The slight exothermic reaction at about 350° C. appearing on curve C-643 is probably due to the combustion of organic matter or the oxidation of ferrous iron. Above 840° C. these curves are very different. The record of the sample heated to 866° and then suddenly cooled shows a well defined exothermic break at about 870° C. Thereafter, no reaction took place and the sample cooled down to room temperature. *X*-ray examination of the resulting material shows the powder pattern to be that of β-Zn_2SiO_4 with an extra line probably belonging to gahnite ($ZnAl_2O_4$).

The exothermic break at 832° C., curve C-643, apparently represents the formation of γ-Zn_2SiO_4. Accordingly, the exothermic break at 870° C. represents the transformation of "γ-Zn_2SiO_4" to β-Zn_2SiO_4 and the area under the curve is a measure of the heat of transformation of the "γ" to the β form.

Table 10. X-Ray Powder Diffraction Data for Sauconite No. 2, the Natural Brown Variety from the Coon Hollow Mine, Arkansas, and for the Same Substance Heated to 327°C.

Sauconite No. 2 Natural Mineral				Sauconite No. 2 Heated to 327° C.			
d spacing	Intensity	Remarks	Probable indices	*d* spacing	Intensity	Remarks	Probable indices
15.4	s		(001)	14.5	vs		(001)
7.77	ms		(002)	7.74	s		(002)
5.58	w	Duco band				present but not measured	
4.60	ms		(020) (110)	4.60	s		(020) (110)
3.87	w		(004)	3.82	m	broad	(004)
3.09	w		(005)	3.07	m	broad	(005)
2.670	s		(130) (200)	2.66	ms	doublet	(130) (200)
1.748	vw		(150) (240)	1.747	vw		(150) (240)
1.718	vw					(?)	
1.544	s		(060)	1.544	vs		(060)
1.334	m		(260) (170)	1.331	w	broad	(260) (170)
1.005	w	broad		1.007	vw	broad	
0.890	w	broad		0.891	vw	broad	

s = strong
ms = medium-strong
w = weak
vw = very weak
vs = very strong

(3) *Phases present in sauconite heated to about 1000° C.*

The products resulting from the dissociation of the various specimens of sauconite which had been heated to at least 1000° C. were examined by the x-ray powder diffraction method. The phases observed are wil-

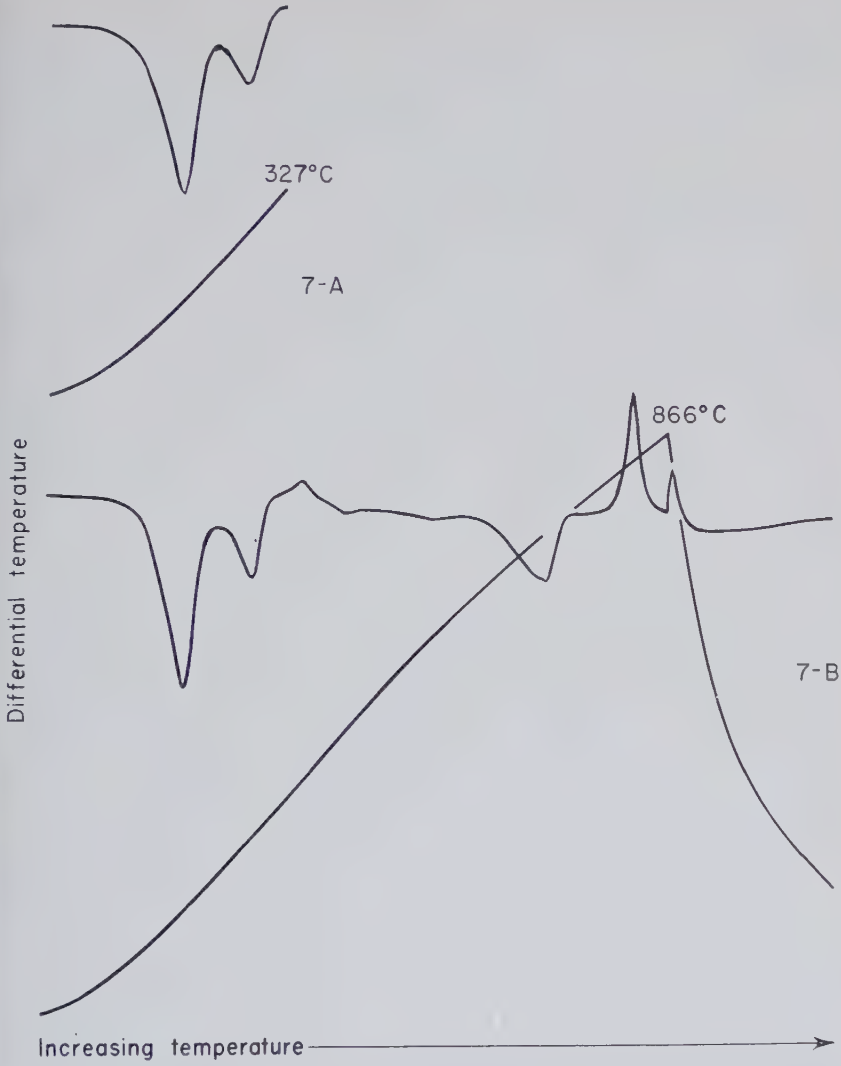

FIG. 7A. Differential thermal analysis curve of a sample of sauconite no. 2, from Boone County, Arkansas, C-639, heated to a temperature of 327° C. and then cooled by removing the furnace from the sample holder.

FIG. 7B. Differential thermal analysis curve of a sample of sauconite no. 2, from Boone County, Arkansas, C-643, heated to 866° C. and then suddenly cooled by removing the furnace from the sample holder.

lemite, gahnite, and cristobalite. A summary of these data is given in Table 11.

TABLE 11. PHASES IDENTIFIED BY *X*-RAY METHODS IN THE SAUCONITES HEATED TO ABOUT 1000° C.

Sauconite used in the experiment	Record No.	Phases present			Relative abundance	*X*-ray powder pattern no.	Notes
		Willemite α-Zn_2SiO_4	Cristobalite SiO_2	Gahnite $ZnAl_2O_4$			
Sauconite No. 2 (ZnO = 36.73%)	C-134	+	+	+	Willemite> Gahnite	3305	
Sauconite No. 2 Ca-Na Sauconite	C-211	+	+	+	Willemite>> Gahnite	3318	
Sauconite No. 2 Na-Sauconite	C-222	+	−	+	Willemite>>> Gahnite	3319	
Sauconite No. 2 H-exchanged	C-209	+	−	+	Willemite>> Gahnite	3306	
Sauconite No. 3 (ZnO = 33.70%)	C-80	+	+	+	Willemite> Gahnite	3303	
Sauconite No. 4 (ZnO = 28.19%)	C-81	+	+	+	Gahnite> Willemite	3304	
Sauconite No. 6 (ZnO = 23.10%)	C-175	+	−	+	Gahnite>>> Willemite	3072	A weak extra line appears at 3.37Å(±). This suggests the presence of mullite ($2SiO_2 \cdot 3Al_2O_3$)
Sauconite No. 6	C-567	+	−	+	Gahnite>>> Willemite	3320	

The equilibrium relations in the system ZnO-Al_2O_3-SiO_2 have been determined by Bunting (1932). One must be cautious in attempting to correlate the results of differential thermal analysis studies with equilibrium diagrams. Differential thermal analysis experiments are almost always performed in such a manner that inequilibrium results. Nevertheless, a comparison of the results of differential thermal analysis studies with the actual equilibrium diagrams is of interest. The chemical analyses of the various sauconites studied were recalculated to a water free basis. In this calculation the very small amounts of MnO, TiO_2 and CuO were neglected. The Fe_2O_3, Na_2O and K_2O were combined with the Al_2O_3 and the resulting sum was considered as Al_2O_3; likewise the MgO and CaO were added to the ZnO. These "corrected" values of ZnO and Al_2O_3 together with the SiO_2 were used to calculate the mole percentages of these oxides in each of the sauconites. The resulting data were plotted on the phase rule diagram of Bunting. See Fig. 8. The phases present in these samples of dissociated sauconite are those which are predicted by an examination of the equilibrium diagram.

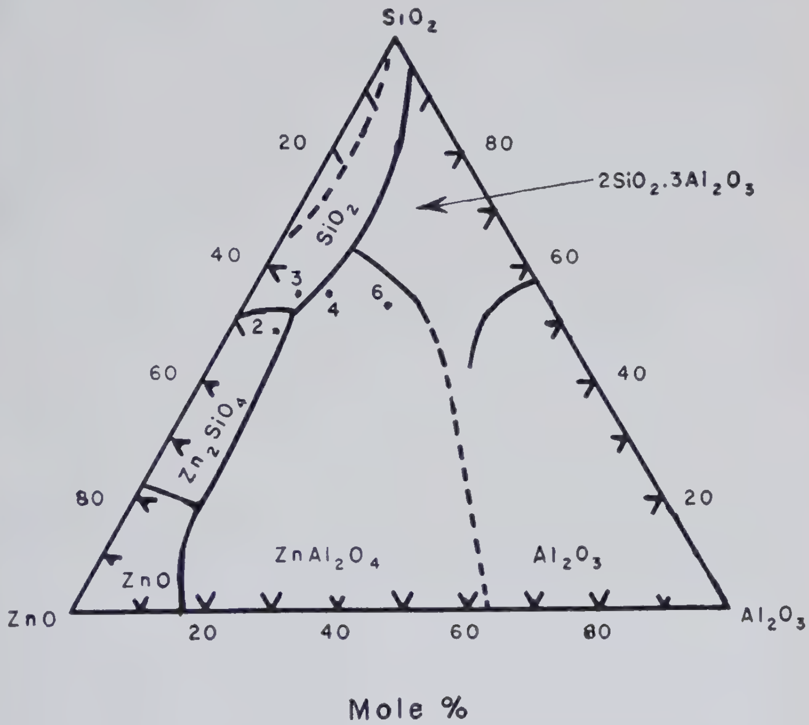

FIG. 8. Phase equilibrium diagram of the system $ZnO-Al_2O_3-SiO_2$, as determined by E. N. Bunting. The numbers 2, 3, 4, and 6 represent the composition of sauconites Nos. 2, 3, 4, and 6.

When samples of sauconite are packed in the hole in the nickel block of the differential thermal analysis apparatus and heated to a temperature of about 1000° C. they usually form as a firm cylinder. The sauconite from the New Discovery Mine yielded the firmest cylinder. This behavior is like that of certain types of montmorillonite.

ACKNOWLEDGMENT

In various parts of the text, acknowledgment is made to others who have furnished data or specimens. J. M. Axelrod discussed with the author his preliminary study of the *x*-ray patterns of sauconite. I am particularly indebted to Theodore Woodward for measuring several of the powder photographs. C. L. Christ offered valuable advice in connection with the *x*-ray studies.

References

1. Alexander, L. T., Hendricks, S. B., and Nelson, R. A. (1939), Part I, Minerals present in soil colloids; Part II, Estimation in some representative soils: *Soil Sci.*, **48,** 257–268; 273–279.
2. Bunting, E. N. (1932), Phase equilibria in the system SiO_2-ZnO-Al_2O_3: *Bur. Standards Jour. Res.*, **8,** 279–287.
3. Caillére, S., and Hénin, S. (1944), Sur l'origine de quelques anomalies présentées par les courbes thermiques de certaines montmorillonites: *Acad. Sci. Paris Comptes rendus*, **219,** 685–686.
4. Cross, C. W. (1877), Vanuxemite: *Naturalists' Bull.*, March, p. 5.
5. Faust, George T. (1948), Thermal analysis of quartz and its use in calibration in thermal analysis studies: *Am. Mineral.*, **33,** 337–345.
6. Faust, George T. (1950), Thermal analysis studies on carbonates I. Aragonite and calcite: *Am. Mineral.*, **35,** 207–224.
7. Genth, F. A. (1875), Mineralogy of Pennsylvania—*Second Geol. Survey. Penn.*, p. 120-B.
8. Grim, R. E., and Rowland, Richards A. (1942), Differential thermal analyses of clay minerals and other hydrous materials: *Am. Mineral.*, **27,** 746–761; 801–818.
9. Gruner, John W. (1935), The structural relationship of nontronites and montmorillonite: *Am. Mineral.*, **20,** 475–483.
10. Hendricks, S. B., Nelson, R. A., and Alexander, L. T. (1940), Hydration mechanism of the clay mineral montmorillonite saturated with various cations: *Am. Chem. Soc. Jour.*, **62,** 1457–1464.
11. Hofmann, Ulrich, Endell, Kurd, and Wilm, Diederick (1933), Kristallstruktur und Quellung von Montmorillonit: *Zeits. Kristallographie*, **86,** 340–349.
12. Ingerson, Earl, Morey, G. W., and Tuttle, O. F. (1948), The systems K_2O-ZnO-SiO_2, ZnO-B_2O_3-SiO_2, and Zn_2SiO_4-Zn_2GeO_4: *Am. Jour. Sci.*, **246,** 31–40.
13. Ito, T., and West, J. (1932), The structure of hemimorphite, $H_2Zn_2SiO_5$: *Zeits. Kristallographie*, **83,** 1–8.
14. Kenngott, G. A. (1868), Übersichte der Resultate mineralogischer Forschungen (1852–1868) für die Jahren 1862–65, Leipzig **1868.**
15. Leverenz, Humboldt W., and Seitz, Frederick (1939), Luminescent materials: *Jour. Applied Physics*, **10,** 479–493.
16. Maegdefrau, Edmund, and Hofmann, Ulrich (1937), Die Kristallstruktur des Montmorillonits: *Zeits. Kristallographie*, **98,** 299–323.
17. Nagelschmidt, Gunther (1938), On the atomic arrangement and variability of the members of the montmorillonite group: *Mineral. Mag.*, **25,** 140–155.
18. Risse, Hugo (1865), Über den Moresnetite, ein neues Zinkoxyd—Thonerdesilikat von Altenberge bei Aachen: *Naturh. Ver. der Rheinlande und Westphalens Correspondenzblatt*, No. 1, pp. 98–99, Vol. **22,** Bonn.
19. Ross, C. S. (1946), Sauconite—A clay mineral of the montmorillonite group: *Am. Mineral.*, **31,** 411–424.
20. Schaller, W. T., and Fairchild, J. G. (1938), Cadmium in smithsonite from New Mexico: *Am. Mineral.*, **23,** 894–897.
21. Schleede, Arthur, and Gruhl, Arno (1923), Über Röntgenographische Beobachtungen an Luminescenz-fähigem Zinksilikat: *Zeits. Electrochemie*, **29,** 411–412.
22. Shepard, C. U. (1876), New Minerals: *Am. Jour. Sci.*, 3rd Ser., **12,** 231.
23. Zambonini, F. (1908), Contributo allo studio dei silicate idrati: *Alti della Real Accad. delle scienze fisische e mathematiche*, **14,** Ser. 2, No. **1,** 1908 (1910).

Manuscript received April 23, 1951.

NOTES ON PRECISION AND ACCURACY OF OPTIC ANGLE DETERMINATION WITH THE UNIVERSAL STAGE

H. W. Fairbairn and T. Podolsky, *Massachusetts Institute of Technology, Cambridge, Massachusetts.*

Abstract

Precision of determination of 2V varies greatly with the method used, with maximum precision being shown by the so-called direct method. Optimum conditions demand double axis measurement and settings at both 45° and 135° positions of the microscope stage. Precision increases roughly with birefringence and also with section thickness. Based on quintuplicate measurements, precision varies between .02° and .6°. Accuracy was tested by using an optic angle goniometer as control instrument. A satisfactory calibration (within a few tenths of a degree) was obtained for five of the six U-stages used for the test.

As an example of the need for information on precision and accuracy, careful work on several high-temperature, unzoned plagioclase grains in a rhyolite shows a range in optic angle of about 6°. With more casual examination this range of angle could easily be ascribed to errors of various kinds. Since refractive index study (even by the double variation method) cannot be substituted for 2V determinations in cases as critical as this, the advantage of mastery of the Universal stage technique is obvious.

Introduction

The increased use of the U-stage in investigations of the optic character and properties of anisotropic crystals is encouraging evidence of its acceptance as standard equipment for quantitative work. Published U-stage measurements however show in many cases a lack of concern about precision and accuracy, both of which can be checked with little extra work and which would seem to be essential in forming conclusions about critical mineralogic and petrologic problems. Fairbairn and Sheppard (1945) dealt with some aspects of precision from the standpoint of single measurements. Although similar studies have undoubtedly been made in other laboratories, the dearth of published data on the subject is somewhat disturbing. Wright (1907) gives data for topaz; more recently Hess (1949) published replicate measurements on monoclinic pyroxene. It is the purpose of this paper to demonstrate the relative precision which may be expected under certain situations and to present also some data regarding the accuracy of U-stage determinations. We are not primarily concerned here with variations *between* crystals in a rock section; that is a purely petrologic problem which can properly be considered only after the precision of single crystal measurements has been evaluated.

Precision of Optic Angle Determinations

The precision, or reproducibility, of a measurement is a matter which vitally concerns every U-stage operator. A fundamental knowledge of proper stage and lamp adjustment, in order to obtain correct centering and approximately parallel illumination, is, of course, a prerequisite. With these details attended to and standardized the degree of precision attainable is controlled by birefringence, thickness, orientation, etc., all of which must be evaluated. A number of methods of determining 2V with the U-stage are known, not all of equal importance for one reason or another. They are discussed in the following sections.

Extinction Angle Procedures

These methods, developed for the U-stage by Federow and Berek, are all based on the fundamental Biot-Fresnel law relating extinction directions to optic axes. The construction of "optic curves" for precise location of an optic axis is an illustration of this law. It is an elegant method, but is too time-consuming for the present generation of petrographers and requires exceedingly careful work with the stereographic net. Federow himself recognized this handicap of the method a half-century ago. Wright (1911) and Johannsen (1918) have described the procedure fully.

The principal use of extinction angle methods at present is as an aid in identification of indicatrix directions and for approximating 2V. Berek (1924), followed by Dodge (in Emmons, 1943), developed this application of the Biot-Fresnel law. Single determinations are rapid, but as a precision method for 2V it leaves much to be desired, since a considerable number of trials are needed before a satisfactory mean value is reached. Thus in a section of anhydrite having Bx_o vertical, 9 replicate extinction angle measurements were needed to obtain the mean of $2V=43.3°$ found by direct measurement (see Table 1). Moreover the error of this mean is 1.6° (based on 9 trials) compared with 0.3° by direct measurement (based on only 5 trials). Undoubtedly for certain orientations the Berek-Dodge method is capable of greater precision than this, but as already mentioned its principal usefulness is as a guide for orientation and optic angle measurement (Emmons 1943, p. 30).

Relative Retardation Method

Long before quantitative work with compensators was possible, it was known that 2V could be approximately determined from the Michel-Lévy interference color chart, based on the relation $\sin^2 V=(\beta-\alpha)/(\gamma-\alpha)=(\Gamma_z/\Gamma_y)$. Until the Berek and other graduated compensators became available, however, the quality of the results obtained was not commensurate with the time expended. The combination of the U-stage (for exact orientation) and a graduated compensator (for exact retardation) now make possible the indirect determination of 2V with moderate precision. Best results are likely to be attained if (1) all necessary retardations can be obtained from one grain (this excludes possible errors due to variable section thickness, or to compositional differences), (2) grains are used having symmetry planes as nearly parallel as possible with the microscope axis. Both these goals are obviously impossible to achieve simultaneously and one must compromise. A determination of 2V with the Berek compensator for barite is typical of the results to be expected by this procedure. A grain was found which was adequate for the entire computation (Table 1). A mean orientation position of its symmetry planes was obtained, based on five individual trials, and the standard error of the angle (normal to the section ∧ microscope axis) was computed. This turned out to be .5°. Five sets of readings of the compensator were made,[1] an average computed and also the error of this mean (.02). From this the retardations can be found and, knowing the error in the U-stage settings and in the compensator readings, the total error in each retardation can be obtained. These are of the order of magnitude of 10 mμ or less. Computation of 2V (or careful reading of the 2V nomogram) gave 39.6°; the error comes out to 2.1°. Direct measurement of optic angle on this same grain gave 40.3° with an error (for 5 measurements) of 0.2°. As with the extinction angle procedure, the theory of the retardation method is superior to the practice, and it is not a satisfactory substitute

TABLE 1. PRECISION OF EXTINCTION ANGLE AND RELATIVE RETARDATION METHODS OF 2V DETERMINATION

Mineral	Extinction Angle Method (based on 9 measurements)	Relative Retardation Method (based on 5 measurements)	Comparison with Double Axis Method (based on 5 measurements)
Anhydrite	43.3 (1.6)		43.3 (.3)
Barite		39.6 (2.1)	40.3 (.2)

Error of each mean is shown in parentheses.

In this and succeeding tables error of the mean is the standard error

$$s_{\bar{x}} = \sqrt{\frac{\Sigma(\bar{x} - x)^2}{n(n-1)}}$$

where $\bar{x}$ = arithmetic mean
x = single measurement
n = number of measurements.

---

[1] For best results the method of using extinction bands several wavelengths higher than the compensation position, as recommended by Mosebach (1949), should be followed.

for the direct measurement of 2V. As a by-product of a birefringence determination, which requires a graduated compensator, 2V can often be determined from the same compensator readings without additional measurement. Since many grains are unsuitably oriented for direct determination of 2V, the method, although not of great precision, is nevertheless useful.

Direct Method

This method is so superior to the previous ones that comparisons can scarcely be made. It requires, for highest precision, orientation of both optic axes, but reasonably good work can also be accomplished with one axis only. It is the method in common use today with the U-stage. Two operations are involved, (*a*) the orientation of the optic plane parallel to the microscope axis, (*b*) the orientation of the optic axes parallel to the microscope axis. As a result of a considerable number of tests, the writers recommend the following procedural details for double axis orientation.

(1) The optic plane is oriented in a vertical and north-south position (for either the 4- or 5-axis stage). No angles need be recorded for this step. The acute bisectrix in the unoriented section must be approximately vertical in order that *both* optic axes can be oriented.

(2) The optic axes positions are read on the outer east-west axis (single readings) for two settings of the microscope axis, approximately 90° apart. The two readings for each axis are averaged; the difference between the two averages is the observed value of 2V.

(3) Steps (1) and (2) are repeated four times, using the same grain. The five values of 2V are averaged and the standard error of this mean is computed.

The duplicate settings of each optic axis for two orientations of the microscope axis increase precision considerably and are well worth the few extra minutes required. The procedure tends to compensate for inaccuracies in the optic plane setting. Data have been obtained (Table 2) for a group of selected minerals to illustrate the error in their means for various birefringences and section thicknesses. Each mean is obtained from measurements of the same grain and, particularly in the example of plagioclase, from the same part of the same grain.* The study is therefore not concerned with variation in optic angle from grain to grain in a rock section, but only with the experimental error of replicate measurements of the same grain. These two goals should not be confused.

Except for barite, each mineral was investigated by two operators,

---

* Except for plagioclase (2) in Table 2, where the mean is the result of measurements at different points in the grain. Since the error of this mean is comparable with those for the other plagioclases, the essential homogeneity of the crystals is reasonably well established.

TABLE 2. PRECISION OF DOUBLE AXIS DETERMINATION OF 2V

Mineral	Operator	Mean 2V, based on 5 settings		Error of mean		Thickness of section t	Birefringence B	Angle of tilt of optic plane
		4-axis stage	5-axis stage*	4-axis stage	5-axis stage*			
Aragonite	H.W.F.	18.05	18.38	.05	.06	.105	.155	None
	T.P.	18.26		.02				
Anhydrite	H.W.F.	42.55	42.95	.25	.13	.012	.044	~10°
	T.P.	42.41	43.13	.30	.20			
Muscovite	H.W.F.	42.80		.16		~.07	~.04	None
	T.P.		42.67		.09			
Barite	H.W.F.		40.3		.2	~.012	.012	~35°
Andalusite	H.W.F.	85.2	84.6	.1	.1	~.09	~.01	None
	T.P.							
Topaz	H.W.F.	65.46	65.03	.13	.2	~.06	.010	None
	T.P.	65.40	65.04	.06	.2			
Plagioclase (1)	H.W.F.	68.2	68.9	.4	.3	~.02	~.008	~15°
	T.P.	69.2	67.7	.6	.1			
Plagioclase (2)	H.W.F.	61.7		.3		~.02	~.008	~10°
	W.F.B.†	61.5		.3				
Plagioclase (3)	H.W.F.		64.3		.3	~.02	~.008	~30°
	L.F.H.†	64.0		.3				
Plagioclase (4)	H.W.F.	63.2		.2		~.02	~.008	~25°
	W.H.†	63.2		.25				

* Stage No. 5 (See Table 5).

† The writers are indebted to W. F. Brace, L. F. Herzog, and W. Holyk for their co-operation in making these plagioclase determinations.

each without knowledge of the other's results. Some were measured with the 4-axis, others with the 5-axis stage, as noted. All readings of the optic axes were made on the east-west axis. The following points are obvious from the table: (1) any two operators obtain errors of comparable order of magnitude for a given mineral; (2) the expected direct relation between precision and birefringence holds throughout, modified to some degree by variations in thickness (precision varies in general with thickness); (3) the effect of angle of tilt of the optic plane is not clear. High angles are expected to lower precision, but the 35° maximum in Table 2 does not seem to be high enough to achieve this; (4) the average error obtained with the 5-axis stage (.17) is essentially the same as with the 4-axis stage (.23). More extensive measurements would be needed, however, to establish this as a general condition. Mechanically the 5-axis instrument is at a disadvantage, but the scope of Table 2 is too limited to indicate this; (5)

the maximum difference between means for any given mineral is 1° (plagioclase); the minimum is .13° (muscovite). This supports the general thesis that increased precision is to be expected where birefringence and thickness are relatively high.[2]

Although offering somewhat lower precision, and a tendency to a bias in the means, the single axis procedure may in certain cases be the only source of 2V data by direct measurement. Table 3 gives information based on the same grains and same general procedure as used for the double axis method. Precision is reduced about one-half and the means vary between 0.6° and 2.8° from the double axis results. The large variations are confined to plagioclase; for all the other minerals the differences are slightly less than 1°. Even with optimum conditions for measurements, therefore (high birefringence and relatively thick sections), the single axis is not a satisfactory substitute for the double axis method and if from necessity it is used, the results must be interpreted with considerable care.

TABLE 3. COMPARISON OF SINGLE AND DOUBLE AXIS DETERMINATIONS OF 2V

Mineral	Single axis mean* (5 settings)	Double axis mean (from Table 1)	Diff. in 2V	Thickness of section t	Birefringence B	Error of single axis mean	Error of double axis mean
Plagioclase (1)	70.8	68.5	2.3	∼.020	∼.007	.4	.2–.3
Plagioclase (2)	63.0	61.6	1.4	∼.020	∼.007	.5	.2–.3
Plagioclase (3)	67.0	64.2	2.8	∼.020	∼.007	.5	.2–.3
Aragonite	18.8	18.2	0.6	∼.105	.155	.1	.05
Andalusite	84.2	84.9	0.7	∼.090	∼.01	.4	.1
Anhydrite	43.8	43.0	0.8	∼.012	.044	.3	.2
Muscovite	41.9	42.7	0.8	∼.07	∼.04	.2	.1
Barite	40.9	40.3	0.6	∼.012	.012	.3	.2

* Measurements on same grains as for double axis mean.

ACCURACY OF OPTIC ANGLE DETERMINATIONS

Evaluation of precision in physical measurements is a relatively simple matter; the same however cannot be said for accuracy, since the bias of the mean of any set of measurements from the true value is unknown. One must therefore be satisfied with an approach to the true value and select an independent and presumably superior method for control. In the case of optic angle measurements the best control instrument for the U-stage is the optic angle goniometer. With this instrument 2V can be determined indirectly with an oriented thin section by measurement of 2E; or directly, using a sphere cut from the selected mineral. Both procedures were carried out, with results as shown in Tables 4 and 5.

---

[2] Orientation on the U-stage by the interference figure method was not possible with our equipment for all the minerals. The writers agree with Hallimond (1950) that this method gives higher precision in symmetry plane settings than is to be expected with conventional extinction position methods, particularly for crystals of low birefringence. An interesting extension of the present study would be a comparison of precision by the interference figure procedure for a range of minerals such as in Table 1.

Table 4. Accuracy of U-Stage Measurements of 2V
(Based on 2E determinations)

Mineral	2E (Optic angle goniometer)	Error in 2E	β	Error in β	2V (calc.)	Error in calc. 2V	2V (measured with U-stage)	Error in measured 2V
Aragonite (H.W.F.)	30.90 (mean of 5 sets of readings)	.03	1.6816 (from Rosenbusch Wülfing Mügge)	.0002 (Assumed value)	18.23	∼.03	18.22 (see Table 1)	.05
(T.P.)	30.97	.06		.0002	18.27	∼.05	18.26	.02
Aragonite (Data from Rosenbusch Wülfing Mügge)	30.90	Not stated	1.6816	Not stated	18.23	Not stated	No data	
Aragonite (Data from Winchell)	30.87	Not stated	1.681 (?)	Not stated	18.18	Not stated	No data	
Topaz (Wright, (1907)	126.2	Unknown	Not stated but probably determined by minimum deviation method	Unknown	66.7	Unknown	66.6	Unknown

An oriented section of aragonite was used for the indirect computation of 2V. In Table 4 the authors' results may be compared with published data for 2E. It is apparent that, whether instrumental or compositional (or both), variations in 2E are satisfactorily small. The intermediate index β must also be relatively constant; even if an uncertainty of ±.0002 in the published value is assumed, the error of the calculated 2V is still quite small. As it was not possible to determine β in our section of aragonite within limits smaller than ±.001, the published value has been accepted. The computed value of 2V is practically identical with the values obtained by U-stage measurement. Even if the uncertainty in β were

±.001, the resultant error in 2V would be less than 0.1° (computed from the differentiated form of sin E/sin V = β). This test of the accuracy of the U-stage may therefore be considered satisfactory.

For the direct method a sphere about $\frac{7}{8}$-inch in diameter was cut from a large, clear, single-crystal fragment of topaz. From the same material an oriented thin section was prepared. The sphere, properly centered on the goniometer, passes light without deviation across the air-topaz boundary surface and gives values directly comparable with those obtained on the U-stage with the thin section. These measurements are given in Table 5. Six U-stages were tested; only one failed to yield 2V values within a few tenths of a degree of the goniometer value. This stage was known however to have a slightly defective bearing and the high values, obtained by both of us, are ascribed to this cause. Two stages gave consistently lower, three gave consistently higher values than the goniometer. The mean for all five is less than 0.2° from the goniometer result. Although in the aragonite measurements the two U-stages tested were closer to the goniometer value than this, we believe that the topaz calibration is preferable,[3] since no assumption regarding refractive index

Table 5. Accuracy of U-Stage Measurements of 2V
(Direct method, using topaz sphere)

Operator	Illumination	Optic angle goniometer	4-axis stages				5-axis stages	
			1	2	3	4	5	6
H.W.F.	Sodium lamp	65.17 (.01)*	65.03 (.15)	65.86 (.08)	65.48 (.09)	65.31 (.17)	65.03 (.2)	66.60 (.09)
	Tungsten lamp	—			65.63 (.16)			66.28 (.04)
T.P.	Sodium lamp	65.18 (.02)			65.15 (.07)		65.04 (.2)	66.54 (.2)
	Tungsten lamp	—			65.65 (.05)			

Mean for all U-stages (excluding #6) 65.35. No. 1 is a Fuess stage; all others are Leitz.
* Numbers in parentheses are standard errors for each mean.

---

[3] A check on the order of magnitude of errors in 2V which would result if the sphere were slightly elliptical was carried out by a graphical method. The sphere, in the circumference parallel to the optic plane, was known to vary in diameter by .0001 inch. Assuming the least favorable orientation of the optic axes relative to this slightly elliptical optic plane section, the error in 2V turns out to be less than .05°. This is of the same order of magnitude as the errors computed for the means in Table 5 and is therefore relatively insignificant.

need be made. In either case a check on the magnitude of the bias in measurements made with a given U-stage can be obtained.[4]

As far as the writers are aware the results of only one previous calibration of a U-stage have been published (Wright, 1907). These figures are included in Table 4 and indicate that even the small, early models of the U-stage were apparently well constructed. As Wright gives no data on precision, further comparison with our work is not possible.

General Discussion

The optic angle of a crystal, if properly determined and evaluated for error, is a significant and highly diagnostic property of a crystal. If carelessly done, without regard for matters of either precision or accuracy, one's time is largely wasted, for a reasonable estimate of 2V can be made from an interference figure without need for a U-stage at all. Furthermore, incorrect petrologic conclusions may be drawn in some instances if optic angle work is poorly done. As an illustration we cite the data for the plagioclase crystals in Table 2. These are phenocrysts from a thin section of a rhyolite from Nevada known to contain high temperature plagioclase.[5] Detailed measurements on four unzoned phenocrysts, using the double-axis procedure, gave four different means* for 2V, ranging from 61.5 to 68.5. Since the error of the means is only 0.3 (approximately) no question can arise regarding the validity of the separate 2V values. But if the single-axis procedure had been used (see Table 3), or some other of the approximate methods, it might have been concluded that the plagioclase was uniform throughout the rock and that discrepancies shown by 2V represented instrumental and operator error. Furthermore, if optical study of these phenocrysts had been limited to the refractive index immersion procedure, the variations indicated by the optic angle investigation would not be detected. If, for example, indices are determined to ±.001 one can easily show that, for the values determined ($\alpha=1.530$, $\beta=1.536$, $\gamma=1.540$), computed values of 2V can vary between 52° and 83°. If the uncertainty is ±.0001, as might be the case with the double variation technique, computed values of 2V will still have a range of 5°. This sensitivity of 2V to extremely small changes in refractive index is of course well known and is a characteristic of the optic indicatrix which, although it demands careful treatment, should be exploited fully rather than avoided. On the other hand, even the most painstaking refractive index investigation may not reveal any but gross inhomogeneities in a group of supposedly uniform crystals. Since the example cited here for plagioclase may have its counterpart in other minerals and in other rocks, no effort should be spared to reveal valid inhomogeneities by carefully controlled optic angle investigation. According to Tuttle (personal communication) one explanation of the range in 2V in these plagioclase phenocrysts might be sluggish inversion from the high to the low form which has progressed further in some grains than in others. Where x-ray spectrometric analysis can be combined with precise optic angle investigation it is probable that many petrologic riddles may be solved. Tuttle and Bowen (1950) have already given some indication of this in their recent work on feldspar. Success is possible however only if meticulous attention to operational details is maintained. It is the hope of the authors that this paper will arouse some long overdue interest in matters pertaining to precision and accuracy in optic angle investigations.

---

[4] Since cleavage fragments of topaz are normal to the acute bisectrix they provide naturally oriented sections and facilitate determination of 2V with the U-stage. The large single-crystal cleavage fragment from which the sphere was cut for this investigation will provide several hundred small cleavage plates suitable for mounting on glass slides. The authors will be glad to supply such cleavage plates without cost to those interested in U-stage standardization.

[5] Specimen loaned to the authors by O. F. Tuttle.

* Hemisphere corrections were made as standard procedure.

Acknowledgments

We are indebted to F. Chayes, R. C. Emmons, H. H. Hess, and F. J. Turner for their comments and suggestions. The authors take all responsibility however for any shortcomings of the paper.

References

Berek, M. (1924), Mikroskopische Mineralbestimmung mit Hilfe der Universaldrehtischmethoden. Gebrüder Borntraeger (Berlin).

Emmons, R. C. (1943), The universal stage: *Geol. Soc. Am. Mem.*, **8.**

Fairbairn, H. W., and Sheppard, C. W. (1945), Maximum error in some mineralogic computations: *Am. Mineral.*, **30,** 673.

Hallimond, A. F. (1950), Universal stage methods: *Mining Mag.*, (July), p. 3.

Hess, H. H. (1949), Chemical composition and optical properties of common clinopyroxenes: *Am. Mineral.*, **34,** 621.

Johannsen, A. (1918), Manual of petrographic methods, Chap. 35. McGraw-Hill (New York).

Mosebach, R. (1949), Eine Differenzmethode zur Erhöhung der Messgenauigkeit normaler Drehkompensatoren: *Heidel. Beitr. Mineral. Petrog.*, **2,** 167.

Tuttle and Bowen (1950), High-temperature albite and contiguous feldspars: *J. Geol.*, **58,** 572.

Wright, F. E. (1907), Measurement of optical axial angle, etc.: *Am. J. Sci.* (4), **24,** 317.

Manuscript received May 10, 1951.

THE CRYSTAL STRUCTURE OF CLAUDETITE (MONOCLINIC As_2O_3)

ALFRED J. FRUEH, JR., *University of Chicago, Chicago, Illinois*

ABSTRACT

From a complete diffraction record of a single crystal of claudetite taken by equi-inclination Weissenburg and Precession techniques, the unit cell dimensions were confirmed as: $a=5.25$ Å, $b=12.87$ Å, $c=4.54$ Å, $\beta=93°49'$. The cell contains four As_2O_3. Due to the apparent faint appearance of an odd order ($0k0$) reflection, doubt was cast upon the existence of a twofold screw axis (2_1). The presence of the 2_1, and hence of the space group $P2_1/n$, was confirmed by the comparison of the Harker-Patterson sections $P(x0z)$ and $P(x\frac{1}{2}z)$. From these sections and from Patterson projections on (001) and (100) the eight arsenic atoms were found to be in two general fourfold positions, one set at $x=.258$, $y=.102$, $z=.040$; the other set at $x=.363$, $y=.352$, $z=.007$; and their symmetry equivalents. From electron density projections and intensity checks, the twelve oxygen atoms were found to be in three general fourfold positions at $x=.45$, $y=.22$, $z=.03$; $x=.62$, $y=.41$, $z=.18$; and $x=.95$, $y=.16$, $z=.13$; and their symmetry equivalents. The structure is one of linked AsO_3 groups sharing all oxygens to form an irregular sheet parallel to the perfect (010) cleavage.

INTRODUCTION

Claudetite, the monoclinic form of As_2O_3, is found in nature as a secondary mineral, formed by the oxidation of realgar, arsenopyrite, or other arsenic minerals (1). The habit of its crystals is tabular, forming thin plates on {010}; both penetration and contact twins on {100} are very common. The crystals show perfect micaceous cleavage parallel to {010}. According to Schulman and Schumb (2), claudetite, the high-temperature form, is the stable form of the dimorphous pair, claudetite-arsenolite, at temperatures as low as 2° C. By calculations based upon the measured temperature dependence of the solubilities, these authors conclude that an enantiotropic relation exists between the two forms, the transition temperature being approximately $-13°$ C. The unit cell and space group of claudetite was investigated by Buerger (3) and the following cell dimensions were determined:

$$a=5.25\text{ Å}$$
$$b=12.87\text{ Å}$$
$$c=4.54\text{ Å}$$
$$\beta=93°49'$$

The cell contains four formula weights of As_2O_3. The diffraction symbol is $2/mP2_1/n$, which uniquely fixes the space group as $P2_1/n(C_{2h}^5)$.

EXPERIMENTAL PROCEDURE

The major portion of the data for the present work was obtained from a naturally occurring crystal of claudetite from Jerome, Arizona. Because of the tabular habit, the extreme ease with which these crystals will de-form plastically, and the scarcity of untwinned crystals, it was impossible to obtain a crystal of optimum size and shape or to peel a crystal down to a desired shape. Consequently, the crystal used had a *b* axis many times shorter than the other axes. No attempt was made to correct for relative absorption. A complete record of the zero, first, second and third levels of the *c* axis was taken by the equi-inclination Weissenburg method using filtered copper radiation. Zero level *a* and *b* axis records were obtained by the Buerger precession method using filtered molybdenum radiation. Zero level *c* axis data were also obtained by the Weissenburg method from a minute tabular crystal grown from a KOH solution of As_2O_3. Intensity data were gathered from the entire diffraction record in a manner similar to that first suggested by Dawton (4) and adapted to Eastman No-Screen *X*-Ray film by workers in the Massachusetts Institute of Technology crystallographic laboratory (5). The intensities were made proportional to F_{hkl}^2 by correcting for Lorentz and polarization factors as described by Buerger and Klein (6, 7).

CONFIRMATION OF SYMMETRY

Close examination of the zero level *c* axis Weissenburg photographs showed increased blackening along the general radiation streak in the vicinity of (030), which cast doubt on the existence of a true 2_1 axis. To ascertain the existence of this symmetry element and thereby confirm the space group as $P2_1/n$, two Harker-Patterson sections (8), one on $P(x0z)$ and the other on $P(x\frac{1}{2}z)$, were computed by means of Patterson-Tunell strips (9) and are shown in Figs. 1*a* and 1*b*. It is apparent from the larger peaks on the section $P(x\frac{1}{2}z)$, representing a *b* axis translation component of $\frac{1}{2}$, that this translation component must exist in the crystal; hence the twofold screw axis and therefore the space group $P2_1/n$ were

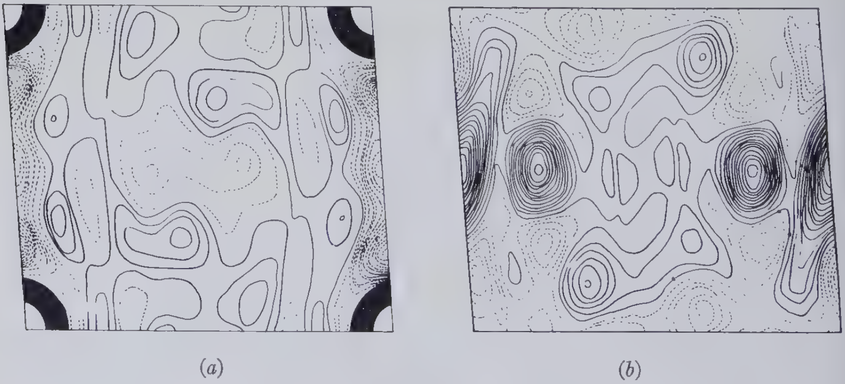
(*a*) (*b*)

FIG. 1. Harker-Patterson sections of claudetite. (*a*) $P\ (x0z)$. (*b*) $P\ (x\frac{1}{2}z)$.

confirmed. The high peak about the origin of the $P(x0z)$ would be present regardless of symmetry since it is the zero vector representing each atom to itself.

LOCATION OF THE ARSENIC ATOMS

The arsenic atoms were located from Patterson projections on the (001) and (100) planes illustrated in Figs. 2 and 3 and from the Harker-Patterson section $P(x\frac{1}{2}z)$ mentioned above. In the latter section one elongated peak appeared, due to the presence of two interactions slightly displaced along the axis of elongation. In order to obtain the center of density of each of these interactions and hence the end of the interatomic distance vectors, two graphical sections were made across one of the other peaks known to be a single interaction, and compared at intervals until it was seen that their sum approximated the elongated peak (Fig. 4). The eight arsenic atoms were found to lie in two general fourfold positions, and the following coordinates were determined: As_{I}, $x=.27$, $y=.10$, $z=.03$; As_{II}, $x=.35$, $y=.35$, $z=.00$. The four equivalent points for the

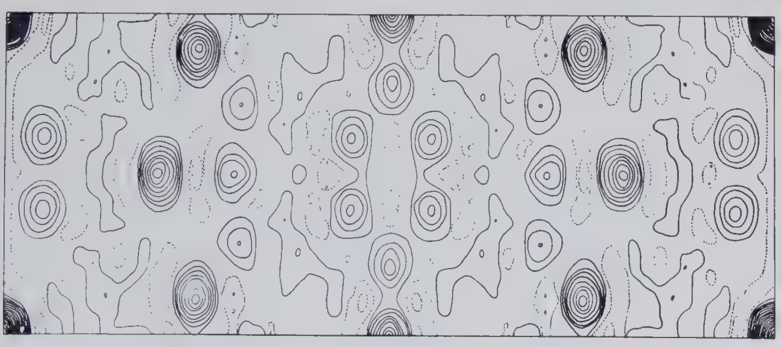

FIG. 2. Patterson projection of claudetite on (001).

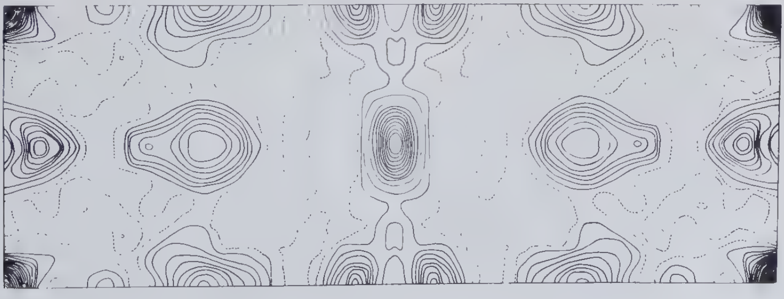

FIG. 3. Patterson projection of claudetite on (100).

general position are: x, y, z; $-x, -y, -z$; $x+\frac{1}{2}, \frac{1}{2}-y, z+\frac{1}{2}$; and $\frac{1}{2}-x, y+\frac{1}{2}, \frac{1}{2}-z$. Not only are all the interactions between arsenic atoms in these locations satisfactorily found on the three vector maps, but also all the sizable peaks on both the Patterson projections can be attributed to interactions between the arsenic atoms. Consequently, it must be assumed that the oxygen-oxygen interactions and the arsenic-oxygen interactions are either masked by arsenic-arsenic interactions or are too comparatively weak to give rise to substantial peaks.

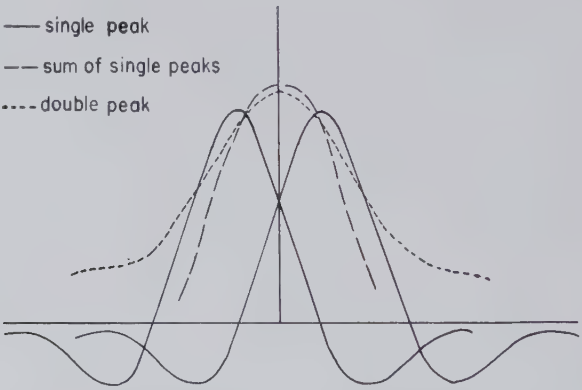

FIG. 4. Graphical sections through single and double Harker-Patterson interaction peaks to determine separation in double peak.

DETERMINATION OF THE OXYGEN PARAMETERS

Electron density projections on (001) and (100) were computed, again by Patterson-Tunell strips, using only those terms whose signs could be unequivocably determined by the arsenic atoms in the locations as found above, the sign determinations being made from the structure factor formula:

$$F_{hkl} = 16 \sum_{n} f_n \cos 2\pi \left(hx + lz + \frac{h+k+l}{4} \right) \cos 2\pi \left(ky - \frac{h+k+l}{4} \right).$$

The Thomas-Fermi scattering factor for heavy atoms and the Hartree scattering factor for light atoms (10) were used in these calculations. Only about 70% of the available reflections were used in constructing these first electron density projections. These projections yielded one possible general fourfold oxygen location, at $x=.45$, $y=.22$, $z=.03$, and its symmetry equivalent. This location permitted the determination of the signs of additional terms which were in turn employed in making additional electron density projections (Figs. 5*a* and 5*b*). Considerable false detail was present about the arsenic peaks in the projections on the (001) and (100) planes.

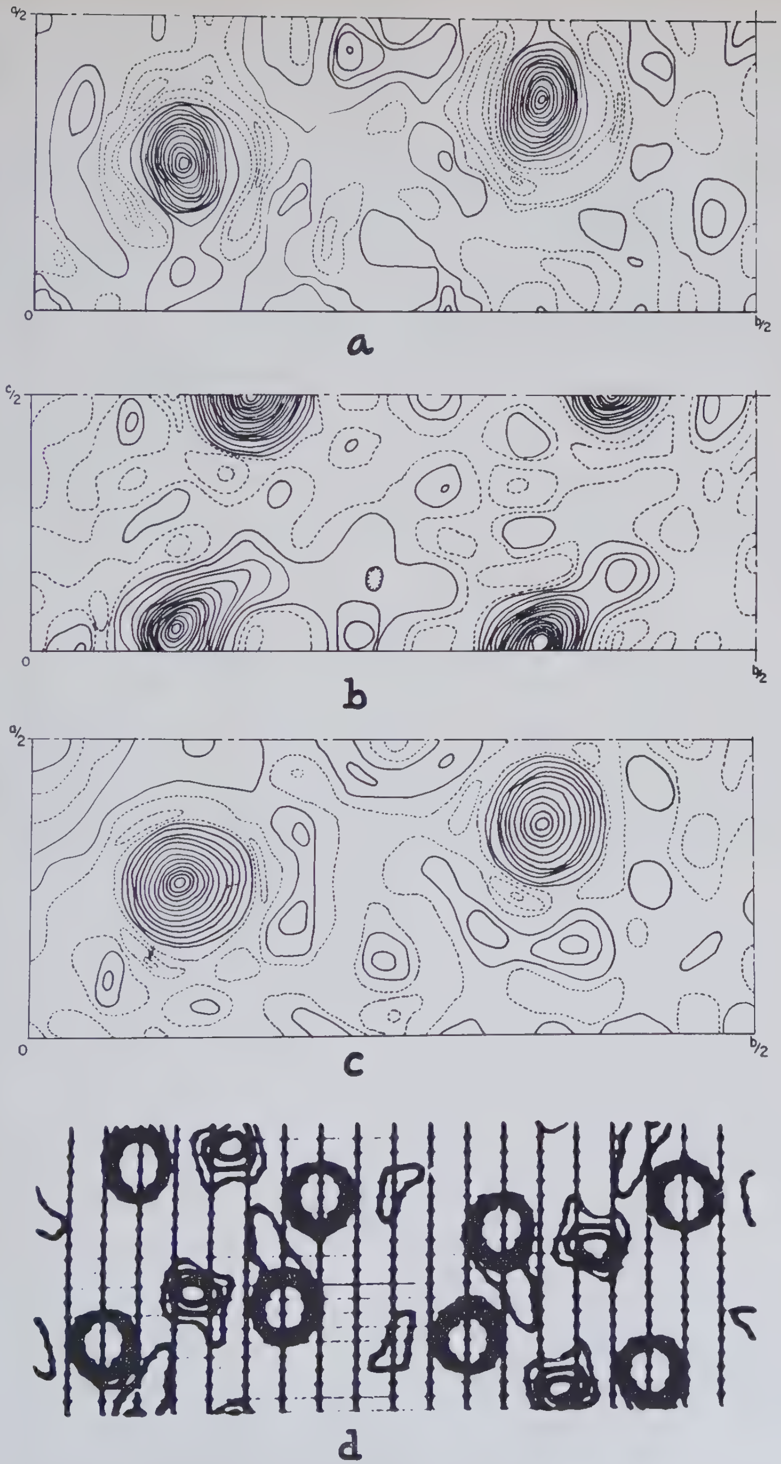

FIG. 5. Electron density projections of claudetite. (*a*) ρ (001) $\frac{1}{4}$ cell. (*b*) ρ (100) $\frac{1}{4}$ cell. (*c*) ρ (001) from calculated arsenic values only. $\frac{1}{4}$ cell. (*d*) ρ (001) from observed values modified by Cesaro Means. Entire cell.

An attempt was made to distinguish between the real oxygen peaks and those peaks due to the false detail about the arsenic atoms. An electron density projection on (001) (Fig. 5*c*) was made using only those terms used in making the same projection as in Fig. 5*a* with F values calculated from the Thomas-Fermi scattering factors of arsenic in the locations determined above. This method was used rather than directly making a difference map (11, 12) expressed by the function:

$$D_{xy} = \rho_0 - \rho_c = \frac{1}{A} \sum_h \sum_k F_0(h0l) - F_c(h0l) e^{2\pi i(hx+ky)}$$

for in the employment of this latter method it would be necessary to determine an atomic form factor, usually expressed in terms of a temperature coefficient, to make the observed values fall off at the same rate as the calculated values. It would also be necessary to scale the F_0 (observed) values with the F_c (calculated) values. By comparing Fig. 5*a* directly with Fig. 5*c* it will be observed that, with the exception of the oxygen peak noted above, most of the peaks on the map made from the observed values are present on the map made from the calculated arsenic values. Therefore, it can be concluded that either the projection of the oxygen peaks coincides with the peaks of arsenic false detail, or the projections of the oxygen peaks are so close to those of the arsenic that they are masked by the arsenic peaks themselves or by the depressions surrounding the peaks. It is also evident that since both maps produced similar amounts of false detail, this false detail can be attributed for the most part to the abrupt termination of the series due to experimental limitations determined by the small cell dimensions in two directions. The application of the temperature factor or absorption corrections would be insufficient to make the Fourier series close.

The series could be made to close falsely by applying the method of the Cesàro means to the coefficients of the series (13). Thus the two-dimensional projection becomes:

$$\rho_{xy} = \frac{1}{A} \sum_h \sum_k F \left(1 - \frac{|h|}{H}\right)\left(1 - \frac{|k|}{K}\right) e^{2\pi i(hx+ky)}$$

where H and K are one greater than the maximum indices h and k used in the series. The results of this series for the (001) projection, as solved by *X-RAC*, are shown in Fig. 5*d*, and it will be noted that the false detail has been removed. Unfortunately, this series exhibits greatly diminished resolving power over the normal series, and any oxygen peaks lying close to arsenics are not resolved. However, the lack of more than one oxygen peak permits the assumption that the other two oxygens lie close to the arsenic in this projection.

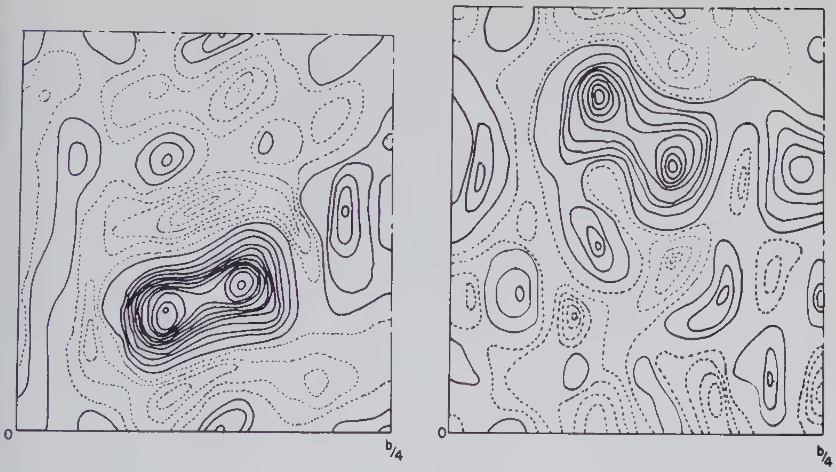

a *b*

FIG. 6. Electron density projections of claudetite. (*a*) ρ (101) $\frac{1}{4}$ cell. (*b*) ρ ($\bar{1}01$) $\frac{1}{4}$ cell.

Electron density projections were then made on the (101) and ($\bar{1}01$) planes (Figs. 6*a* and 6*b*), and from these the remaining oxygen parameters were determined to be approximately: $x=.65$, $y=.40$, $z=.14$; and $x=.94$, $y=.14$, $z=.10$. As the contribution of any one oxygen atom has a negligible effect on the signs of the terms of the Fourier series in the electron density projections, the Fourier technique of parameter refining could not be used. Refining was carried out by a system of comparing observed with calculated intensities. The final parameters are listed in Table 1 and in Table 2. The intensities calculated from these parameters are compared with those observed and corrected.

TABLE 1

	x	y	z
As_{I}	.258	.102	.040
As_{II}	.363	.352	.007
O_{I}	.45	.22	.03
O_{II}	.62	.41	.18
O_{III}	.95	.16	.13

Because the scattering power of arsenic is four times that of oxygen at low angles, increasing to over seven times that of oxygen at higher angles, the oxygen parameters can only be determined with limited accuracy.

TABLE 2*a*. ZERO LEVEL *c* AXIS. OBSERVED DATA FROM EQUI-INCLINATION WEISSENBURG RECORD TAKEN WITH COPPER Kα RADIATION AND CORRECTED FOR LORENTZ AND POLARIZATION FACTORS

Index	Sin θ	$\|F\|$ Calculated	F Observed
0 2 0	.120	4	4
0 4 0	.240	24	17
0 6 0	.360	1	2
0 8 0	.480	8	13
0 10 0	.600	0	0
0 12 0	.719	4	6
0 14 0	.839	0	0
0 16 0	.959	11	18
1 1 0	.159	9	8
1 2 0	.190	4	6
1 3 0	.232	10	8
1 4 0	.281	13	11
1 5 0	.339	3	5
1 6 0	.389	1	2
1 7 0	.445	9	12
1 8 0	.502	19	21
1 9 0	.561	6	7
1 10 0	.617	1	1
1 11 0	.676	2	5
1 12 0	.735	12	23
1 13 0	.794	5	8
1 14 0	.852	1	0
1 15 0	.911	0	0
1 16 0	.971	9	12
2 0 0	.294	10	6
2 1 0	.300	12	12
2 2 0	.317	6	7
2 3 0	.345	1	2
2 4 0	.379	10	12
2 5 0	.420	11	12
2 6 0	.464	7	9
2 7 0	.513	3	4
2 8 0	.563	4	6
2 9 0	.612	8	11
2 10 0	.668	7	11
2 11 0	.722	6	10
2 12 0	.777	1	6
2 13 0	.833	4	6
2 14 0	.889	6	11
2 15 0	.946	6	11

TABLE 2*a* (*Continued*)

Index	Sin θ	$\lvert F \rvert$ Calculated	F Observed
3 1 0	.445	4	2
3 2 0	.457	15	16
3 3 0	.476	8	11
3 4 0	.502	3	5
3 5 0	.533	0	0
3 6 0	.569	10	13
3 7 0	.609	6	9
3 8 0	.651	2	4
3 9 0	.695	3	6
3 10 0	.744	0	0
3 11 0	.794	5	6
3 12 0	.844	3	7
3 13 0	.895	6	10
3 14 0	.948	4	7
4 0 0	.588	0	0
4 1 0	.591	0	0
4 2 0	.600	4	7
4 3 0	.616	3	4
4 4 0	.635	1	0
4 5 0	.660	2	5
4 6 0	.689	11	15
4 7 0	.722	1	0
4 8 0	.759	0	0
4 9 0	.796	1	0
4 10 0	.840	13	18
4 11 0	.884	0	2
4 12 0	.929	0	0
4 13 0	.976	1	1
5 1 0	.738	4	3
5 2 0	.744	13	16
5 3 0	.756	4	2
5 4 0	.773	0	1
5 5 0	.794	3	4
5 6 0	.818	8	9
5 7 0	.846	2	0
6 0 0	.882	4	2
6 1 0	.884	1	0
6 2 0	.890	2	1
6 3 0	.900	0	0
6 4 0	.914	3	0
6 5 0	.932	6	6
6 6 0	.952	7	10
6 7 0	.976	4	5

TABLE 2b. ZERO LEVEL *a* AXIS. OBSERVED DATA FROM PRECESSION RECORD TAKEN WITH MOLYBDENUM Kα RADIATION AND CORRECTED FOR LORENTZ AND POLARIZATION FACTORS

Index	Sin θ	$\|F\|$ Calculated	F Observed
0 2 0	.055	4	—
0 4 0	.111	24	18
0 6 0	.166	1	2
0 8 0	.221	7	7
0 10 0	.277	0	0
0 12 0	.332	4	0
0 14 0	.387	0	0
0 16 0	.442	11	6
0 1 1	.083	3	4
0 2 1	.096	2	3
0 3 1	.114	5	5
0 4 1	.135	2	0
0 5 1	.159	7	7
0 6 1	.184	0	0
0 7 1	.211	13	10
0 8 1	.235	0	0
0 9 1	.260	13	11
0 10 1	.287	0	0
0 11 1	.314	10	6
0 12 1	.341	1	0
0 13 1	.368	9	5
0 14 1	.393	1	0
0 15 1	.422	9	5
0 0 2	.157	23	18
0 1 2	.159	8	8
0 2 2	.166	3	3
0 3 2	.177	3	6
0 4 2	.192	15	12
0 5 2	.209	2	0
0 6 2	.228	1	0
0 7 2	.249	4	5
0 8 2	.271	7	4
0 9 2	.293	1	0
0 10 2	.319	1	0
0 11 2	.342	1	2
0 12 2	.367	2	1
0 13 2	.393	4	2
0 14 2	.418	1	0
0 15 2	.444	1	0
0 16 2	.469	8	2

Table 2*b* (*Continued*)

Index	Sin θ	$\lvert F \rvert$ Calculated	F Observed
0 1 3	.236	0	0
0 2 3	.241	6	6
0 3 3	.249	7	6
0 4 3	.260	3	2
0 5 3	.273	7	6
0 6 3	.288	3	4
0 7 3	.304	12	8
0 8 3	.323	6	4
0 9 3	.341	11	7
0 10 3	.363	0	0
0 11 3	.384	9	6
0 12 3	.407	5	2
0 13 3	.429	8	5
0 14 3	.453	2	0
0 15 3	.477	5	6
0 0 4	.313	12	8
0 1 4	.314	5	3
0 2 4	.318	1	0
0 3 4	.324	5	4
0 4 4	.332	9	5
0 5 4	.342	1	0
0 6 4	.354	1	2
0 7 4	.368	5	5
0 8 4	.384	2	0
0 9 4	.400	4	0
0 10 4	.418	3	0
0 11 4	.437	1	4
0 12 4	.456	0	2
0 13 4	.477	3	2
0 1 5	.393	3	0
0 2 5	.395	5	3
0 3 5	.400	6	5
0 4 5	.407	5	4
0 5 5	.415	3	0
0 6 5	.426	4	0
0 7 5	.437	7	5
0 8 5	.450	9	6
0 9 5	.463	5	5

TABLE 2*c*. SECOND LEVEL *c* AXIS. OBSERVED DATA FROM EQUI-INCLINATION WEISSENBURG RECORD TAKEN WITH COPPER Kα RADIATION AND CORRECTED FOR LORENTZ AND POLARIZATION FACTORS

Index	Sin θ	$\|F\|$ Calculated	F Observed
0 0 2	.340	23	—
0 1 2	.345	8	—
0 2 2	.360	3	2
0 3 2	.384	3	7
0 4 2	.416	15	15
0 5 2	.453	2	2
0 6 2	.495	1	1
0 7 2	.540	5	8
0 8 2	.588	7	8
0 9 2	.636	2	0
0 10 2	.689	2	0
0 11 2	.742	1	3
0 12 2	.796	3	3
0 13 2	.852	4	3
0 14 2	.905	2	0
0 15 2	.961	2	0
1 1 2	.379	2	2
1 2 2	.393	4	3
1 3 2	.415	5	3
1 4 2	.445	7	11
1 5 2	.480	5	6
1 6 2	.519	2	3
1 7 2	.563	10	12
1 8 2	.608	11	19
1 9 2	.655	8	15
1 10 2	.707	0	0
1 11 2	.758	7	8
1 12 2	.812	11	18
1 13 2	.864	6	7
1 14 2	.919	1	0
1 15 2	.974	5	5
$\bar{1}$ 1 2	.370	7	10
$\bar{1}$ 2 2	.385	3	2
$\bar{1}$ 3 2	.412	6	7
$\bar{1}$ 4 2	.437	9	10
$\bar{1}$ 5 2	.473	6	5
$\bar{1}$ 6 2	.513	1	2
$\bar{1}$ 7 2	.557	5	4
$\bar{1}$ 8 2	.603	15	22
$\bar{1}$ 9 2	.649	0	0
$\bar{1}$ 10 2	.702	2	0
$\bar{1}$ 11 2	.754	0	0

TABLE 2c (*Continued*)

Index	Sin θ	|F| Calculated	F Observed
$\bar{1}$ 12 2	.807	12	20
$\bar{1}$ 13 2	.861	1	1
$\bar{1}$ 14 2	.915	1	0
$\bar{1}$ 15 2	.971	2	4
2 0 2	.457	8	10
2 1 2	.460	12	12
2 2 2	.472	6	4
2 3 2	.491	9	8
2 4 2	.516	9	12
2 5 2	.546	8	10
2 6 2	.581	6	6
2 7 2	.620	4	3
2 8 2	.663	3	3
2 9 2	.705	4	3
2 10 2	.754	7	7
2 11 2	.802	1	1
2 12 2	.852	1	3
2 13 2	.904	0	2
2 14 2	.955	6	7
$\bar{2}$ 0 2	.442	11	17
$\bar{2}$ 1 2	.446	10	12
$\bar{2}$ 2 2	.458	2	0
$\bar{2}$ 3 2	.477	0	0
$\bar{2}$ 4 2	.503	10	12
$\bar{2}$ 5 2	.534	9	11
$\bar{2}$ 6 2	.570	2	3
$\bar{2}$ 7 2	.609	5	6
$\bar{2}$ 8 2	.652	4	4
$\bar{2}$ 9 2	.695	8	12
$\bar{2}$ 10 2	.745	4	4
$\bar{2}$ 11 2	.794	8	10
$\bar{2}$ 12 2	.844	2	0
$\bar{2}$ 13 2	.896	5	7
$\bar{2}$ 14 2	.949	4	3
$\bar{2}$ 15 2	.999	8	15
3 1 2	.518	0	0
3 2 2	.588	12	13
3 3 2	.593	4	5
3 4 2	.614	3	3
3 5 2	.640	6	8
3 6 2	.670	9	8
3 7 2	.704	6	7

TABLE 2c (*Continued*)

Index	Sin θ	$\lvert F \rvert$ Calculated	F Observed
3 8 2	.741	3	4
3 9 2	.780	5	10
3 10 2	.824	1	0
3 11 2	.868	8	10
3 12 2	.915	3	4
3 13 2	.963	7	15
$\bar{3}$ 1 2	.551	7	10
$\bar{3}$ 2 2	.565	14	14
$\bar{3}$ 3 2	.576	10	13
$\bar{3}$ 4 2	.598	2	2
$\bar{3}$ 5 2	.624	2	3
$\bar{3}$ 6 2	.655	9	9
$\bar{3}$ 7 2	.690	8	11
$\bar{3}$ 8 2	.728	2	2
$\bar{3}$ 9 2	.767	2	2
$\bar{3}$ 10 2	.812	0	0
$\bar{3}$ 11 2	.857	4	3
$\bar{3}$ 12 2	.904	4	4
$\bar{3}$ 13 2	.953	5	6
$\bar{3}$ 14 2	.999	4	5
4 0 2	.689	1	1
4 1 2	.691	4	5
4 2 2	.699	4	4
4 3 2	.712	5	7
4 4 2	.729	1	0
4 5 2	.751	3	5
4 6 2	.777	6	6
4 7 2	.807	3	4
4 8 2	.839	1	0
4 9 2	.873	0	0
4 10 2	.913	12	21
$\bar{4}$ 0 2	.669	0	2
$\bar{4}$ 1 2	.672	0	1
$\bar{4}$ 2 2	.680	5	6
$\bar{4}$ 3 2	.693	1	0
$\bar{4}$ 4 2	.711	0	0
$\bar{4}$ 5 2	.733	3	4
$\bar{4}$ 6 2	.754	13	15
$\bar{4}$ 7 2	.790	5	3
$\bar{4}$ 8 2	.823	0	0
$\bar{4}$ 9 2	.858	3	3
$\bar{4}$ 10 2	.898	15	21
$\bar{4}$ 11 2	.939	3	4

TABLE 2c (*Continued*)

Index			Sin θ	$\|F\|$ Calculated	F Observed
5	1	2	.822	4	4
5	2	2	.828	12	20
5	3	2	.839	4	2
5	4	2	.854	1	0
5	5	2	.872	4	4
5	6	2	.895	7	8
5	7	2	.921	2	0
5	8	2	.950	0	0
5	9	2	.980	3	3
$\bar{5}$	1	2	.801	0	0
$\bar{5}$	2	2	.808	15	20
$\bar{5}$	3	2	.819	2	0
$\bar{5}$	4	2	.834	0	0
$\bar{5}$	5	2	.854	2	0
$\bar{5}$	6	2	.876	9	10
$\bar{5}$	7	2	.903	3	3
$\bar{5}$	8	2	.932	2	0
$\bar{5}$	9	2	.964	4	2
6	0	2	.955	0	0
6	1	2	.957	1	0
6	2	2	.963	2	3
6	3	2	.972	1	2
6	4	2	.985	0	0
$\bar{6}$	0	2	.934	5	3
$\bar{6}$	1	2	.936	6	5
$\bar{6}$	2	2	.942	2	1
$\bar{6}$	3	2	.952	5	2
$\bar{6}$	4	2	.965	3	0
$\bar{6}$	5	2	.981	6	5
$\bar{6}$	6	2	.999	8	15

DISCUSSION OF THE STRUCTURE

The structure of claudetite can be looked upon as consisting of infinite zigzag chains of

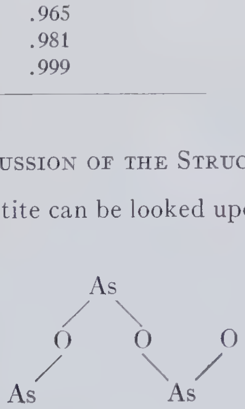

extending in the direction of the *c* axis and being linked together into irregular sheets perpendicular to the *b* axis by additional As-O-As bonds. Thus each arsenic atom is surrounded by three oxygen atoms, and each oxygen has two close arsenic neighbors. The structure is illustrated in Fig. 7.

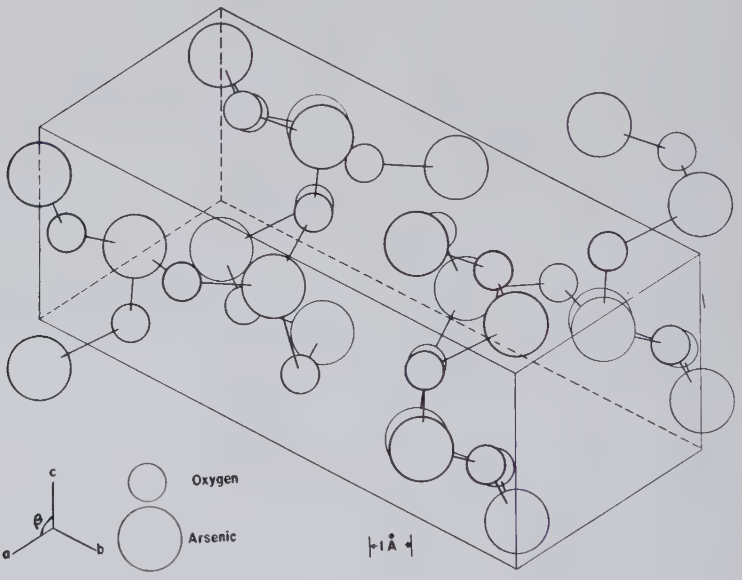

Fig. 7. Crystal structure of claudetite.

Table 3 contains the important interatomic distances.

The As-O distance found in claudetite is the same as the As-O distance of 1.80±.02 Å found in the As_4O_6 molecule in the gaseous state and the distance of 1.80±.05 Å found in arsenolite (14). Because of the difficulty in obtaining accuracy in the determination of the oxygen parameters, it would be misleading to quote any greater accuracy in the O-O parameters than that given in the table. However, it can be seen that the greater density of claudetite over arsenolite can be accounted for by the closer O-O distances. The closest O-O distance in arsenolite is 2.73±.07 Å.

It can be seen that the prominent cleavage and tabular habit of claudetite can be explained by the above structure. The polymorphic relationship between claudetite and arsenolite will be the subject of a future paper.

TABLE 3. SOME IMPORTANT INTERATOMIC DISTANCES IN CLAUDETITE

Atom	Neighbor	Distance
As_I	As_I	3.79
As_{II}	As_{II}	4.07
As_I	As_{II}	3.02
	As_{II}	3.27
	As_{II}	3.30
As_I	O_I	1.82
	O_{II}	1.79
	O_{III}	1.82
As_{II}	O_I	1.77
	O_{II}	1.74
	O_{III}	1.77
O_I	O_{II}	3.0
	O_{II}	2.8
	O_{III}	2.8
	O_{III}	2.4
O_{II}	O_{II}	2.9
	O_{III}	2.8
	O_{III}	2.4

ACKNOWLEDGMENTS

The author is indebted to Professor Martin J. Buerger for his counsel especially during the initial part of the work which was performed in his laboratory in partial fulfillment of the Master's degree at the Massachusetts Institute of Technology. Thanks are also due to Professor R. Pepinsky for suggesting the method of the Cesàro means and for the use of X-RAC. The technical assistance of Anne T. Frueh and W. L. Peterson is gratefully acknowledged.

REFERENCES

1. PALACHE, C., BERMAN, H., AND FRONDEL, C., *Dana's System of Mineralogy*, Seventh Edition, **1**, 195–197 (1944).
2. SCHULMAN, J., AND SCHUMB, W., The polymorphism of arsenic oxide: *Jour. Am. Chem. Soc.*, **65**, 878–883 (1943).
3. BUERGER, M. J., The unit cell and space group of claudetite, As_2O_3: *Am. Mineral.*, **27**, 216 (1942).
4. DAWTON, R., The integration of large numbers of *x*-ray crystal reflections: *Proc. Phys. Soc. London*, **50**, 919–925 (1938).
5. KLEIN, G. E., The crystal structure of nepheline: Master's thesis, Department of Geology, Massachusetts Institute of Technology (1947).
6. BUERGER, M. J., AND KLEIN, G., Correction of *x*-ray diffraction intensities for Lorentz and polarization factors: *Jour. App. Phys.*, **16**, 408–418 (1945).
7. BUERGER, M. J., AND KLEIN, G., Correction of diffraction amplitudes for Lorentz and polarization factors: *Jour. App. Phys.*, **17**, 285–306 (1946).

8. Harker, D., The application of the three-dimensional Patterson method and the crystal structure of proustite and pyrargyrite: *Jour. Chem. Phys.*, **4,** 381–390 (1936).
9. Patterson, A. L., and Tunell, G., A method for the summation of Fourier series used in the *x*-ray analysis of crystal structures: *Am. Mineral.*, **27,** 655–679 (1942).
10. *Inter. Tabellen z. Best. v. Kristallstrukturen*, Band **II,** 571–572 (1935).
11. Finbak, C., and Norman, N., Subtraction of atom images from a Fourier synthesis of a crystal lattice: *Acta Chem. Scand.*, **2,** 813–827 (1948).
12. Cochran, W., The structure of pyrimidines and purines, Part V: *Acta Cryst.*, **4,** 81–92 (1951).
13. Pepinsky, R., The application of Cesàro means and Parseval's relations in the Fourier analysis of crystals: Abst. *Am. Cryst. Assn.*, Winter meeting, Feb., **1951.**
14. Almin, K. E., and Westgren, A., The lattice parameters of the cubic As_2O_3 and Sb_2O_3: *Arkiv for Kemi, Mineralogie och Geologie*, **15B,** No. 22, 1–6 (1942).

Manuscript received May 28, 1951.

STRUCTURAL TRANSFORMATIONS IN AMPHIBOLES AT ELEVATED TEMPERATURES*

MARK WITTELS,** *Massachusetts Institute of Technology, Cambridge, Mass.*

ABSTRACT

A thermal investigation of the amphiboles revealed some structural transformations occurring in three magnesian varieties at about 830° C. *X*-ray and optical methods of analysis were employed in the study of these transitions, in addition to a differential thermal technique that was used for calorimetric determinations.

Magnesian anthophyllite undergoes a reversible crystallographic contraction of about 0.45% in the *c*-axis direction at 830° C. The heat evolved by the transformation is of the order of 3 calories per gram.

At 825° C. tremolite contracts in the *c*-axis direction. The transformation is irreversible and evolves 2.76 calories per gram.

By an *x*-ray method of analysis the approximate axial contractions of richterite near 825° C. were determined. The calculated contractions are $a_0=0.33\%$, $b_0=0.44\%$, and $c_0=0.55\%$. The transformation is not reversible and evolves an undetermined amount of heat. Between the temperatures of 700° C. and 825° C. the average coefficient of linear thermal contraction is 2.8×10^{-5} per deg. C. This coefficient is of the same order of magnitude as the linear coefficients of expansion for many metals.

Further investigation by high temperature *x*-ray, optical, and dilatometric methods are necessary to define the transformations more precisely.

INTRODUCTION

At temperatures below those required for structural disintegration certain species of amphiboles undergo characteristic transformations. Magnesian anthophyllite, tremolite, and richterite are three varieties which exhibit these properties. The chemical analyses of five specimens studied are shown below.

Spec.	Reference	SiO_2	Al_2O_3	TiO_2	Fe_2O_3	MgO	FeO	MnO	Na_2O	CaO	K_2O	H_2O	F	Total
A	CC200A[1]	57.02	1.40	—	—	28.81	8.71	0.09	0.66	1.48	—	1.59	—	99.76
B	U. S. Nat. Mus. No. 13895	n.d.	0.28	n.d.	n.d.	n.d.	3.35	n.d.	n.d.	0.36	n.d.	n.d.	n.d.	—
C	Harvard No. 97956	n.d.	0.13	0.08	n.d.	24.8	n.d.	0.26	—	13.7	n.d.	n.d.	0.27	—
D	Posnjak and Bowen[2]	58.59	0.10	—	—	24.78	—	—	0.12	13.95	0.10	2.31	—	99.95
E	Sundius[3]	57.74	0.37	tr	0.29	23.67	tr	2.40	3.14	9.01	0.64	2.39	0.37	99.86

[1] Rabbitt, J. C., A new study of the anthophyllite series: *Am. Mineral.*, **33**, 263–298 (1948).

[2] Posnjak, E., and Bowen, N. L., The role of water in tremolite: *Am. J. Sci.*, **22**, 203–214 (1931).

[3] Sundius, N., The position of richterite in the amphibole group: *Geol. För. För.*, **67**, 266–270 (1945).

The evidence for describing these transformations was collected by these methods: (1) differential thermal analysis, (2) *x*-ray powder diffraction, and (3) optical studies. This paper is a presentation of the initial investigation of these phenomena.

---

* An investigation as part of a Ph.D. thesis by the author.

** Now at the Oak Ridge National Laboratory, Oak Ridge, Tenn.

MAGNESIAN ANTHOPHYLLITE

The differential thermal analyses in this investigation were made at a heating rate of 30° C. per minute in a furnace evacuated to 1 mm. Hg pressure. Thermal analyses under these conditions revealed a transformation occurring in magnesian anthophyllite at about 830° C. Thermographic curves *A* and *B* in Fig. 1† show a major exothermic reaction at this temperature. The general nature of the reaction peak has the earmarks of a displacive[1] transformation except for the fact that heat is evolved with rise in temperature.

The reaction was not reversed thermographically (by cooling), but this may be due to its proximity to the reaction temperature for structural disintegration. Initial rupturing of a few bonds at temperatures slightly above 850° C. may prevent the thermographic reversal of this transformation.

Quenching experiments failed to indicate that any high form exists above 830° C. and this added to the difficulty in determining the nature of the transformation. The evolution of heat attending the rise in temperature from 800° C. to 850° C. can be explained if the mineral is in a high form at 20° C., but the stability of a high form at this low temperature is very difficult to explain on thermodynamic grounds.

Additional evidence for a structural change at 830° C. was obtained by a high temperature optical examination in the nature of a dilatometric test. A contraction in the direction of the *c*-axis was recorded at 830° C. and was found reversible when the temperature 830° C. was not exceeded. This observation correlates well with the thermographic nonreversibility at slightly higher temperatures. The optical analysis was simple. A single needle of anthophyllite was heated on a platinum resistor and was observed through a microscope as the temperature rose. An eyepiece equipped with a scale enabled the observer to record linear changes. A shrinkage of 0.45% in the *c*-axis direction was recorded at 830° C. The data shown below is in proper sequence reading downward and indicates the reversibility of the transformation when 830° C. is not exceeded.

---

† The endothermic reactions occurring above 1000° C. are the thermographic records of the structural disintegration of the amphiboles. These will be discussed in a later paper which will include a study of some ferrous amphiboles.

[1] Buerger, M. J., The role of temperature in mineralogy: *Am. Mineral.*, **33,** 101–121 (1948).

Specimen	*Temp. °C.* (±10°)	*Length* (*c*)
B	100	100.00
	300	100.00
	500	100.00
	800	100.00
	830	99.55
	775	100.00
	830	99.55
	930	99.55
	1050	99.55

Estimated accuracy ±15%

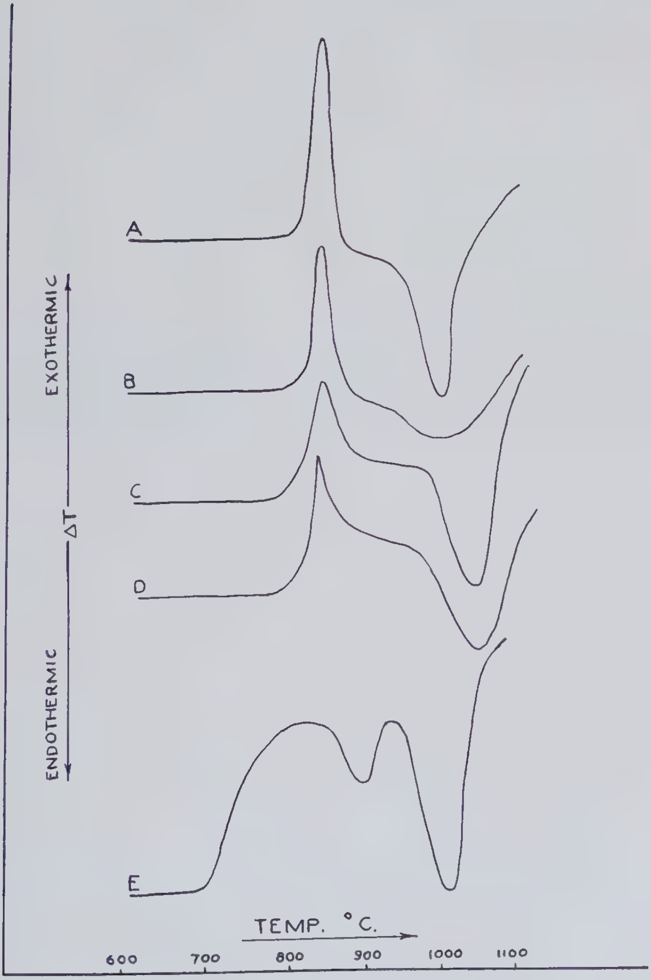

FIG. 1. Thermographic curves of amphiboles.

The thermographic investigation also included the determination of the heat evolved by the transformation. The accuracy of these determinations are high as a direct result of the negligible baseline deviation[2] in the thermographic curves.

Specimen	*Heat Evolved Cal. per gram* (±10%)
A	3.50
B	2.84

The difference in the heat determinations for the two specimens is probably due to slight variations in the chemical compositions.

TREMOLITE

The thermographic curves for tremolite (C and D) reveal a sharp exothermic reaction taking place about 825° C., with a base-line shift at the completion of the reaction. The general configuration of the reaction peaks are similar to the thermal curves showing the alpha→beta quartz inversion; both occur over a narrow range of temperature and are marked by a sharp change in thermal conductivity at the completion of the reaction.

As in the magnesian anthophyllites, the peculiar phenomenon of heat evolution with rise in temperature takes place in the tremolite transformation. In addition, the reaction was not reversed thermographically possibly for the same reason that was applied to the orthorhombic species, namely, the rupturing of some bonds at temperatures slightly above 825° C. Quenching experiments failed to reveal the existence of any high form above 825° C. This, too, paralleled the results for the magnesian anthophyllites.

The high temperature optical examination revealed a contraction in the *c*-axis direction at 825° C. which was not reversed. A shrinkage of 0.65% was observed as indicated by the results shown below.

	Specimen	*Temp. °C.* (±10°)	*Length* (*c*)
	C	100	100.00
		300	100.00
		500	100.00
(Estimated accuracy)		775	100.00
(±15%)		825	99.35
		775	99.35
		825	99.35
		900	99.35
		1050	99.35

---

[2] Wittels, M., The differential thermal analyzer as a microcalorimeter: *Am. Mineral.*, **36**, 615–521 (1951).

The base-line shift in the thermographic curves of tremolite at about 900° C. made precise calorimetric measurements indeterminate. However, by reversing the sequence of area measurement an approximate calorimetric determination was made possible. This was accomplished by extending the base-line at reaction completion to the lower temperature portion of the curve and employing the area thus obtained. The base-line shift also indicated that the measured area would be too small by a factor of about one-half. In order to obtain a more accurate heat of transformation the measured values were multiplied by 1.5. Both specimens evolved 2.76 calories per gram in the reaction as determined by this approximate method. It should be noted that this value is of the same order of magnitude as those obtained in the anthophyllite analysis.

RICHTERITE

At 700° C. richterite (Fig. 1, E) starts to undergo an exothermic transformation that approaches a peak about 825° C. This reaction is not rapid and evolves more heat than the corresponding reaction for tremolite. The reaction is thermographically irreversible even when the peak temperature is not exceeded.

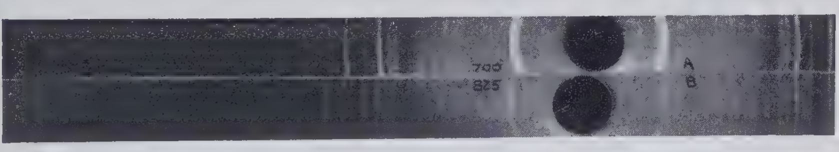

FIG. 2. Camera radius 114.6 mm., ($\mathrm{Cu}_{K\alpha}$ radiation). Forward reflections only. A. Richterite quenched from 700° C. B. Richterite quenched from 825° C.

Quenching experiments established a structural change in the nature of a crystallographic contraction. *X*-ray powder diffraction patterns revealed a slight increase in the values for θ as seen in Fig. 2. In other words, the d spacings were slightly reduced. No new lines appeared nor were any of the original lines extinguished in the patterns of specimens quenched at 825° C. A decrease in the distances between interatomic planes in a crystal results in a volumetric contraction of the crystal structure which can be mathematically evaluated if the values for Δd are known and the various lines indexed. Shinoda[3] derived the equations for the changes in the lattice constants with respect to changes in d for all the crystal systems except monoclinic and triclinic by differentiation of the basic relations for each system. Differentiation of the formula for the monoclinic system

---

[3] Shinoda, G., *X*-ray investigations on the thermal expansion of solids: *Mem. Coll. of Sci., Kyoto Imp. Univ. A*, **16**, 193 (1933).

$$d_{hkl} = \frac{1}{\sqrt{\dfrac{\dfrac{h^2}{a^2} + \dfrac{l^2}{c^2} - \dfrac{2hl \cos \beta}{ac}}{\sin^2 \beta} + \dfrac{k^2}{b^2}}}$$

obviously results in a complex and unwieldy expression due to the presence of the radical and the β terms.

Since x-ray powder diffraction patterns do not give a high order of precision, an approximate method was employed in the determination of the changes in the lattice constants of richterite at 825° C. Although there are four constants in the monoclinic crystals, a, b, c, and β, only the axial changes were calculated. Two assumptions were made in this approximate method:

(1) Since the tables compiled by Strunz[4] do not include the cell constants for richterite, the constants for tremolite were substituted: $a_0 = 9.78$ Å, $b_0 = 17.8$ Å, $c_0 = 5.26$ Å, and $\beta = 106°2'$.

(2) The crystal was assumed to be orthorhombic because β approaches 90°.

The last assumption did not introduce any large error into the analysis and permitted the use of Shinoda's equation for the thermal expansion of orthorhombic crystals:

$$\frac{\Delta d}{d} = \frac{1}{\dfrac{h^2}{a^2} + \dfrac{k^2}{b^2} + \dfrac{l^2}{c^2}} \left[\frac{h^2 \Delta a}{a^2 a} + \frac{k^2 \Delta b}{b^2 b} + \frac{l^2 \Delta c}{c^2 c} \right].$$

By using this formula and the assumptions above the following changes were derived:

(hkl)	$d_{700°\text{C.}}$	$d_{825°\text{C.}}$	Δd	$-\Delta a$	$-\Delta b$	$-\Delta c$
(300)	3.1367	3.1260	0.0107	0.033361	0.072548	0.028815
(550)	1.6548	1.6489	0.0059			
(003)	1.5882	1.5795	0.0087			

				Axial contractions in %		
	a_0	b_0	c_0	a_0	b_0	c_0
(Axes in Å)	9.78	17.8	5.26	0.33	0.44	0.55

The axial contractions are of the same order of magnitude as those for magnesian anthophyllite (0.45%) and tremolite (0.65%). The systematic and random errors of the analysis make the accuracy of the determination ±25%.

---

[4] Strunz, H., Minerallen Tabellen, Leipzig, (1941).

Becker[5] gives the following expression for the average linear thermal coefficient of expansion of a solid by the x-ray powder diffraction method:

$$1 + \alpha(t_2 - t_1) = \frac{\sin \frac{\theta_1}{2}}{\sin \frac{\theta_2}{2}}$$

α is the average coefficient of linear thermal expansion between temperatures t_1 and t_2, θ_1 is the angle at t_1, and θ_2 is the angle at t_2. This equation is employed here for the determination of the average linear thermal coefficient of contraction.

(hkl)	700° C.		$\Delta\theta/2$	825° C.		$1+\alpha(t_2-t_1)$
	$\theta_1/2$	$\sin \theta_1/2$		$\theta_2/2$	$\sin \theta_2/2$	
(300)	7° 6.4′	0.12398	0°1.5′	7° 7.9′	0.12414	0.99871
(550)	13°52.1′	0.23969	0°3′	13°55.1′	0.24054	0.99646
(003)	14°30′	0.25038	0°5.3′	14°35.3′	0.25188	0.99402
Average						0.99639

Average coefficient of linear thermal contraction is

$$\alpha = \frac{0.99639 - 1.00000}{825 - 700} = 2.8 \times 10^{-5} \text{ per deg. C.}$$

The significance of this coefficient is more apparent when one realizes that the coefficient of linear thermal expansion is of the order of magnitude of 10^{-5} per degree Centigrade in many metals.

Discussion

The similarities in the thermal behavior of these minerals are characteristic. The temperature range, the heat of transformation, and the degree of contraction, are the features which make this comparison striking. All of the transformations occur near 825° C. For two varieties the heat of reaction was of the order of 3 calories per gram. This heat determination may be compared with the heat of transformation in the $\alpha \rightarrow \beta$ quartz inversion, which is of the same order of magnitude. Calculated and observed values of linear thermal contraction were of the order of 0.50% for all three species.

Of equal interest is the fact that these minerals are of metamorphic origin and of comparable chemical composition. They are magnesian-type amphiboles that are sesquioxide-poor. However, it was seen that the presence of considerable FeO (Spec. A, 8.71%) did not interfere with the transformation or prevent it from occurring. Also, other notable constituents did not hinder or prevent the changes from taking place. These are CaO, MnO, and Na_2O.

---

[5] Becker, K., Eine röntgenographische Methode zur Bestimmung des Wärmeausdehnungskoeffizienten bei Hohen Temperaturen: *Z. Physik*, **40**, 37 (1926–7).

The transformations give an indication of being very closely related to the silicon-oxygen double-chains, since all the specimens are free, comparatively, from Al^{+++} substitution in those chains. What significance all this may have from a general mineralogic or geologic viewpoint is uncertain with the small amount of evidence on hand at present. The crystallization temperature of these minerals, below 825° C., only confirms information that is already well-known.

Three additional methods of analysis should help to clarify some of the problems encountered in this investigation. These are (1) high temperature *x*-ray studies, (2) investigation of optical properties at elevated temperatures, and (3) dilatometric tests at transition temperatures on good single crystals.

The results of this investigation indicate that perhaps many important thermal properties of the common rock-forming minerals have been overlooked through the absence of sensitive thermal apparatus.

ACKNOWLEDGMENTS

The mineral samples, without which this investigation could not have been made, were kindly given to the author by Doctors N. Sundius, H. S. Yoder, Jr., J. C. Rabbitt, E. P. Henderson, and by Professor C. Frondel.

Manuscript received March 27, 1951.

CHLORITOID FROM RAWLINSVILLE, LANCASTER COUNTY, PENNSYLVANIA

ANNA HIETANEN,[1] *U. S. Geological Survey, Washington, D. C.*

ABSTRACT

Chloritoid occurs in a mica schist near Rawlinsville, Pa. Measurements on the universal stage showed that most chloritoid flakes from this area are monoclinic with $X=b$, but some are triclinic. Polysynthetic twinning on (001), which is also the direction of cleavage, is common. The new twinning axes, [210], [120] and [310], in addition to the known axes, [110] and [130], were measured.

A chloritoid from South Carolina also shows both monoclinic and triclinic symmetry, the monoclinic variety having $Y=b$.

The indices of refraction of chloritoid from Lancaster County are as follows: $\alpha=1.719$, $\beta=1.721$ and $\gamma=1.725$, all ± 0.001. The formula calculated for the Lancaster County material on the basis of a chemical analysis is: $(\mathrm{Fe}'', \mathrm{Mn}, \mathrm{Mg})_{1.9}(\mathrm{Fe}''', \mathrm{Al})_{2.2}(\mathrm{Al}_{1.9}\mathrm{Si}_{2.1})\mathrm{O}_{10.4}(\mathrm{OH})_{3.7}$, in which $\mathrm{Fe}'':\mathrm{Mn}:\mathrm{Mg}=1.37:0.07:0.48$, and $\mathrm{Fe}''':\mathrm{Al}=0.2:2.0$.

INTRODUCTION

The descriptions of the optical properties of the chloritoids found in the literature are rather controversial. There is considerable doubt whether this mineral shows varying optic orientations when monoclinic and whether or not a triclinic form exists.

The present writer collected a hand specimen of chloritoid schist near Rawlinsville, Lancaster County, Pa., in December 1939. The chloritoid was studied optically and chemically in the Institute of Geology at the University of Helsinki during the following winter. A study of the twinning was undertaken later. Careful measurements of this mineral on the universal stage and of a chloritoid from Chesterfield County, S. C., seem to suggest that the mineral can be either monoclinic with X or $Y=b$, or triclinic.

X-ray study of the recorded triclinic forms would be necessary to prove the true symmetry.

OCCURRENCE

Chloritoid occurs as dark aggregates in a pinkish white schist at a road cut a mile east of Rawlinsville in southern Lancaster County, Pa. (the locality is the same as mentioned on p. 121 in Cloos and Hietanen, 1941). The specimen used for investigation is medium grained and contains abundant chloritoid. The chloritoid flakes range from 2 to 3 mm. in diameter and show the usual radiating arrangement. Chloritoids from the schists in the Appalachian area have been described from Dutchess County, N. Y., by Barth and Balk (1934) and from the Deep River region in North Carolina by Stuckey (1926). Milne (1949) recently made a detailed study including x-ray determinations, of a chloritoid from Megantic County, Quebec.

---

[1] Publication authorized by the Director, U. S. Geological Survey.

THE CHLORITOID SCHIST

The muscovite-chlorite schist in which the chloritoid occurs as newly crystallized aggregates is fine grained and was strongly deformed prior to the crystallization of the chloritoid. A minute, intense wrinkling of the early muscovite flakes and the fracture cleavage are easily visible under the microscope (Figs. 1 and 2). Some newly crystallized muscovite flakes ranging from $\frac{1}{2}$ to 1 mm. in length grow across the older wrinkled ones. Chlorite also is found in two generations; the older small flakes occur with the early muscovite, whereas the later larger flakes are grouped around the chloritoids.

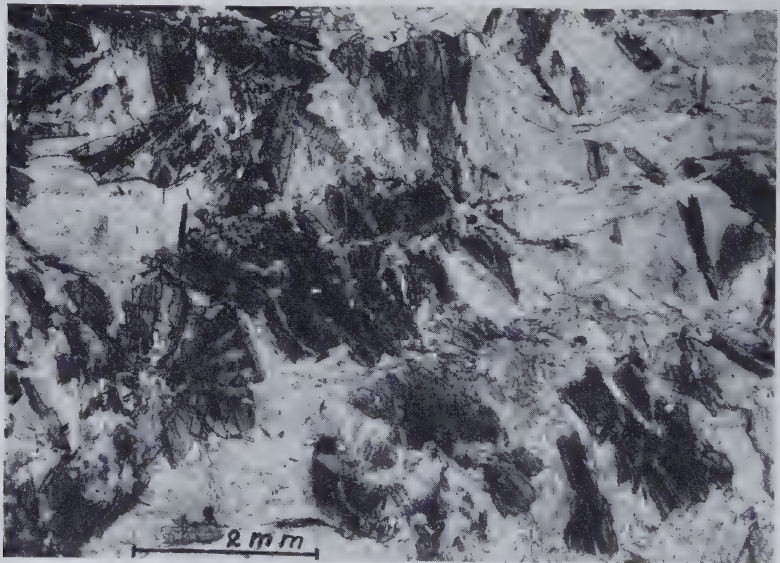

FIG. 1. Chloritoid schist near Rawlinsville, Lancaster County, Pennsylvania. The dark mineral is chloritoid.

Tiny twinned grains and prisms of rutile occur as inclusions throughout the rock. Their orientation indicates them to be early: they follow the wrinkled texture shown by the muscovite, even when they are included in chloritoid. Larger prisms are later: they follow shear planes and irregular surfaces which probably represent healed cracks. As a rule the late muscovite and chlorite are free of the rutile inclusions. Thus the sequence of crystallization was as follows:

First stage: rutile I, muscovite I, chlorite I.
Second stage: chloritoid, muscovite II, chlorite II, rutile II.

The amount of quartz in the schist varies considerably even in the hand specimen. It may range from about 10 to 60 per cent. A few small albite grains occur as an additional constituent. The chemical and mineralogical composition of the chloritoid schist is shown in Table 1. The amounts of K_2O and Na_2O are small and the amount of FeO is large compared with the amounts shown by analyses of surrounding biotite schist and muscovite-chlorite schists (see tables of analyses in Cloos and Hietanen, 1941). The crystallization of chloritoid instead of chlorite is mainly due to this difference in the chemical composition.

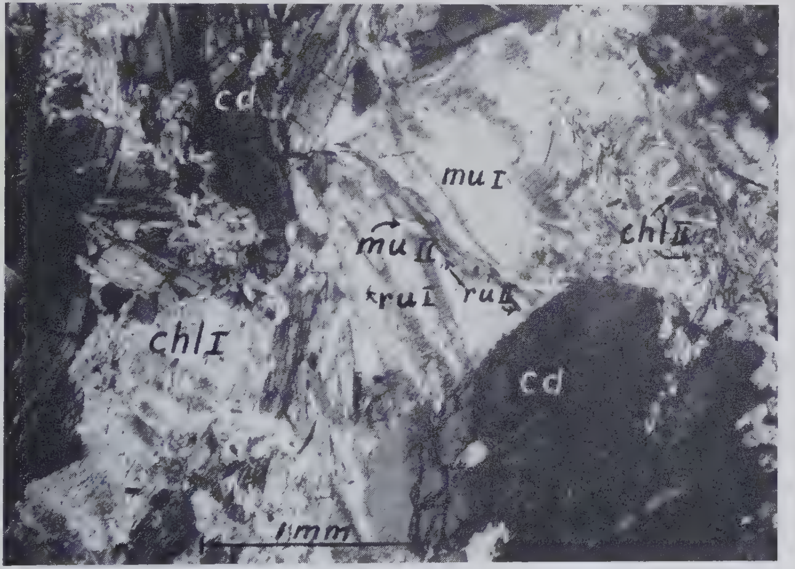

Fig. 2. Twinning in chloritoid (cd) from Lancaster County. Second generation muscovite (mu II), chlorite (chl II), and rutile (ru II) transect the older wrinkled muscovite (mu I) and chlorite (chl I).

Chloritoid is usually considered to be a stress mineral and appeared to be so in other nearby localities in Lancaster County and the Norristown quadrangle, Pa. (Cloos and Hietanen, 1941, pp. 122, 123, 152, and Table 15). At Rawlinsville, however, the largest flakes occur next to the quartz veins and they are clearly crystallized after the shearing movements, which caused the microfolding of the micas. Probably the chloritoid at this locality crystallized also at an earlier stage, as it did in the

Table 1. Chemical and Mineralogical Composition of the Muscovite-chlorite-chloritoid Schist at Rawlinsville, Lancaster County, Pa.

Analyzed by Miss Elsa Ståhlberg

SiO_2	70.12	quartz	56
TiO_2	0.67	chloritoid	26
Al_2O_3	15.48	muscovite	11
Fe_2O_3	0.68	chlorite	5
FeO	5.98	albite	1
MnO	0.23	rutile	1
MgO	2.17		
CaO	0.16		100
Na_2O	0.33		
K_2O	0.99		
P_2O_5	0.00		
H_2O+	2.88		
H_2O-	0.32		
	100.01		

surrounding schists (Cloos and Hietanen, 1941, p. 119) and recrystallized later as large flakes under the influence of the watery solutions, which deposited the vein quartz. The occurrence is comparable with the one described by Friedlaender (1930) from Crestlianderstobel, Switzerland, where large recrystallized chloritoid flakes occur in later quartz veins which show only minor traces of strain. Friedlaender, in accord with Riecke (1895), assumes that the chloritoid has a greater solubility under stress. It therefore might go into solution under stress and is redeposited in places of less stress. Some other stress minerals, as for instance kyanite, are found in quartz veins which were deposited toward the end of or after the shearing movements (Hietanen, 1938, pp. 90–91). Therefore, stress does not seem to be essential for the formation of these minerals, but unlike the anti-stress minerals, they are stable also under stress. Chloritoid, like many other minerals which may occur as porphyroblasts, seems to stay mobile until the late stages of recrystallization.

Chloritoid

General appearance. The chloritoid flakes grow across the old structure, which is somewhat disturbed in the immediate surroundings of the flakes. A part of each flake, commonly a part of the rim, is free of relict rutile inclusions. The flakes show one good cleavage, poor parting, and polysynthetic twinning.

Optical properties. The pleochroism of the chloritoid from Lancaster County is similar to that described in the literature for chloritoids in general (Winchell, 1933): X = green, Y = blue, Z = colorless. Absorption is thus Y>X>Z. Z makes an angle of 13° with the pole of (001). The indices of refraction determined in immersion liquids are as follows:

$$\alpha = 1.719 \pm 0.001$$
$$\beta = 1.721 \pm 0.001$$
$$\gamma = 1.725 \pm 0.001$$

The optic angle was measured by universal stage, $2V = 56° \pm 2°$. These properties are closest to those determined by Milne for the chloritoid from Megantic County except for lower birefringence and somewhat smaller optic angle. The birefringence is $\gamma - \alpha = 0.006$, the same as found by Barth and Balk (1934) for the chloritoid from Dutchess County.

Twinning and optic orientation of chloritoid. The composition face of the twinning lamellae is parallel to the basal cleavage. Two sets of twinning lamellae show an inclined extinction. The optic orientation of several flakes showing distinct lamellae were measured and the results are shown in Figs. 3, 4, and 5. Figures 3 and 4 show monoclinic symmetry with $X = b$, but Fig. 5 shows triclinic symmetry.

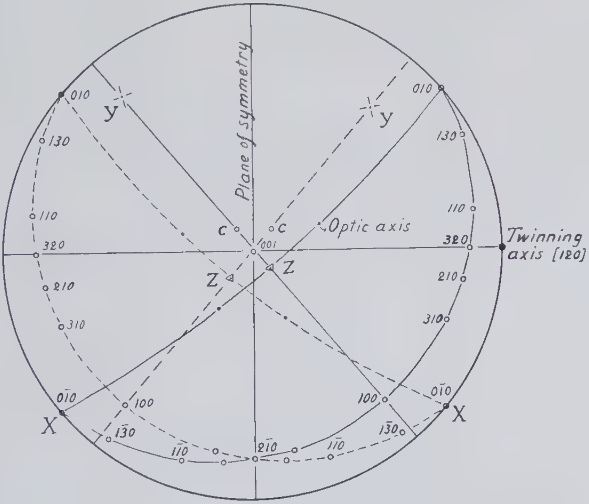

FIG. 3. Optic orientation of the two twinned lamellae in a chloritoid from Lancaster County. The twinning axis is the zone-axis [120]. $X = b$, $c = c$ axis.

If the cell dimensions measured by Milne (1949) are assumed to hold for the monoclinic varieties, the twinning law shown in Fig. 3 is as follows: The composition face is the base (001), the twinning axis is a line of intersection between the base and the face (210), and is the zone-axis [120]. Figure 4 shows a different law; namely that the twinning axis is a

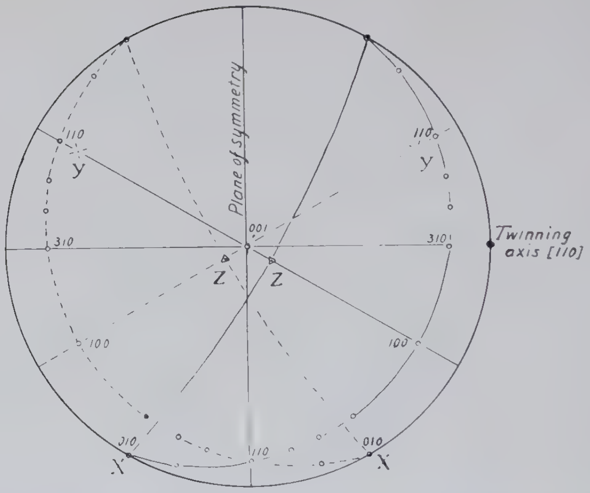

FIG. 4. Orientation of two sets of twinning lamellae in a chloritoid from the same thin section as Fig. 1. Twinning axis is [110]. $X=b$.

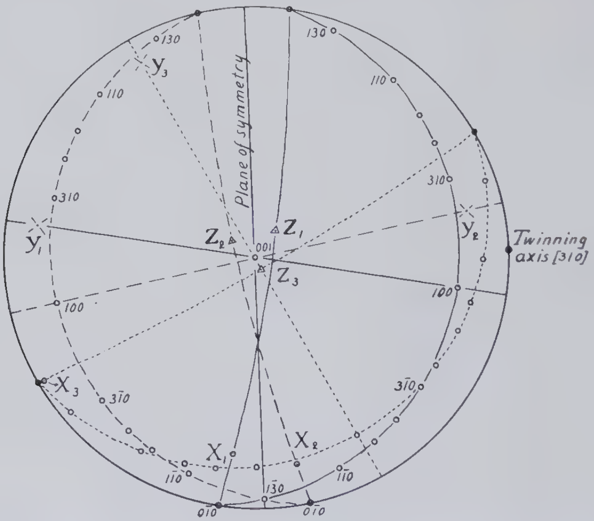

FIG. 5. Orientation of three sets of lamellae in a chloritoid from Lancaster County. Two sets are clearly triclinic and twinned; the third set is very nearly monoclinic.

line of intersection between the base (001) and the face (110), and is the zone-axis [110]. In Fig. 3 the zone-axis [230] in one set of lamellae falls over [230] in the other set of lamellae. In Fig. 4 the two zone-axis [130] in each set of lamellae coincide and lie in the plane of symmetry (Pl. S. in Fig. 4). The twinning axis [210] also was measured.

Figure 5 shows measurements of three sets of lamellae parallel to the cleavage. Two sets are twins and are clearly triclinic, whereas the third set is nearly monoclinic and is intergrown with the others parallel to the base. The twinning axis would probably be the zone-axis [310].

For comparison a number of twinned chloritoid flakes from a chloritoid schist from Chesterfield County, S. C., were measured on the universal stage. The thin section was kindly lent to the author by Miss Jewell Glass, who had determined the optical properties, finding some flakes to be optically negative. In some grains she suspected a triclinic symmetry. Measurements on the universal stage confirmed these properties and it appeared that here also, as in Lancaster County, both monoclinic and triclinic symmetry occur in various sets of lamellae of a twinned crystal. The twinning on a flake with three sets of lamellae is shown in Fig. 6. This twinning is comparable with the one shown in Fig. 4 but the optic orientation is different, Y being parallel to *b*. The twinning axis is [110]. The composition face is (001) as usual.

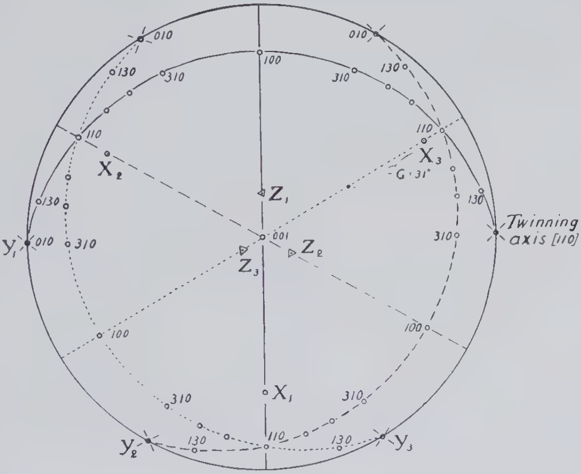

FIG. 6. Orientation of three sets of twinned lamellae in a chloritoid from Chesterfield County, South Carolina. This grain is optically negative, has $Y=b$, and the twinning axis is the zone-axis [110].

These measurements show that the optic orientation and the twinning laws of the chloritoid may vary even in the same thin section. Various orientations have been described in the literature. Barth and Balk (1934) measured 30 chloritoid flakes in a chloritoid schist from Dutchess County, N. Y., and found that all showed Y parallel to the cleavage (001), thus $Y=b$. The angle between the optic planes of the twinned individuals is 60° in their diagram, and the twinning axis is [110].

Simpson (1915) reports a similar orientation Y = b from Yampi Sound, Australia. Shannon (1926) described a chloritoid with X = b from Lemhi County, Idaho. The chloritoid from the Champion mine, Michigan, was first reported by Lane, Keller, and Sharpless (1891) to be triclinic with X near the cleavage plane and Y making an angle of 20° with it. Milne (1949) restudied the mineral, but failed to give a direct comment about the optic orientation. He described in the same paper a chloritoid with X = b from Megantic County, Quebec, and established the optic orientation in this mineral by x-rays and universal stage. The twinning axis in the Quebec mineral is, according to Milne, the zone-axis [130]. Thus the pole of (310) face would fall over the pole of (310) of the other individual and the angle between the optic planes would be about 120°.

X-ray study. A powder pattern of the chloritoid from Lancaster County was made by Fred A. Hildebrand. The data (Table 2) compare well with that of the known chloritoids.

Chemical composition. The chloritoid was separated from the schist

TABLE 2. *X*-RAY POWDER DATA OF CHLORITOID FROM RAWLINSVILLE, LANCASTER COUNTY, PENNSYLVANIA

I	*d* (meas.)	*I*	*d* (meas.)
1	8.9	3	2.12
5	4.90	1	2.07
3	4.68	3	2.04
10	4.44	½	1.982
1	3.80	2	1.878
1	3.58	½	1.857
1	3.53	½	1.836
1	3.41	2	1.798
3	3.26	1	1.744
2	3.08	1	1.723
6	2.97	1	1.702
1	2.92	1	1.687
3	2.76	2	1.646
4	2.69	1	1.629
3	2.63	1	1.597
3	2.48	6	1.579
3	2.45	4	1.561
5	2.36	3	1.551
1	2.33	½	1.504
5	2.31	½	1.496
1	2.25	4	1.482
1	2.22	1	1.463
1	2.18	½	1.442
		3	1.403

by means of Clerici solution. The fraction with a specific gravity from 3.517 to 3.522 was used for the chemical analyses. The mineral was clean except for minute rutile inclusions. Therefore the true composition of the chloritoid (Anal. 2, Table 3) was calculated after subtracting TiO_2 and H_2O- from the original analysis (Anal. 1, Table 3). The relative number of atoms contained in a chloritoid molecule was calculated on the basis of the corrected analysis. Using the structural formula suggested by Milne (1949), the composition of the chloritoid from Lancaster County would be as follows: $(Fe'', Mn, Mg)_{1.9}\ (Fe''', Al)_{2.2}\ (Al_{1.9}Si_{2.1})\ O_{10.4}(OH)_{3.7}$, in which $Fe'':Mn:Mg = 1.37:0.07:0.48$ and $Fe''':Al = 0.2:2.0$. This is close to the assumed ideal formula: $(Fe'', Mg)_2(Al, Fe''')_2(Al_2Si_2)O_{10}(OH)_4$.

TABLE 3. CHLORITOID FROM RAWLINSVILLE, LANCASTER COUNTY, PENNSYLVANIA
Analyzed by Miss Elsa Ståhlberg

	1	2	Atomic ratios for analysis 2		
SiO_2	24.90	25.12	Si	2.09	4.00
TiO_2	0.63	—	Al	3.95	
Al_2O_3	39.93	40.25	Fe'''	0.20	2.24
Fe_2O_3	3.20	3.22	Fe''	1.37	
FeO	19.44	19.62	Mn	0.07	1.92
MnO	1.04	1.05	Mg	0.48	
CaO	0.00	0.00	K	0.01	
MgO	3.85	3.89	OH	3.75	
Na_2O	0.00	0.00	O	10.46	
K_2O	0.09	0.09			
H_2O+	6.70	6.76			
H_2O-	0.14	—			
	99.92	100.00			

Comparison of the earlier published chemical analyses of chloritoid shows that there is very little variation in the chemical composition of this mineral in spite of the considerable variation of the optical properties. A slight decrease in the indices of refraction can be observed with increasing amounts of Mg replacing the Fe.''

CONCLUSIONS

Chloritoid may be either triclinic or monoclinic with varying orientation. $X = b$ has been reported from Lemhi County, Idaho (Shannon, 1926); Megantic County, Quebec (Milne, 1949); and Lancaster County, Pa. (this paper). Y = *b* is reported from Dutchess County, N. Y. (Barth and Balk, 1934); from Yampi Sound, Australia (Simpson, 1915); and from Chesterfield County, S. C. (this paper). Both monoclinic and triclinic symmetry occur together at certain localities. In the monoclinic chloritoid where X or Y coincide with *b*, the two other axes have a variable position in the plane of symmetry. The angle between Z and the pole of (001) varies even in the twinned individuals. The smallest measured value for this angle was 4° and the largest 50°, and both occurred on the chloritoid from South Carolina. 2V is highly variable in the same mineral and either Z or X may bisect the acute angle. Polysynthetic twinning is common. The composition face is always (001), and the twinning axis lies parallel to the composition face. Its direction in this face, however, varies.

A more thorough study of chloritoids from various localities will be necessary to establish the relations between the two monoclinic varieties (X = *b* and Y = *b*) and a triclinic form.

REFERENCES

BARTH, T. F. W., AND BALK, ROBERT, 1934, Chloritoid from Dutchess County, New York: *Am. Mineral.*, **19**, no. 8, 345–350.

CLOOS, ERNST, AND HIETANEN, ANNA, 1941, Geology of the "Martic Overthrust" and the Glenarm series in Pennsylvania and Maryland: *G. S. A., Special Paper* **35**, 207 p.

FRIEDLAENDER, C., 1930, Der Chloritoid vom Crestlianderstobel: *Schweiz. Min. Pet. Mitt.*, **9**, 247–264.

HIETANEN, ANNA, 1938, On the petrology of Finnish quartzites: *Comm. Geol. Finl., Bull.* **122**, 118 p.

LANE, A. C., KELLER, A. F., AND SHARPLESS, F. F., 1891, Notes on Michigan minerals: *Am. Jour. Sci.*, **42**, 499–508.

MILNE, I. H., 1949, Chloritoid from Megantic County, Quebec: *Am. Mineral.*, **34**, nos. 5 and 6, 422–434.

RIECKE, E., 1895, Über das Gleichgewicht zwischen einem festen homogenen deformierten Körper und einer flüssigen Phase: *Ann. d. Physik*, **54**, 731–738.

SHANNON, EARL V., 1926, The minerals of Idaho: *U. S. Nat. Mus., Bull.* **131**, 1–483.

SIMPSON, E. S., 1915, On chloritoid and its congeners: *Geol. Surv. W. Australia, Bull.* **64**, 64–78.

STUCKEY, J. L., 1926, Chloritoid from the Deep River region, North Caroloina: *Am. Mineral.*, **11**, no. 7, 186–188.

WINCHELL, A. N., 1933, Elements of Optical Mineralogy. Wiley & Sons, New York, 459 p.

Manuscript received May 28, 1951.

THE GEOLOGY AND PARAGENESIS OF THE LORD HILL PEGMATITE, STONEHAM, MAINE

H. H. Woodard, *University of Chicago, Chicago, Illinois*

Abstract

A field and laboratory study of the Lord Hill pegmatite, Stoneham, Maine, indicates that the pegmatite magma was mechanically injected into diorite country rock but that small amounts of quartz, muscovite, and microcline were introduced to the country rock producing a two-foot wide granitized halo around the pegmatite. Partial assimilation of the wall rock has contaminated and chemically altered at least the outermost zone of the pegmatite.

The internal structure consists of zones, replacement bodies, and fracture and cavity fillings. Three zones are recognized: border zone (outermost), wall zone, and core (innermost). Replacement bodies of cleavelandite and perthite are restricted to the core. Fracture and cavity fillings are numerous both in replacement bodies and in unreplaced core.

Twenty-four minerals have been identified, and their paragenetic relations determined.

Introduction

The Lord Hill pegmatite is one of a group of pegmatites of the Paris-Rumford district, in southwestern Maine. The general features of the Paris Rumford pegmatites have been described by Bastin (1911) and Sterrett (1923). The Lord Hill pegmatite lies at an elevation of 1,240 feet and caps the summit of Lord Hill, located in the north-central part of the north-west ninth of the Fryeburg, Maine, quadrangle.

Intermittent mining of the Paris-Rumford pegmatites for gem stones, feldspar, and mica has been carried on for a period of about eighty years. No appreciable development of the Lord Hill pegmatite was carried out until the summer of 1947. At this time the Whitehall Company prospected the pegmatite for concentrations of block perthite. The total amount of feldspar removed during operations now lies in a stockpile on the main dump and does not exceed 5,000 tons. There appears to be no commercial concentration of book muscovite in the pegmatite.

Field work consisted of making an extensive collection of specimens in 1947 while prospecting operations were still in progress. The pegmatite was mapped with plane table and telescopic alidade in September 1948 and the zoning of the pegmatite was studied at this time (Pl. 1).

The writer is indebted to Dr. A. H. McNair of Dartmouth College for proposing the present study and for supervising the field work. Valuable criticism of the laboratory work, along with a critical review of the manuscript, was made by Dr. J. B. Lyons and Dr. R. E. Stoiber, both of Dartmouth College. The author also wishes to thank Mr. C. E. Ferrin for his expert assistance in the field.

STRUCTURAL FEATURES

General statement. Exposures of pegmatite in the Paris-Rumford district are confined chiefly to a roughly circular area of approximately 1,400 square miles which lies on the east side of the White Mountains. The district is in rough country formed of many low mountains and hills, with many lakes and ponds in the intervening depressions. Many of these hills are capped with pegmatite. Dale (1923) has classified the country rocks as metamorphosed sediments and volcanics of early and middle Paleozoic age(?). These are cut by extensive bodies of granites and granodiorites of middle and late Paleozoic age(?). Bastin (1911) finds that most of the pegmatites of the district are confined to schistose country rocks. Some, however, are found within bodies of granite or other intrusions; the Lord Hill pegmatite, for example, occurs within a diorite body of local distribution.

General structure of the pegmatite. The Lord Hill pegmatite is roughly circular in plan with the east-west outcrop diameter approximating 1,500 feet and the north-south outcrop diameter approximating 1,000 feet.

Contact of the pegmatite with wall rock is poorly exposed except on the southwestern border near the two main cuts where it is concordant with a poorly-defined foliation in the country rock (Pl. 1). In the small southwestern cut, however, the contact is distinctly discordant. At all the exposed contacts the pegmatite appears to dip outward at angles of 60 degrees or more. The author is of the opinion that these dips are not representative of the actual form of the pegmatite. Recent studies show that internal structure is a more reliable criterion for determining attitude, owing to the irregular shape of many pegmatites. That the Lord Hill pegmatite is probably a relatively flat-lying sheet is evidenced by the sub-horizontal zoning as shown in the main cuts, and the topographic expression of the pegmatite as a whole. Cameron, Larrabee, et al. (in preparation) state that many of the pegmatites in the Paris-Rumford district are similarly flat-lying or gently dipping sheets.

The wall rock has an ill-defined foliation produced by the partial alignment of biotite. This poor foliation strikes west-northwest and dips 50° SW to vertical. South and east of the main pegmatite numerous pegmatite stringers and quartz pods have been injected into the diorite. Most of these lenses are concordant with the wall-rock foliation, and approximate lit-par-lit injections; but some of the larger bodies, are discordant. In several cases these lenses and pods have their longest dimension approximately vertical.

Erosion has only slightly unroofed the pegmatite. This fact is in-

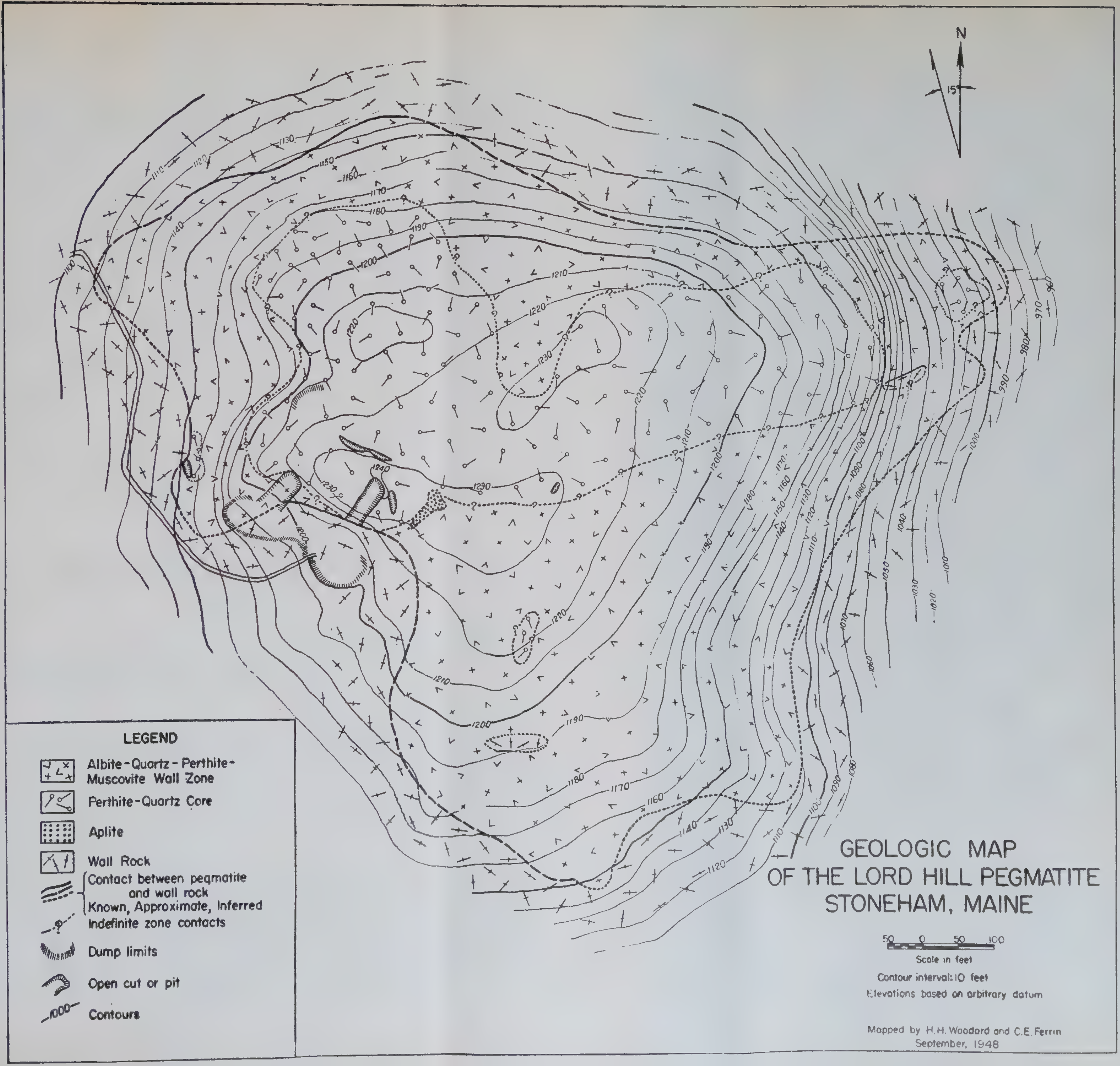

GEOLOGIC MAP
OF THE LORD HILL PEGMATITE
STONEHAM, MAINE

Contour interval: 10 feet
Elevations based on arbitrary datum

Mapped by H. H. Woodard and C. E. Ferrin
September, 1948

dicated by the large number of stoped blocks of wall rock and early-formed aplite which were engulfed and frozen into the pegmatite during solidification. Owing to the scale of the geologic map many of the smaller stoped blocks were not mapped.

Structural and Petrologic Relations of the Wall Rock with the Pegmatite. The country rock was originally an oligoclase ($Ab_{75}An_{25}$) diorite rich in biotite and containing minor amounts of apatite, hornblende, sphene (?), and quartz. However, most of the exposed wall rock now contains up to 30 per cent quartz as myrmekitic intergrowths with calcic plagioclase. The probable explanation of the myrmekite is that after the consolidation of the diorite, calcium was introduced into it and calcic plagioclase formed by replacement of oligoclase. The resulting SiO_2 exsolved produced with plagioclase a myrmekite. Plagioclase in the myrmekitic portion of the diorite ranges from andesine ($Ab_{60}An_{40}$) to bytownite ($Ab_{13}An_{79}$). Small plagioclase crystals show a preferred crystallographic orientation of the quartz intergrowths throughout the whole grain, but large plagioclase crystals show several groupings of preferred orientation within single grain boundaries. The origin of the introduced calcium is unknown.

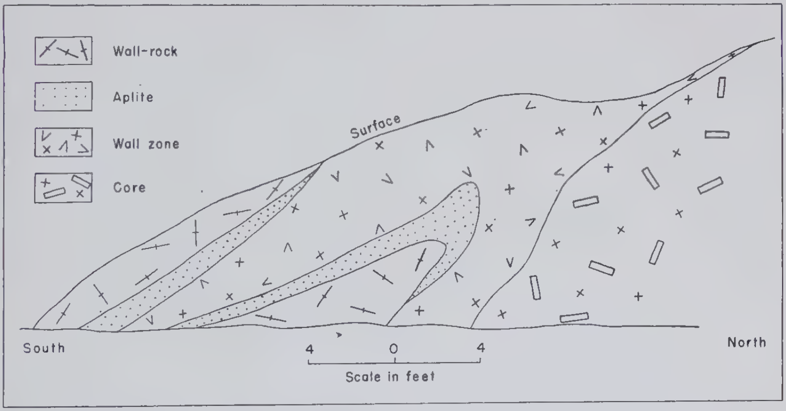

FIG. 1. Diagrammatic sketch of the west wall of the easternmost main cut. Sharp contacts between the wall rock, aplite border zone, and wall zone are apparent. The core is only four feet from wall rock at this locality.

Where observed, the pegmatite country-rock contacts are sharp and well-defined (Fig. 1). Locally, biotite is segregated into clusters within the diorite close to the contact. There is no evidence of large-scale replacement of country rock. However, some small, partially assimilated wall-rock inclusions have a relict rim of biotite left at the contact, and relict lenses of biotite are contained in the adjoining pegmatite several inches from the contact. These biotite lenses resemble minute schlieren and are aligned at an angle to the strike of the contact. This seems to indicate there there was movement within the pegmatite during the assimilation of the inclusions (Fig. 2). Locally, the diorite wall rock and some of the diorite inclusions have been impregnated with quartz, microcline, and muscovite, and are therefore granitized. This granitized halo never has an observable width greater than two feet. In the field granitized diorite does not resemble the aplite-textured border zone in any way, but retains the typical diorite texture except that the poor foliation of the original diorite has been destroyed. However, thin section analysis of the aplite border zone indicates that small areas of this zone are composed in part of assimilated wall-rock materials.

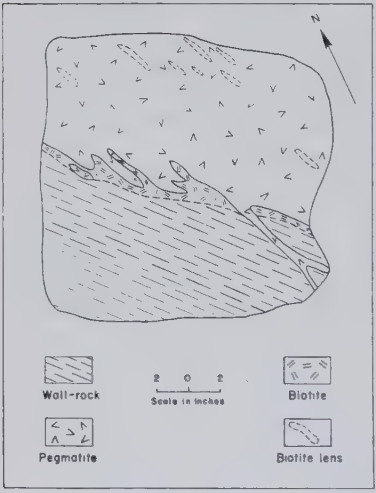

FIG. 2

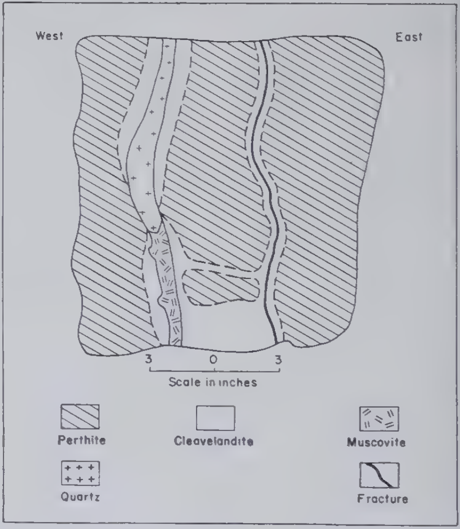

FIG. 3

FIG. 2. Map plan of part of the contact of a small diorite wall-rock inclusion in pegmatite (wall zone). A relict biotite rim is present around the inclusion, and small relict biotite lenses are aligned in the pegmatite.

FIG. 3. Perthite crystal partially replaced by cleavelandite. The cleavelandite was localized by fractures. Quartz-muscovite vein is later than cleavelandite.

The stoped blocks of aplite border zone have two rims of garnets associated with them. At the contact with pegmatite a one-sixteenth inch band, composed entirely of small, pink spessartite(?) crystals, has developed. These same garnets are abundant in the aplite inclusions, but are noticeably scarcer at the centers than nearer the contact. In many of the smaller inclusions they persist throughout the entire body. These garnets are intimately associated with late quartz, green apatite and cleavelandite and they were probably formed by late residual liquors which used the contact as a minor passageway. The second rim of garnets has developed one to two feet from the contact in the enveloping body of pegmatite (Pl. 2). These garnets are brownish-red in color, have a high luster, and are usually several inches in diameter. They formed around earlier crystals of milky yellow apatite. This second rim of garnets may represent the original outline of the stoped block of aplite. However, no proof for this possible explanation was observed.

As has been noted above the effects of assimilation and granitization are small and local features. The large number of stoped blocks of aplite and of relatively unaltered, randomly oriented wall-rock inclusions, along with the sharp pegmatite-country rock contacts suggests that stoping or some other type of mechanical injection was much more effective than assimilation and replacement.

Internal structure. Zones, replacement bodies, and fracture and cavity fillings may be recognized within the Lord Hill pegmatite. The accompanying geologic map shows only the main zones, the scale of the map making it impossible to plot the replacement bodies and fracture and cavity fillings (Pl. 1).

In general the zones are composed chiefly of quartz, perthite, cleavelandite, albite, microcline, and muscovite with minor amounts of other minerals.

Border Zone. The border zone is the outermost zone and for the most part is very thin, ranging from 2 to 8 inches in thickness. Mineral constituents vary from place to place owing to local contamination through partial assimilation of wall rock. Microcline, perthite, oligoclase ($Ab_{72}An_{28}$), biotite, and muscovite are the chief minerals and form a typical fine-grained, equigranular, aplitic-textured rock.

The plagioclase shows features of possible genetic significance. In the border zone, a reverse zoning of oligoclase crystals to slightly more calcic exteriors is very evident. Associated with this reverse zoning are myrmekitic intergrowths of quartz and plagioclase. In some cases the intergrowths are confined to the more calcic borders of the oligoclase crystals, but in others, they persist throughout the grain. The reverse zoning of the plagioclase was possibly caused by crystallization from the pegmatite magma of more calcic plagioclase around preexisting crystals of myrmekitic oligoclase. One may advance the explanation that, on partial assimilation of wall rock by the pegmatite magma, the oligoclase persisted as crystal inclusions. The myrmekitic andesine to bytownite of the diorite was reacted upon by the pegmatite magma to produce oligoclase which retained the original myrmekitic quartz intergrowths. The liquor was locally enriched in calcium, and consequently a calcic

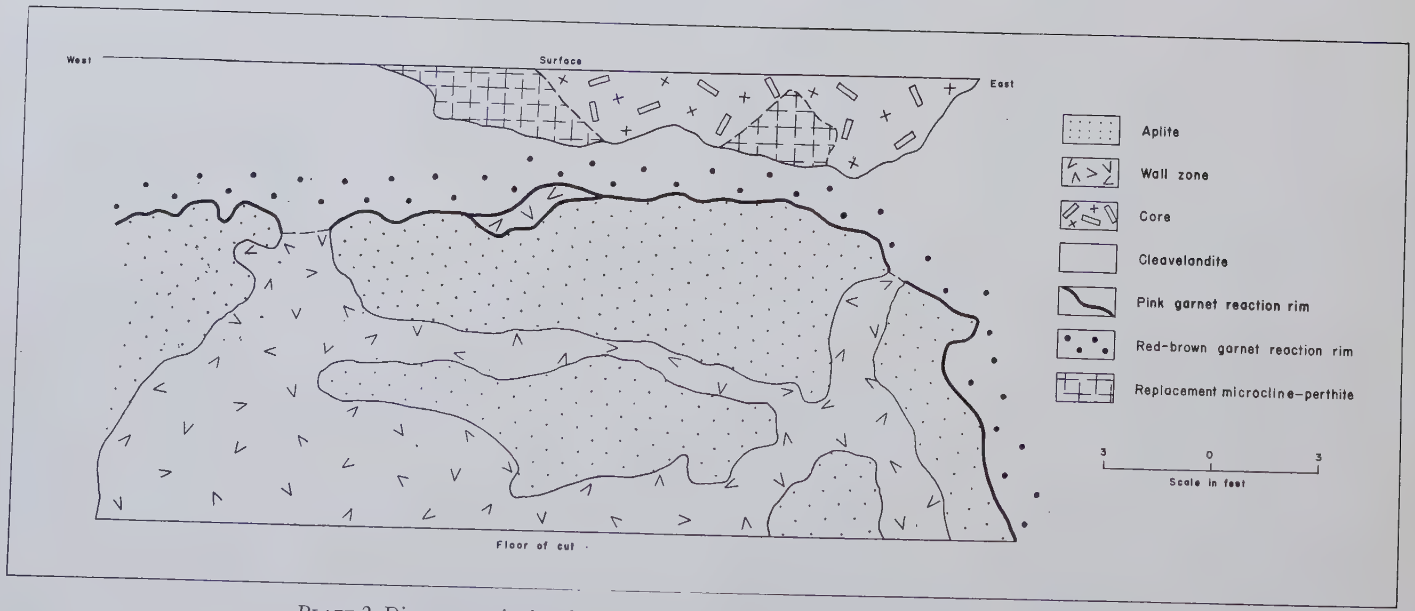

PLATE 2. Diagrammatic sketch showing a stoped block of aplite and associated garnet rims.

border precipitated around the oligoclase inclusions. Equilibrium never was attained because of the relatively rapid cooling of the border zone. An alternative explanation to the above hypothesis is that the reverse zoning of the plagioclase in the border zone was caused by the same solutions which caused the myrmekitic intergrowths in the diorite wall rock. The calcium may have been derived from calcium-bearing wall rock minerals during assimilation by the pegmatite. However, this would necessitate a re-introduction of this calcium to the wall rock in order to produce the wall rock myrmekite. This seems unlikely. The difference in composition of the myrmekitic plagioclase in the border zone ($Ab_{72}An_{28}$) and the myrmekitic plagioclase in the wall rock ($Ab_{60}An_{40}-Ab_{13}An_{79}$) indicates that the calcium necessary to produce these two features was not derived from the same source, for had it been, both plagioclases would be of the same composition.

Crystal growth as shown in thin sections indicates that microcline, perthite, quartz, muscovite, and small amounts of micropegmatite crystallized at approximately the same time. Oligoclase (in part) and biotite are earlier in origin and, as previously stated, are believed to have been derived from the diorite wall rock.

Wall Zone. The wall zone lies inside the border zone, and for the most part is considerably thicker. Width of outcrop ranges from 3 feet in the vicinity of the main cuts to more than 500 feet on the southeastern prong. Field observations show sharp contact relations between this zone and the border zone. Study of thin sections, however, reveal a one-half inch zone in which grain size grades from the aplite size of the border zone into the coarse-grained pegmatite wall zone. The grain size of the zone in general is evenly textured, with crystals up to 1½ inches in diameter. Locally, the grain size changes rapidly and ranges from a granitoid textured rock with grains up to one-fourth inch in diameter, to the normal grain size of the zone.

Albite, quartz, perthite, and muscovite are the chief minerals, with small amounts of oligoclase, biotite, and spessartite (?) also present. The oligoclase ($Ab_{72}An_{28}$) occurs adjacent to the border zone-wall zone contact and has a more calcic exterior. The cause of this reverse zoning has been discussed in the preceding section on the border zone. Perthite content increases from the border zone inward, and the inner contact of the zone is drawn approximately at the place where perthite becomes the most abundant mineral (Pl. 1). Many aplite blocks and country rock blocks, ranging from 1 foot to 100 feet in greatest dimension, form inclusions in this zone. They were apparently stoped from the walls during intrusion. The apparent large size of some of the aplite blocks is difficult to explain when one considers the exposed width of the aplite border zone. It is possible that these few large blocks have a small, unobserved third dimension.

Core. The core consists of four separate bodies which are not connected in surface exposures. As a whole the core forms the central portion of the pegmatite. Its nearest approach to the wall rock is along the southeastern hanging wall, where the two are only four feet apart. On the southern prong it is separated from the wall rock by over 500 feet of wall-zone outcrop. The chief minerals of the core are perthite, quartz, muscovite, and cleavelandite, with minor amounts of albite, biotite, fluorite, spessartite(?), and topaz.

Grain size ranges from 1½ inches in diameter to crystals 8 feet long by 4 feet wide. Interstitial, granitoid-textured quartz, albite and muscovite are abundant, and the smaller perthite crystals are graphically intergrown with quartz.

Three concentrations of block perthite occur in the pegmatite. The largest of these is found close to the southern hanging wall where the two main cuts were opened. This portion of the core has been replaced to a large extent by cleavelandite and its associated minerals; almost one-half the volume now being cleavelandite. The second largest concentration of block perthite, and the one showing the largest perthite crystals, crops out on the northeastern prong of the pegmatite. This outcrop shows little or no cleavelandite, and only small quantities of muscovite are present. However, interstitial quartz with some albite is quite common. The third area of block perthite crops out in the small western-most open pit and has a low perthite content. The boundaries of these concentrations are indefinite and unknown. They probably grade imperceptibly into finer-grained core minerals, which in turn grade outward into wall zone.

The core contains many inclusions of aplite. In one locality wall-zone pegmatite intrudes and cuts aplite. This block of wall-zone pegmatite and aplite was itself stoped, and is now preserved as a large inclusion in the core. The core displays crosscutting relations to both the aplite and the wall zone of the stoped block, and is, then, the last part of the original granitoid pegmatite to crystallize (Pl. 2).

Replacement bodies and fracture and cavity fillings. Replacement bodies are common in the core, especially near the two main open cuts. They range from roughly radial bodies to irregular masses and are often controlled by pre-existing fractures. Small tabular replacements parallel to fracture walls are also common (Fig. 3). Cleavelandite is the chief mineral formed by replacement. However, perthite replacement bodies are also present, especially in the large westernmost cut where they are three to five feet in diameter. Both cleavelandite and perthite replace, corrode, and vein the original core minerals and are thus later in age. Associated with cleavelandite are many cavities or vugs, which contain the rarer mineral constituents. Most of these cavities are small and average between one and five inches in diameter. One vug which was opened during the 1947 operations measured approximately 5×7×10 feet.

Fracture fillings of quartz and muscovite are numerous. They cut all earlier minerals and range in age from pre-albitization to the last stages of the cavity phase.

Descriptive Mineralogy

Perthite, quartz and albite make up 99 per cent of the pegmatite. Figure 4 diagrammatically represents the order of precipitation of the minerals in the pegmatite.

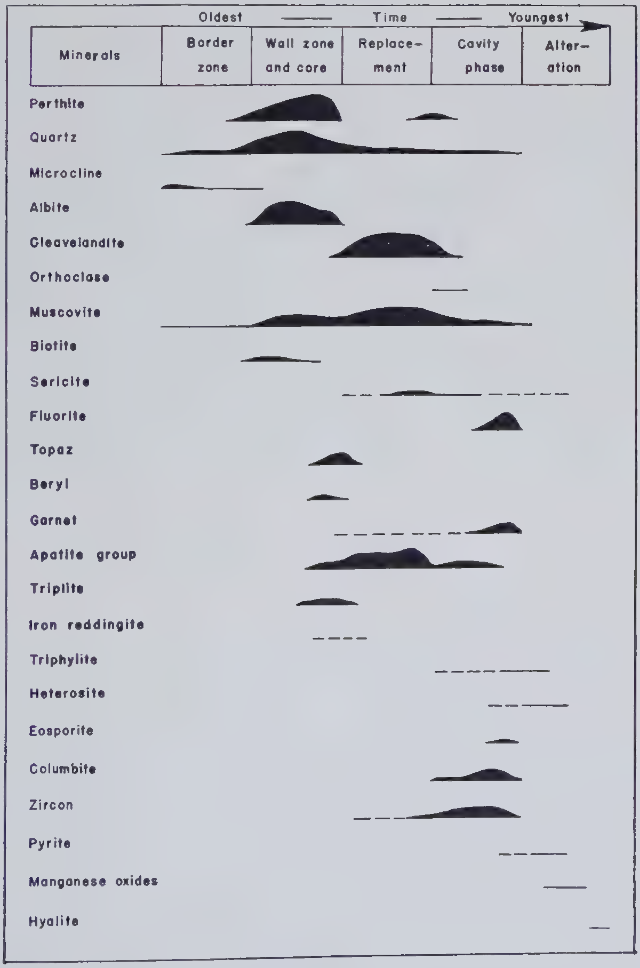

Fig. 4. Paragenetic sequence of the minerals in the Lord Hill pegmatite. Time divisions and vertical dimensions are schematic and do not represent true proportions.

Perthite. At least 95 per cent of the perthite in the pegmatite formed during the original crystallization. However, replacement bodies, dikes, and a few cavity fillings of perthite occur in the core, close to the wall zone-core contact. This perthite is especially abundant at the face of the large western open cut (Pl. 2). It is always a late mineral and in part replaces cleavelandite. The replacement bodies and cavity fillings are always dirty gray, whereas the dikes are white. The color difference is caused by many microscopic opaque inclusions, which are present in the dirty gray varieties and absent in the white dikes.

The dikes range between one-fourth and three-fourths of an inch in width. They have parallel walls, and form almost perfect tabular bodies, which are, in fact, single crystals which retain the same crystallographic orientation throughout the entire observed length of the dikes. The dikes are apparently fillings of straight-walled fractures, but in some cases they terminate in cavities in replacement perthite. Euhedral crystals, commonly intergrown with fluorapatite, cap the dikes which terminate in cavities. In all cases the dikes cut sharply across the perthitic structure of the replacement perthite. This, plus the fact that some terminate in cavities in the replacement perthite, testify to the dikes later age.

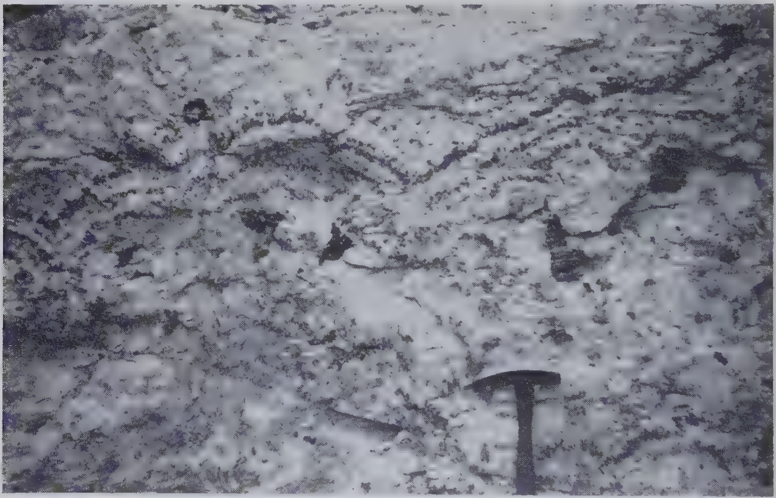

FIG. 5. Triple halos of ball peen muscovite around cleavelandite replacement bodies. The large black crystals are normal muscovite.

Several small cavities in both replacement perthite and cleavelandite contained euhedral, dirty gray crystals of perthite.

Quartz. Cavities developed in the cleavelandite often contain many euhedral quartz crystals. One large cavity contained several tons of quartz crystals, both of the smoky and milky variety.

Orthoclase. The Lord Hill pegmatite, like most pegmatites, contains only minor amounts of orthoclase. Locally, in small cavities in replacement cleavelandite, euhedral, pink, lustrous, orthoclase crystals are developed. Many of the cavities were completely filled by these crystals. The time of crystallization is closely associated with the late replacements and dikes of perthite which were discussed above.

Orthoclase refractive indices measured in sodium light are: $\alpha=1.518$, $\beta=1.524$, $\gamma=1.527$. No polysynthetic twinning could be observed optically.

Muscovite. Large amounts of gray, green, or rum muscovite are associated with cleavelandite. The greatest percentage of this muscovite is of the curved or "ball peen" variety, and is localized as halos around the periphery of cleavelandite bodies (Fig. 5). The external features of the ball peen variety are quite striking when observed in hand specimens. The muscovite crystals appear as though they had been struck innumerable times with a peening hammer; first by heavy blows producing major indentations, and then by lesser blows which superimpose minor indentations on the major curved surfaces. The term botryoidal probably best fits these external characteristics (Fig. 6). Shainin (1946) describes curved muscovite crystals from Branchville, Connecticut, and ascribes them to growth on curved surfaces of radial bodies of cleavelandite. There is no evidence for a similar mode of origin for the ball peen mica of the Lord Hill pegmatite.

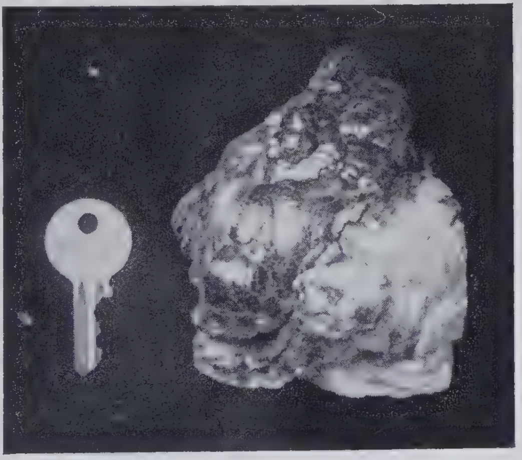

FIG. 6. A typical specimen of ball peen muscovite. Note the broad curved surfaces with innumerable small curved surfaces superimposed upon them. The white mineral is cleavelandite.

This mica is usually associated with quartz, and a large percentage shows an extremely fine, graphic intergrowth with this mineral. This association possibly indicates a replacement of the feldspar in graphic granite by muscovite, but there is no evidence for such replacement having taken place. Commonly, the mica appears contemporaneous with and in some specimens later than quartz and may in part replace it. Shear planes, developed in the muscovite roughly perpendicular to the cleavage, are common, and drag on both sides of the shear planes is locally developed. In thin section the mica always exhibits strong strain shadows. One specimen consists of a large book of green muscovite which grades from perfectly normal, flat folia on one side of the specimen into gray, ball peen folia on the other. This suggests that the ball peening has nothing to do with the quartz with which it is usually associated but rather is an alteration of preexisting, normal muscovite. The structure may be due to late volume increase because of the addition of materials to the preexisting muscovite. The shear planes and strain shadows which are developed, plus the fact that many curved specimens appear as an alteration product of earlier muscovite, lend support to this argument. If this is true, however, the added materials do not change the axial angle and refractive indices of the muscovite in any way, these optics being as follows: biaxial negative, $2V=45°$; $\alpha=1.560$, $\gamma=1.598$.

Two types of muscovite are common as cavity fillings in cleavelandite. The first type is a yellow-green, talc-like muscovite that was deposited as radiating groups coating cavity walls. The other type is a cream colored variety which grows as small radiating groups in cavities.

Sericite. Sericite, a fine-grained variety of muscovite, occurs rarely as fine-grained plumose masses in cleavelandite. These masses are up to 3 inches in diameter and range in color from pink to brown. A light pink variety of sericite occurs sparingly interlayered with sheaves of cleavelandite. Both varieties of sericite appear to have indices of refraction similar to that of muscovite.

Fluorite. Fluorite, a major accessory mineral in the pegmatite, is restricted to cavities in cleavelandite. Exceptional crystals are developed in many of the cavities. The most common habit is a cube modified by octahedral faces, but perfect octahedrons are rarely developed. The modified cubes commonly reach one-half inch in diameter, whereas octahedrons are considerably smaller. There is a marked difference in color depending on the type of crystal. The modified cubes are zoned to an extremely dark purple exterior. This exterior zone terminates abruptly inward against a light purple zone, which in turn grades into a pink zone and then a colorless center. The pink zone may or may not be present in a single crystal. The octahedral crystals in all observed specimens had no dark purple zone on their exterior but were either colorless, pink, or light purple with patches of darker purple present.

Beryl. Three types of beryl are present in the pegmatite. All types are rare.

The most abundant is a milky yellow variety which occurs with and encloses the phosphate triplite. Both of these minerals occur with original core minerals and probably crystallized during late core formation. It has the following optical and physical properties: uniaxial negative; $\epsilon=1.565$, $\omega=1.572$; basal cleavage. According to Winchell (1933, p. 213) the above indices indicate an alkali content of less than 0.5 per cent.

A pale green variety of beryl is veined and corroded by muscovite and cleavelandite. Optical properties are as follows: uniaxial negative; $\epsilon=1.574$, $\omega=1.580$. These indices indicate an alkali content of 1.2 per cent.

One fragment of a clear, blue-green aquamarine crystal was found on the dump. Indices of refraction are the same as those for the pale green variety.

Topaz. Clear, pale green to colorless topaz is the second most abundant accessory mineral in the pegmatite. It occurs in highly fractured masses which are commonly several inches in diameter. In all cases it is corroded by cleavelandite or yellow-green muscovite.

Optical properties of topaz: biaxial positive, $2V=65°$; $\alpha=1.617$, $\beta=1.620$, $\gamma=1.629$; $r>v$ distinct; perfect basal cleavage.

Apatite. Several types of apatite are present in the pegmatite. They are described in order of decreasing abundance.

A dark blue-green apatite is closely related in age to albitization, some being veined and corroded by cleavelandite and some showing mutual relations with cleavelandite. It occurs in irregular highly fractured masses up to several inches in diameter. Optical properties are as follows: $2V=15°$; $\alpha=1.644$, $\beta=1.648$, $\gamma=1.648$; pleochroism slight, α=yellow-blue, γ=light blue; $X>Z$.

The second type of apatite always occurs as euhedral crystals filling cavities in replacement bodies of perthite and cleavelandite or as intergrowths with late perthite dikes. Thus this type of apatite is post albitization, and contemporaneous with the perthite dikes. Several crystal habits are represented.

The most common crystal habit is elongate parallel to the *c* crystallographic axis, and probably has the $c\{0001\}$, $m\{10\bar{1}0\}$, $x\{10\bar{1}1\}$, $r\{10\bar{1}2\}$, and $s\{11\bar{2}1\}$ faces developed. These crystals range in size from one-quarter to one-half inch in length and are beautifully zoned from a clear, gray-green center to a clear, colorless exterior.

The second most common habit probably has the $c\{0001\}$, $m\{10\bar{1}0\}$, $a\{11\bar{2}0\}$, $r\{10\bar{1}2\}$, and $x\{10\bar{1}1\}$ faces developed. It is consistently gray-blue in color. However, several crystals contained a colorless interior and were zoned to a gray-blue exterior. The optical properties of this habit are identical to other varieties present, except that it is not strictly uniaxial but has a negative 2V of 15°. In this respect it resembles the earlier described dark blue-green apatite.

The third most common habit has a facial development which is very complex, and probably the following faces are represented: $c\{0001\}$, $m\{10\bar{1}0\}$, $a\{11\bar{2}0\}$, $r\{10\bar{1}2\}$, $x\{10\bar{1}1\}$, $y\{20\bar{2}1\}$, $z\{30\bar{3}1\}$, $s\{11\bar{2}1\}$ and $i\{12\bar{3}2\}$. The largest crystal observed was flattened parallel to $s\{11\bar{2}1\}$, but another crystal shows $y\{20\bar{2}1\}$ as the most highly developed form. The crystals are zoned from clear, gray-green at the center to a clear, colorless exterior.

The least common habit occurs in long prismatic crystals with only the $c\{0001\}$, $m\{10\bar{1}0\}$, and $r\{10\bar{1}2\}$ faces developed, and is clear, pale green, gray-blue, or colorless.

Optical properties of all euhedral apatite: uniaxial negative; $\epsilon=1.631$, $\omega=1.634$. Cleavages: $\{0001\}$ and $\{01\bar{1}0\}$ imperfect.

The third type of apatite present in the pegmatite is localized in cleavelandite, and has only been found as centers of the large garnet crystals which form a zone around aplite inclusions. The garnet veins and encloses the apatite center, and is distinctly later. The mineral is milky yellow in color, highly fractured, and has the following optical properties: uniaxial negative; $\epsilon=1.635$, $\omega=1.639$; perfect basal cleavage.

Triplite. Triplite is common in the pegmatite. It is associated with, and included within milky yellow beryl, which crystallized concurrently with the quartz and feldspar of the core.

The mineral is salmon-colored and commonly stained on the exterior by late manganese oxides. It has the following optical and physical properties: biaxial positive, 2V=85° (estimated); $r>v$ distinct; $\alpha=1.673$, $\beta=1.685$, $\gamma=1.698$; one perfect and one poor cleavage.

Iron reddingite. One specimen of iron reddingite was observed in the Lord Hill pegmatite. It occurred as a lustrous, dark red, highly fractured, circular mass 3 inches in diameter and 1 inch thick.

Optical properties of iron reddingite: biaxial positive, 2V=80° (estimated); $r>v$ distinct; $\alpha=1.669$, $\beta=1.681$, $\gamma=1.697$; pleochroism, α=colorless, β=light brown; cleavage, one perfect—probably $\{100\}$.

Heterosite(?). This mineral is associated with manganese oxide stain, and is a late alteration product. It is found very rarely as extremly thin, red-violet patches on yellow beryl and triplite crystals. All indices of refraction are above 1.788, and pleochroism is strong—carmine red to violet to greenish brown.

Eosphorite. One cavity in cleavelandite yielded numerous small orthorhombic crystals of eosphorite up to 3 millimeters in length. It occurs as radiating groups growing upon a yellow drusy mineral, which was not identified. The crystal habit is long, prismatic, and tabular parallel to the $a\{100\}$ face. The form is simple, with the $a\{100\}$, $b\{010\}$, and $p\{111\}$ faces developed. The crystals are zoned from a colorless interior to a wine yellow exterior.

The optical properties of the Lord Hill eosphorite differ somewhat from those given by Larsen and Berman (1934). The mineral is biaxial negative, 2V=62°; $r>v$ distinct; $\alpha=1.643$, $\beta=1.666$, $\gamma=1.672$; optic orientation, $Y=a$, $Z=c$: pleochroism weak with γ=colorless and α=yellow-brown; one perfect cleavage parallel $\{100\}$.

Columbite. Many small crystals of columbite are found in cavities and imbedded in cleavelandite bodies. Most of the crystals are thin, tabular and one-fourth inch or less in length, and have one of two probable sets of faces developed: (1) $a\{100\}$, $b\{010\}$, $d\{170\}$, $m\{110\}$, $k\{011\}$, $o\{131\}$ and $u\{111\}$; (2) $a\{100\}$, $b\{010\}$, $c\{001\}$, $m\{110\}$, and $e\{201\}$. The specific gravity of this columbite was determined as 5.64. Thus an approximate Ta_2O_5 content of 15 per cent is indicated (Palache, et al., 1946, p. 786).

Zircon. Commonly small euhedral crystals of zircon are found embedded in either cleavelandite or gray muscovite. Occasionally it is associated with deep purple fluorite and colorless fluorapatite. Most crystals have a yellow-brown halo surrounding them, which is probably due to radioactive effects on the surrounding minerals. The mineral has two good cleavages at right angles.

Unidentified mineral. A yellow platy mineral, which resembles autunite, forms a crust on fracture walls. It is one of the latest minerals in the pegmatite.

Larsen and Berman (1934) list no minerals which have the optical properties determined for this specimen. Determinations are poor, however, because of the mineral's rarity. It is biaxial negative with $2V=40°$ (estimated); $r>v$ strong; strong horizontal dispersion of the vibration directions; ultra-blue, abnormal interference colors; $\beta=1.604$, $\gamma=1.610$; at least three good cleavage directions.

Conclusions on Paragenesis

The geologic and petrologic relations of the Lord Hill pegmatite have led to the conclusion that the pegmatite has slightly granitized its walls and at the same time has assimilated some material.

Reference to Fig. 4, Plate 1, and the preceding sections on the mineralogy and structure of this deposit suggest the following conclusions:

(1) A residual magma rich in K, Na, Si and the rarer elements was mechanically injected into oligoclase diorite country rock.

(2) This residual magma crystallized in a definite sequence. The first minerals crystallized were those rich in potash, soda, and silica. It is these minerals which chiefly comprise the border zone of the pegmatite. The wall zone and core, which were still mobile while the border zone was crystallizing, respectively then crystallized. When these two zones crystallized the order of crystallization was similar to that of an igneous melt. Albite is the most abundant mineral in the wall zone, and potassium feldspar is the chief mineral in the core. There was an enrichment in the rest magma of the minor amounts of rare elements. The development of the zones occurred in an essentially closed chemical system.

(3) Na rich solutions reacted on favorable areas of the core replacing the original zone minerals with cleavelandite. These solutions may represent a new addition of material to the pegmatite (open system).

(4) Hydrothermal solutions deposited phosphates and fluorides in cavities along with other rarer components.

References

Bastin, E. S. (1911), Geology of the pegmatites and associated rocks of Maine: *U. S. Geol. Survey, Bull.* **445.**

Cameron, E. N., Larrabee, D. M., McNair, A. H., Page, J. J., Shainin, V. E., and Stewart, G. W., New England mica deposits (in preparation).

Dale, T. N. (1923), The commercial granites of New England: *U. S. Geol. Survey, Bull.* **738,** 209.

LARSEN, E. S., AND BERMAN, HARRY (1934), The microscopic determination of the non-opaque minerals: *U. S. Geol. Survey, Bull.* **848,** 179.

PALACHE, C., BERMAN, H., AND FRONDEL, C. (1948), *Dana's System of Mineralogy:* vol. **1,** p. 786, New York, John Wiley and Sons.

SHAININ, V. E. (1946), The Branchville, Connecticut, pegmatite: *Am. Mineral.,* **31,** 336–338.

STERRETT, D. B. (1923), Mica deposits of the United States: *U. S. Geol. Survey, Bull.* **740,** 94–100.

WINCHELL, A. N. (1933), Elements of Optical Mineralogy, Part II. Description of minerals: New York, John Wiley and Sons.

WRIGHT, F. E. (1911), The methods of petrographic-microscopic research: *Carnegie Inst. Washington, Pub.* **158,** 147–200.

Manuscript received June 1, 1951.

PETROLOGICAL STUDIES ON PLAGIOCLASE TWINS*

Masao Gorai†

Abstract

The differences in the type of plagioclase twinning in igneous and metamorphic rocks are described. Plagioclase twins are divided, from a petrological point of view, into the C-twin and the A-twin. Frequencies of untwinned plagioclase and twin types in various endogenous rocks are described and the genesis of the C-twin which characterizes the volcanic and plutonic rocks is interpreted. Lastly, a plagioclase twin method for determining the origin of various granitic rocks is proposed and discussed.

Introduction and Acknowledgments

The present study has been under investigation since 1944 for the purpose of determining the petrological significance of plagioclase twins. As a result of this investigation it was found that there exists a clear difference in plagioclase twinning in igneous and metamorphic rocks.

Thus albite and pericline (acline) twins are present commonly in the igneous as well as in the metamorphic rocks, while the other twins (Carlsbad, etc.) are confined to, or characteristic of, the volcanic and plutonic rocks. This difference in the type of plagioclase twinning may be attributed to the difference in the mechanism of plagioclase crystallization.

According to the above interpretation the writer has tried to deduce the mechanism of plagioclase crystallization in some rocks formed near the boundary between magmatic and metamorphic processes, and from this also to postulate the environmental conditions under which these rocks were formed.

It is hoped that the plagioclase twin method proposed in the present paper may throw new light on the so-called "granite problem."

The writer wishes to express his sincere gratitude to the late Dr.

---

* Preliminary reports of this study were published in the following articles:

Study of plagioclase twins, considered from a petrological point of view (in Japanese): *Jour. Assoc. Geol. Collaboration*, **1**, No. 1, 3–6 (1947).

Plagioclase twins in the igneous and metamorphic rocks (in Japanese): *Jour. Geol. Soc. Japan*, **54**, No. 635, 89 (1948).

Proposal of twin method for the study of the granite problem: *Jour. Geol. Soc. Japan*, **56**, No. 655, 149–156 (1950).

Method of distinguishing C-twin and A-twin of plagioclase under ordinary polarization microscope (in Japanese with English summary): *Jour. Geol. Soc. Japan*, **56**, No. 660, 441–443 (1950).

The features of plagioclase twinning in various granitic rocks: *Jour. Geol. Soc. Japan*, **56**, No. 663, 515–518, 1950.

† Geological and Mineralogical Institute, Tokyo Kyōiku-Daigaku (Univ. of Education), Tokyo, Japan.

Kenichi Sugi who kindly guided him during this study, and also to Dr. Shōji Ijiri, Mr. Akiho Miyashiro, Dr. Tatsurō Matsumoto, Mr. George Kojima, Dr. Kenzo Yagi and Mr. Hiroshi Kanō for their many valuable suggestions and criticisms. His thanks are also due to Dr. N. L. Bowen and Dr. F. Chayes for their critical reading of the manuscript. Lastly, he is indebted to Mr. Yono Sotozaki and Miss Takako Ishikawa who assisted him in the preparation of the article.

Approximate Frequencies of Each Twinning Law in Various Endogenous rocks

The chief purpose of this study is to indicate the difference between plagioclase twins characteristic of igneous and metamorphic rocks. Up to the present time the twinning laws of about 1500 plagioclase twins from various endogenous rocks have been determined by the Fedorov method.[1]

Table 1. Approximate Frequencies of Each Twinning Law in the Plagioclases of Volcanic and Allied Rocks

An%		Ab	Pe	Ac	Pe or Ac	Sum	Ca	Ab-Ca	AlB	Ab-AlB	Ma	AlA (Ma-Ac)	Ba	X	Sum	Whole sum
0– 24	P	4	—	—	2	6	2	2	—	—	—	—	—	—	4	10
	G	5	—	—	—	5	3	4	—	—	—	—	—	—	7	12
25– 49	P	85	3	2	26	116	24	23	1	5	3	3	—	4	63	179
	G	19	—	—	4	23	14	10	—	—	—	—	—	—	24	47
50– 74	P	71	6	3	15	95	44	24	1	1	5	3	2	1	81	176
	G	68	—	1	6	75	36	25	—	1	2	—	—	—	64	139
75–100	P	56	5	2	13	76	37	29	1	2	1	1	2	1	74	150
	G	30	—	4	4	38	30	12	—	1	—	1	—	—	44	82
Sum	P	216	14	7	56	293	107	78	3	8	9	7	4	6	222	515
	G	122	—	5	14	141	83	51	—	2	2	1	—	—	139	280
Whole sum		338	14	12	70	434	190	129	3	10	11	8	4	6	361	795

Ab=albite, Pe=pericline, Ac=acline, Ca=Carlsbad, Ab-Ca=albite-Carlsbad, AlB=AlaB, Ab-AlB =Albite-AlaB, Ma=Manebach, AlA (Ma-Ac)=AlaA (Manebach-acline), Ba=Baveno, X=unknown twin, P=phenocrystic plagioclase, G=groundmass plagioclase.

Table 1 shows the approximate frequencies of different types of twins in various volcanic rocks (including so-called hypabyssal rocks such as quartz-porphyries, porphyrites, diabases, and gabbroic rocks of volcanic origin). As seen from the table, albite, pericline (plus acline),[2] Carlsbad and albite-Carlsbad twins are very common, while the other twins are of relatively rare occurrence. It is noteworthy that there are no marked differences between the type of twinning in the phenocrysts and groundmass of the plagioclases, except that the former are somewhat richer in pericline (acline) and the rare twins (Manebach, etc.).

---

[1] Index of hemisphere is 1.516, that of immersion liquid (cedarwood oil) 1.518 at 21° C. Angle of inclination (*h*) was not compensated. The observations with the universal stage and the plotting of Wulff's net were carried out simultaneously. The twinning laws were determined according to Reinhard's diagrams.

TABLE 2. APPROXIMATE FREQUENCIES OF EACH TWINNING LAW IN THE PLAGIOCLASES OF PLUTONIC ROCKS

An%	Ab	Pe	Ac	Pe or Ac	Sum	Ca	Ab-Ca	Ca or Ab-Ca	Ab-AlB	Ma	AlA or (Ma-Ac)	Ba	X	Sum	Whole sum
0– 24	31	—	—	3	34	—	—	17	—	—	1	—	1	19	53
25– 49	35	7	2	8	52	—	—	28	—	—	1	—	1	30	82
50–100	103	18	7	40	168	40	35	—	2	1	1	1	—	80	248
Sum	169	25	9	51	254	40	35	45	2	1	3	1	2	129	383

Table 2 shows the frequencies of each form of twin in the plagioclases of various plutonic rocks (gabbroic to granitic rocks occurring as so-called batholiths and stocks). As in the volcanic rocks mentioned above, albite, pericline (acline), Carlsbad and albite-Carlsbad twins are common, while the other twins are very scarce.

TABLE 3. APPROXIMATE FREQUENCIES OF EACH TWINNING LAW IN THE PLAGIOCLASES OF SCHISTS AND GNEISSES

An%	Ab	Pe	Ac	Pe or Ac	Sum	Ca	Ab-Ca	Sum	Whole sum
25– 49	62	2	1	18	83	—	1	1	84
50– 74	18	3	1	2	24	—	—	—	24
75–100	13	27	1	1	42	1	—	1	43
Sum	93	32	3	21	149	1	1	2	151

Table 3 shows the frequencies of twin forms in the plagioclases of various schists and gneisses of amphibolite facies.[3] As seen from this table the type of plagioclase twinning in these metamorphic rocks is quite different from that in the volcanic and plutonic rocks. Although albite and pericline (acline) twins are common, the other twins are very scarce, Carlsbad and albite-Carlsbad twins being rarely encountered. Pericline (acline) twins are more common in extremely calcic plagioclases than in the sodic varities. The same tendency is also observed in the plagioclases of volcanic and plutonic rocks above described, although it is not shown in Tables 1 and 2.

---

[2] As the differentiation of pericline from acline twins is not always easy, especially in the case of intermediate plagioclases, these twins are treated together.

[3] Excluding the gneisses of marked migmatitic appearance (so-called injection gneiss, etc.).

Table 4. Approximate Frequencies of Each Twinning Law in the Plagioclases of Hornfelsic Rocks

An%	Ab	Pe	Ac	Pe or Ac	Sum	Ca	Ab-Ca	Ab-AlB	Sum	Whole sum
25– 49	32	1	1	9	43	3	1	—	4	47
50– 74	43	5	2	10	60	6	3	1	10	70
75–100	9	2	1	3	15	—	2	—	2	17
Sum	84	8	4	22	118	9	6	1	16	134

Table 4 shows the type of plagioclase twinning in hornfelsic rocks, probably of pyroxene-hornfels facies. As seen from this table the frequencies of different plagioclase twins in these hornfelsic rocks are rather similar to those in the schists and gneisses above described. It is noteworthy, however, that the hornfelses are somewhat richer in Carlsbad and albite-Carlsbad twins than the schists and gneisses, although the frequencies of these twins shown in table 4 are somewhat overestimated.

The above described features of plagioclase twinning in various endogenous rocks may be summarized as follows:

(i) Albite and pericline (acline) twins are very common in the igneous as well as in the metamorphic rocks.

(ii) Carlsbad and albite-Carlsbad twins are common in the volcanic and plutonic rocks, while rare in the metamorphic rocks.

(iii) The other twins (Manebach, etc.) are almost entirely confined to the volcanic and plutonic rocks, where they are of relatively rare occurrence.

Grouping of Plagioclase Twins from a Petrological Point of View

As indicated in the foregoing paragraph albite and pericline (acline) twins are commonly present in the igneous as well as in the metamorphic rocks, while the other twins are almost confined to, or are characteristic of, the volcanic and plutonic rocks. Accordingly, the plagioclase twins are divided, from a petrological point of view, into the following two groups:

C-twin. This includes twins according to the laws[4] that are restricted to, or characteristic of, the volcanic and plutonic rocks.

A-twin. This includes twins according to the laws[5] that are commonly present in the igneous as well as in the metamorphic rocks.

It is easy to determine the approximate frequencies of these C-twins and A-twins in each rock, because they are readily distinguished with the ordinary petrographic microscope (without universal stage).

First, twinned plagioclases are divided into the following four types:

Type 1. Polysynthetic twins (1, 2, 4 of Fig. 1) and their modifications (3, 5).

Type 2. Simple twins (6, 7) and their modifications (8, 9, 10).

Type 3. Complex twins and their modifications; this is subdivided into *3a* (11–15) and *3b* (16–20).

Type 4. Penetration twins (21–25).

Fortunately there are intimate relations between these four types of twinned plagioclases and the twinning laws. Thus the twins of type 1 are almost always those according to the albite or pericline (acline) laws, and consequently fall in type A.[6] The twins of type 3 are almost always complex twins related to albite, Carlsbad and albite-Carlsbad laws, being rarely related to albite, Ala B and albite-Ala B laws. Therefore, they are always C-twins. The twins of type 4 are also C-twins, because they are always twinned after the laws characteristic of the volcanic and plutonic rocks (Carlsbad, etc.). However, the twins of type 2 include, in general, both C-twins and A-twins, and the differentiation of the former from the latter is not always easy. The following three cases may be distinguished for the twins of type 2:

(i) The different twin units of a crystal show different retardation when the twinning line is placed in or near the 45° position with reference to the cross hairs.

(ii) The twin units show, in that position, nearly equal retardation, but show different retardation when a gypsum plate is inserted.

(iii) The twin units show, in that position, equal retardation even when the gypsum plate is inserted.

Of these the first two cases are C-twins (Carlsbad twin), while the third case is practically indeterminate.[7]

---

[4] Carlsbad, albite-Carlsbad, Manebach, Baveno, AlaB, albite-AlaB, AlaA or Manebach-acline laws. Of these the first two are the most common.

[5] Albite and pericline (acline) laws.

[6] Excepting rare instances in some basaltic rocks, in which the twins of Type 1 are sometimes twinned after the Carlsbad law.

[7] The twins of the third case are either A-twin (albite or pericline) or C-twin (albite-Carlsbad); the differentiation is impossible without universal stage.

The approximate frequencies of C-twins and A-twins in each rock are thus easily estimated from those of the above four types of twinned plagioclases determined with the ordinary petrographic microscope. The frequencies of these four types are determined by counting successively the grains of each type (generally 100-200 grains in each slice) which pass the central portion of the field of microscope, moving the slice regularly on a mechanical stage.[8] The frequencies of untwinned plagioclases are also recorded together with those of the two twin types.

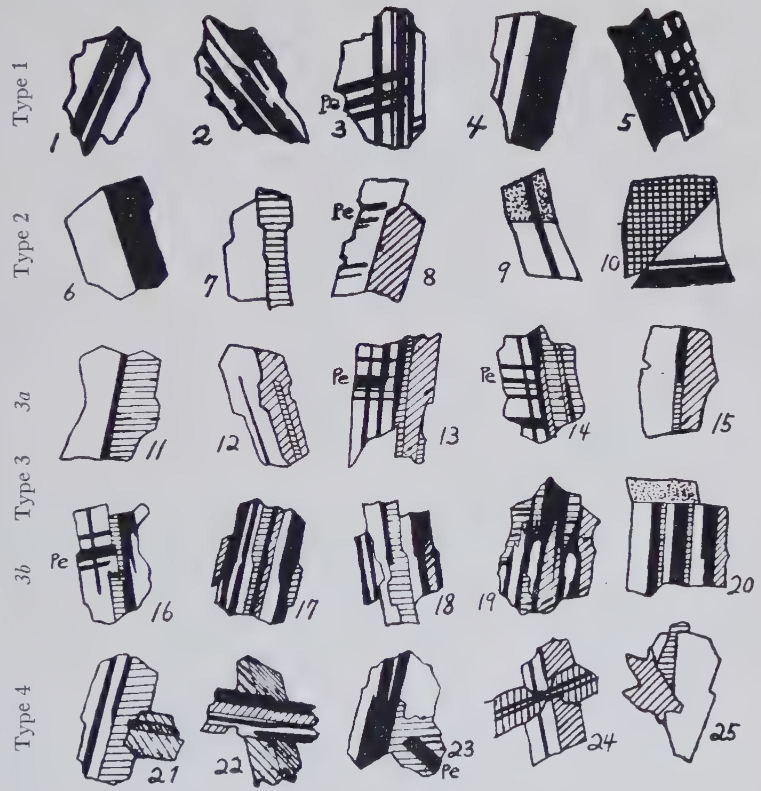

FIG. 1. Four types of twinned plagioclases.
Type 1. Polysynthetic twins and their modifications.
Type 2. Simple twins and their modifications.
Type 3. Complex twins and their modifications.
Type 4. Penetration twins.

---

[8] Therefore large grains may sometimes be counted twice or more.

Frequencies of Untwinned Plagioclase and Twin Types in Various Endogenous Rocks

Figure 2 shows the ratios of untwinned plagioclase (U), C-twin (C), and A-twin (A), of the phenocrystic plagioclases in various volcanic and related rocks. As seen from this diagram each point (each rock) falls in a narrow field, more basic rocks being relatively richer in C-twins. The same features are observed in the groundmass plagioclases of volcanic and allied rocks (Fig. 3). The frequencies of U, A and C depend, however, on the average compositions of the plagioclase rather than on the chemical compositions of the entire rocks. Thus, as seen from Fig. 4, there are regular relationships between the average compositions of plagioclase and the frequencies of untwinned plagioclase and twin types in each rock. This relationship is more pronounced in Fig. 5, which shows the relationship between the average compositions of plagioclase and the frequencies of C-twin in the labradoritic to anorthitic feldspars in andesitic to basaltic rocks.

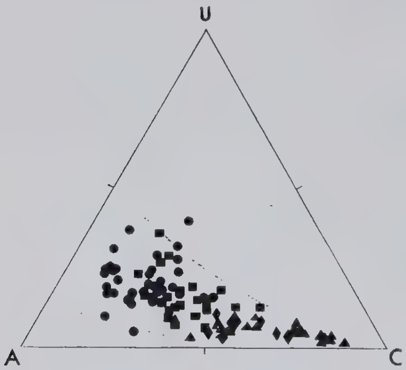

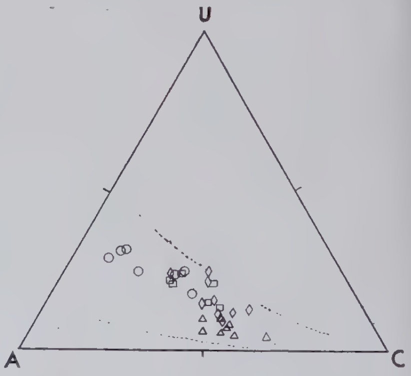

Fig. 2 (left). U:A:C ratios in the phenocrystic plagioclase of volcanic and allied rocks.
Fig. 3 (right). U:A:C ratios in the groundmass plagioclase of volcanic and allied rocks.
Triangle = basalts and related types.
Rhomb = Pyroxene andesites and related types.
Square = hornblende andesites, dacites, and related types.
Circle = liparites, trachytes, and related types.

The U:A:C ratios in various plutonic rocks[9] are shown in Fig. 6. Figure 7 illustrates the relations between the average compositions of plagioclase and the frequencies of U, A and C. As seen from these diagrams the features of plagioclase twinning in these plutonic rocks are

[9] Gabbroic to granitic rocks occurring in batholiths and stocks, rocks with marked shearing effects being excluded.

very similar to those in the volcanic and allied rocks described above.

The ratios of U, A and C in various schists and gneisses[10] of amphibolite facies are shown in Fig. 8. As seen from this figure the features of plagioclase twinning in these metamorphic rocks are quite different from those of the plagioclases in the volcanic and plutonic rocks, C-twins being almost lacking.[11]

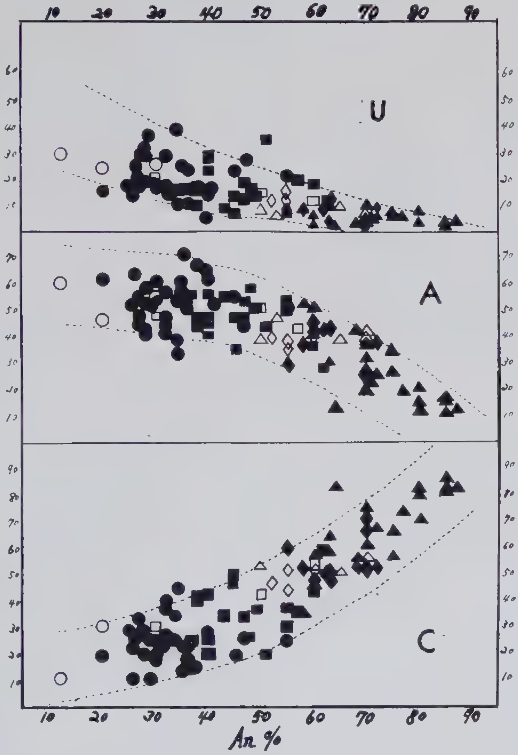

FIG. 4. Relationship between the average An% of plagioclase and the frequencies of U, A and C in volcanic and allied rocks.

It is noteworthy, moreover, that the frequency of twinned plagioclase (A-twin) in these metamorphic rocks has nothing to do with the average composition of the plagioclase, but depends on the average grain size of the plagioclase in each rock (Figs. 9 and 10).

---

[10] Excluding the gneisses of marked migmatitic appearance.

[11] Universal stage determinations show that the Type 2 twins (simple twins) in these metamorphic rocks are always albite or pericline (acline) twins, namely A-twins.

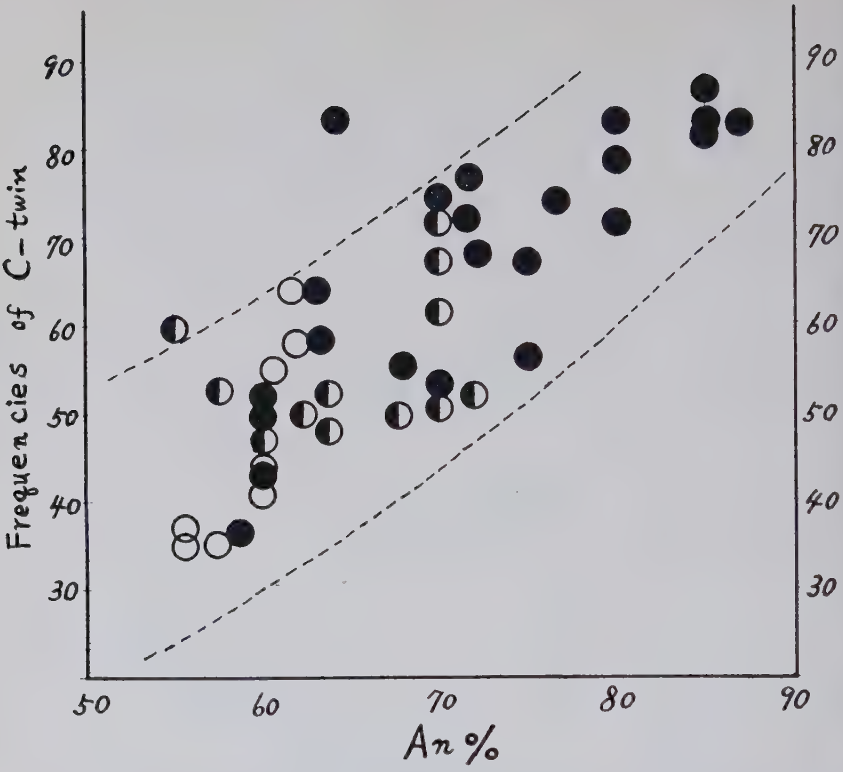

FIG. 5. Relationship between the average An% of plagioclase and the frequencies of C-twins in the basaltic and andesitic effusives and related rocks.

Solid circle = basalts and related types.

Semi-solid circle = pyroxene andesites and allied types.

Open circle = hornblende andesites and allied types.

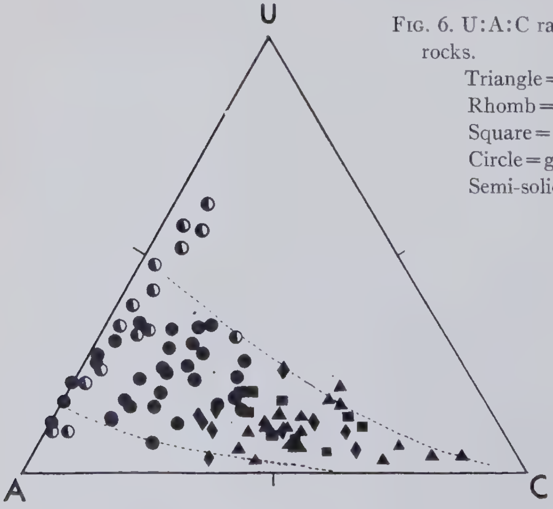

FIG. 6. U:A:C ratios in the plagioclase of plutonic rocks.

Triangle = gabbros.

Rhomb = diorites.

Square = quartz diorites.

Circle = granites, granodiorites.

Semi-solid circle = aplites, pegmatites.

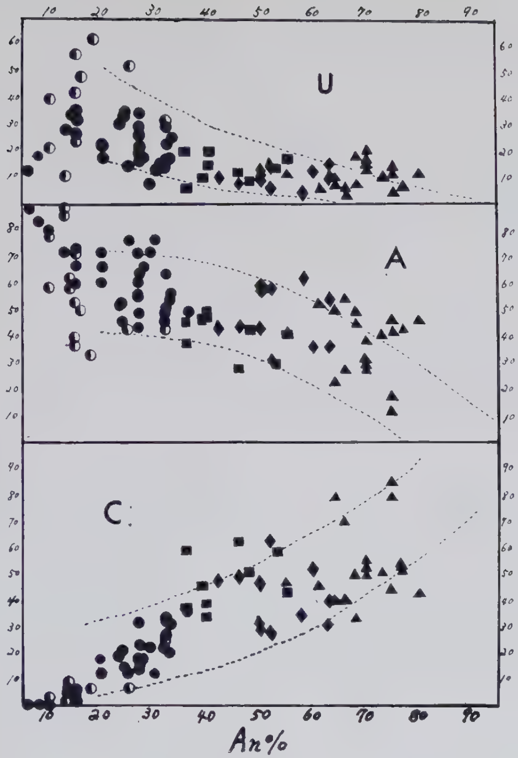

Fig. 7. Relationship between the average An% of plagioclase and the frequencies of U, A and C in plutonic rocks.

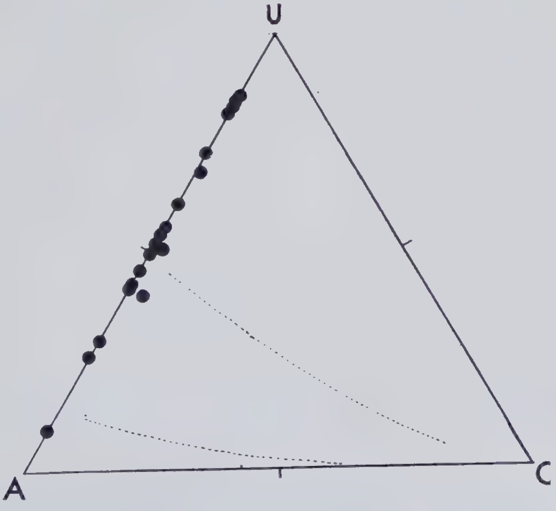

Fig. 8. U:A:C ratios in the plagioclase of schists and gneisses.

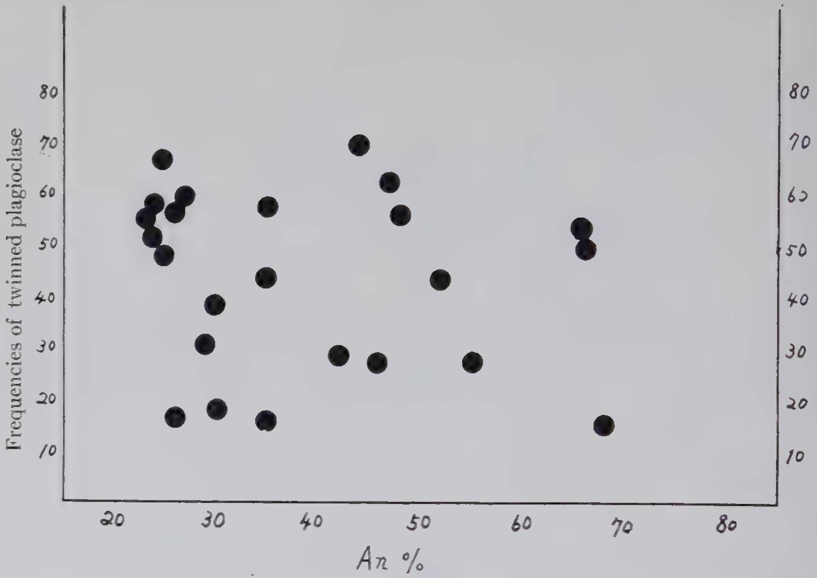

FIG. 9. Relationship between the average An% of plagioclase and the frequencies of twinned plagioclase in schists and gneisses.

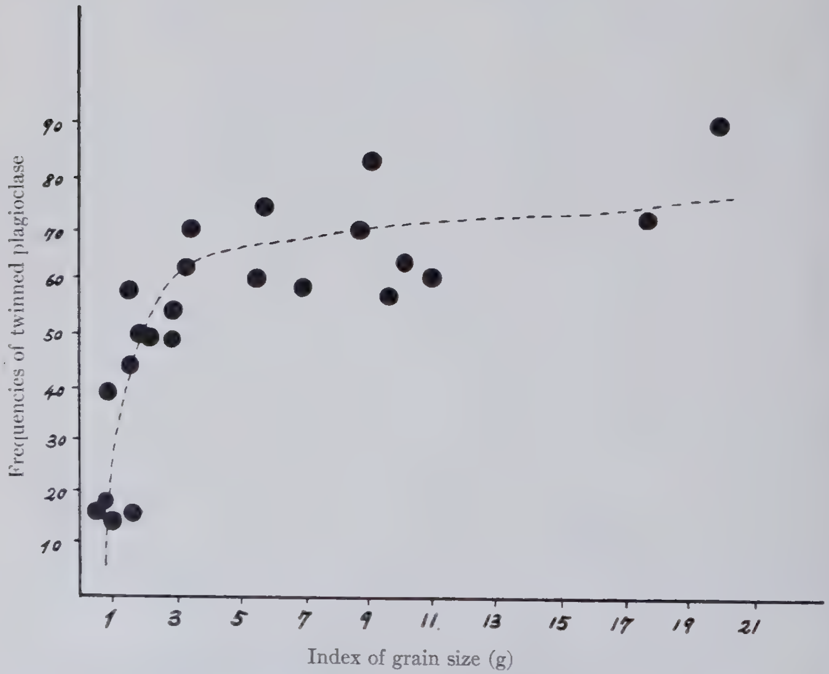

FIG. 10. Relationship between the average grain size (g) of plagioclase and the frequencies of twinned plagioclase in schists and gneisses.

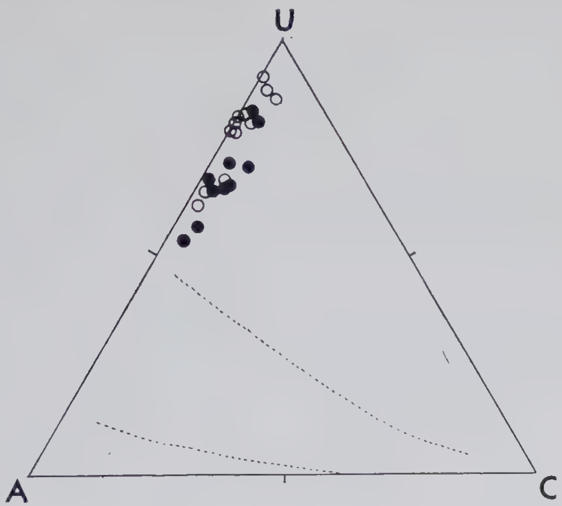

FIG. 11. U:A:C ratios in the plagioclase of hornfelsic rocks.
Open circle = Rocks constituting metamorphic aureoles.
Solid circle = Rocks occurring as xenoliths in the plutonic rocks.

Figure 11 shows the U:A:C ratios in hornfelsic rocks probably of pyroxene-hornfels facies. As seen from this figure each point (each rock) falls, as in the schists and gneisses above described, on or near the U-A line. The hornfelses are, however, generally richer in untwinned plagioclase,[12] and somewhat richer in C-twins as compared with schists and gneisses. It is noteworthy, moreover, that the hornfelses occurring as xenoliths in the plutonic rocks are generally richer in C-twins than those constituting the metamorphic aureoles surrounding the plutonic masses.

SOME CONSIDERATIONS ON THE GENESIS OF C-TWINS

As described in the foregoing paragraphs, some kinds of twins are commonly present in the igneous as well as in metamorphic rocks, while others are confined to, or characteristic of, the volcanic and plutonic types. The genesis of C-twins, which characterize the volcanic and plutonic rocks, is, therefore, a matter of particular interest. It is almost unquestionable that most of the plagioclases in the volcanic rocks are of igneous (magmatic) origin. However the origin of plagioclases in the plutonic rocks is not so definite. The plagioclases of the schists, gneisses, and hornfelses discussed in the preceding paragraphs may be considered as representatives of the plagioclases of metamorphic (recrystallization) origin.

---

[12] This is due to the circumstance that plagioclase twinning in the hornfelses is generally finer than that in the schists and gneisses.

As already mentioned the difference in plagioclase twinning between the volcanic and metamorphic rocks is most pronounced in the twins grouped under C-twins. This relation is expressed as follows: The plagioclase of igneous (magmatic) rocks exhibits, in general, fairly high relative frequency of C-twins, while the plagioclase of metamorphic (recrystallized) rocks rarely shows this type of twinning. The factor which controls the formation of C-twins (it will be called C-factor subsequently) is apparently connected with physical, chemical, or physico-chemical circumstances at the time of plagioclase formation. These circumstances differ obviously in the crystallization of plagioclase in rock magma from those in the so-called recrystallization resulting in the formation of metamorphic rocks. Accordingly, it is conceivable that the C-factor is connected with the crystallization of plagioclase from rock magma.

This interpretation at once raises, however, the question of why C-twins occur at all, though rarely, in some metamorphic rocks.[13] This problem is difficult to solve conclusively, because at present little is known about the details of recrystallization in rock metamorphism.

As many authors have stated, the constituents of the metamorphic rocks may gradually dissolve under favorable conditions, resulting in the formation of a solution phase. If this is true, one can expect the occasional occurrence of plagioclases crystallizing directly from a melt phase in such high grade metamorphics as gneisses or hornfelses. The existence of C-twins in these high-grade metamorphics is thus not incompatible with the interpretation of the C-factor mentioned above.

As already described, the frequencies of C-twins in the volcanic rocks depend on the average compositions of the plagioclase in each rock, the rocks with more calcic plagioclase being, in general, relatively richer in C-twins. The writer proposes as a working hypothesis that the C-factor is connected with the crystallization of plagioclase from a melt phase and that its frequency of realization is controlled by the composition of the crystallizing plagioclase.

Proposal of Plagioclase Twin Method

The chief purpose of the present study is to determine the petrological significance of plagioclase twins. The discovery of the difference in twinning, between the igneous and metamorphic plagioclases is, in this connection, very significant.

One of the outstanding unsolved problems of petrology is the origin of rocks generated near the boundary between the magmatic and metamorphic processes, which involves the so-called "granite problem." The study of plagioclase twins may throw new light on this problem.

---

[13] It is evident, from various petrographic observations, that C-twins in these metamorphic rocks are not relicts of original constituents.

On the basis of his interpretation of the C-factor above mentioned, the writer has tried to deduce the mechanism of plagioclase crystallization in rocks of this type and also the mechanism of formation of such rocks.

(a) *The features of plagioclase twinning in various granitic rocks of Japan.*

As already described, plagioclase twinning in the granitic to granodioritic rocks[14] occurring as batholiths and stocks is very similar to that in the volcanic (liparitic to dacitic) rocks. Relative frequencies in the two suites are shown in Figs. 13*a* and 14*a*.

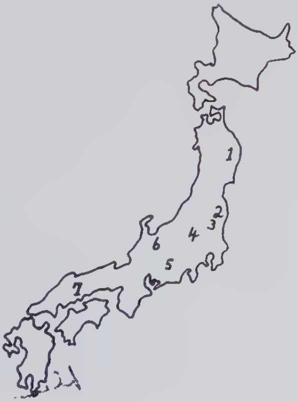

Fig. 12. Outline map of Japan showing localities of the granitic rocks studied.

1. Kitakami Mountainland.
2. Abukuma Plateau.
3. Tsukuba District.
4. Jōetsu District.
5. Ryōke Region.
6. Hida Plateau.
7. Chyūgoku Mountainland.

The features of plagioclase twinning in the granitic rocks[15] occurring as dikes and sheets (minor intrusions) associated with the granites above mentioned are shown in Fig. 13*b* and Fig. 14*b*. As seen from these figures the features of plagioclase twinning of these granitic rocks are, as in the granites above mentioned, similar to those of typical igneous rocks, excepting three rocks whose types of plagioclase twinning are metamorphic.

---

[14] Of these granitic rocks, 4 are from Kitakami Mountainland, 13 from Abukuma Plateau, 3 from Jōetsu District, 6 from Ryōke Region, and 2 from Chūgoku Mountainland (Fig. 12).

[15] Of these, 20 are from Abukuma, 5 from Jōetsu.

Figure 13*c* and Fig. 14*c* show the features of twinning of the granitic to aplitic rocks[16] occurring as lit-par-lit veins in so-called injection gneisses formed from pelitic sediments. The features of twinning in these granitic rocks are fairly similar to those of typical metamorphic rocks, excepting two rocks which carry some C-twins.

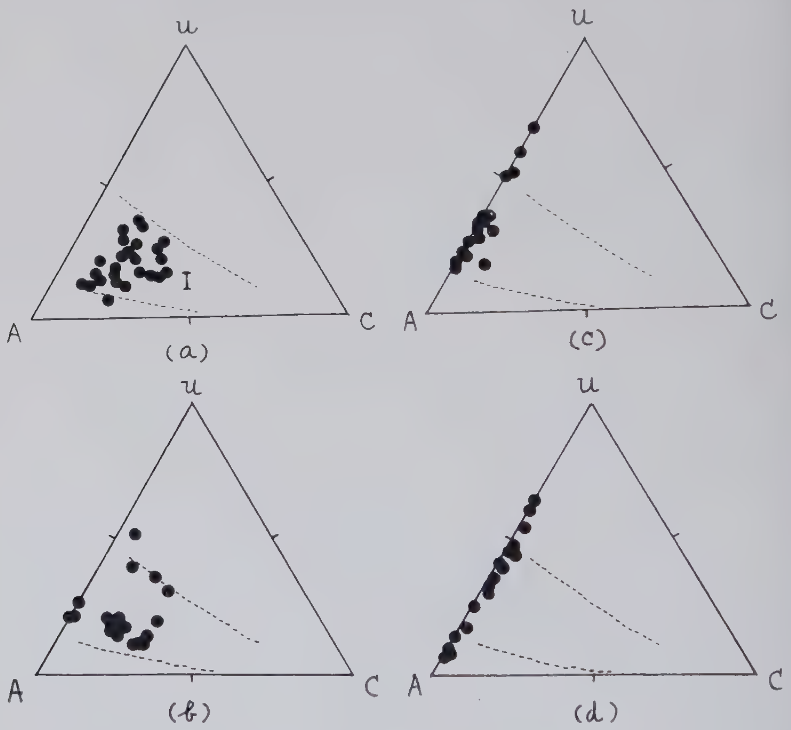

FIG. 13. U:A:C ratios in the plagioclase of various granitic rocks.
(*a*) Granitic rocks occurring as batholiths and stocks.
(*b*) Granitic rocks occurring as dikes and sheets.
(*c*) Granitic rocks occurring as lit-par-lit veins of injection-gneisses.
(*d*) Plutonic-looking rocks of Hida Plateau.
I = Field of typical igneous plagioclase.

Figure 13*d* and Fig. 14*d* show the features of twinning in the plutonic-looking (nebulitic) rocks of Hida Plateau. These plutonic-looking rocks include granitic, monzonitic, and quartz dioritic rocks which are at a glance indistinguishable in mineral composition and texture from typical plutonic rocks. They are intimately associated with gneissic rocks of

---

[16] Of these, 12 are from Abukuma, 2 from Tsukuba, and 13 from Ryōke.

TABLE 5

	1	2
U	12	9
A	88	44
C	0	47
An%	30	35

1—Granitic rock.
2—Tonalite.

more metamorphic appearances in transitional fashion, and have been commonly accepted as orthogneisses injected into gneisses of sedimentary origin. As seen from the figures the features of twinning in these plutonic-looking rocks are, as in the granites of lit-par-lit veins, fairly similar to those of typical metamorphic rocks.

Table 5 shows the modes of twinning in the granitic and tonalitic

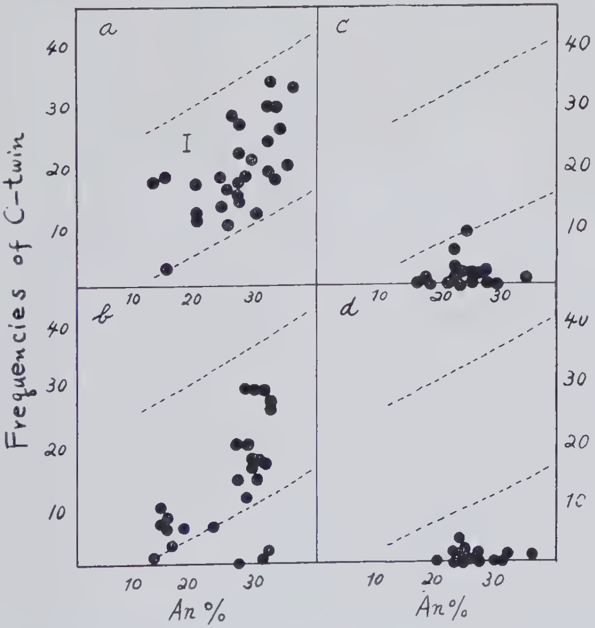

FIG. 14. Relations between the average An% of plagioclase and the frequencies of C-twins in various granitic rocks.

a, *b*, *c*, *d* correspond to those in Fig. 13.

I = Field of typical igneous plagioclase.

rocks at a gneiss-tonalite contact zone of Takanuki District, Abukuma Plateau. Here biotite-gneiss is invaded by tonalite, the marginal part of the former adjacent to the latter being non-gneissose and granitic in appearance. The junction of the granitic rock and the tonalite is fairly distinct, while the relation between this granitic rock and biotite-gneiss is gradational. Under the microscope the granitic rock closely resembles the tonalite in mineral composition (oligoclase, quartz and biotite) and texture (ordinary granitic texture), the two being almost indistinguishable by ordinary petrographic observations. However, as seen from the table these two rocks are quite different with respect to the type of plagioclase twinning. Thus the feature of twinning in the granitic rock is clearly metamorphic, that of the tonalite being markedly igneous.

(b) *Two types of granitic rocks, with respect to the type of plagioclase twinning.*

As described above some granites are igneous, while the others are metamorphic, with respect to the type of plagioclase twinning. Accordingly the granitic rocks may be divided into the following two types:

(i) I-granite, in which the type of plagioclase twinning is igneous.

(ii) M-granite, in which the type of plagioclase twinning is metamorphic.

It is interesting to note that there exist intimate relations between the types of occurrence and the features of plagioclase twinning. Thus most of the granitic rocks occurring as definite intrusive bodies (batholiths, stocks, dikes, and sheets) are I-granites, while the granitic rocks intimately associated with gneissic rocks in transitional fashion (lit-par-lit veins in injection gneisses, plutonic-looking rocks of Hida Plateau, etc.) largely belong to the M-granites.

It seems permissible, therefore, to infer that the I-granites above mentioned are of magmatic origin, while the M-granites are products of some metamorphic processes (granitization). There is no evidence unfavorable to this interpretation.[17]

The so-called "granite problem" which has attracted the attention of many petrologists during the past twenty years is, in short, whether granites are igneous (products of magmatic consolidation) or metamorphic (products of granitization). The plagioclase twin method proposed in the present paper may throw new light on this problem.

---

[17] It is noteworthy, in this connection, that the three exceptional rocks (M-granites) of minor intrusions previously described occur as sheet-like bodies intercalated with biotite gneisses of pelitic sedimentary origin. These M-granites might be products of granitization, probably of sandstones intercalated with pelitic sediments.

SUMMARY

(i) Albite and pericline (acline) twins are commonly present in the igneous as well as in the metamorphic rocks, while the other twins are confined to, or characteristic of, volcanic and plutonic rocks, Carlsbad and albite-Carlsbad twins being the most common.

(ii) Plagioclase twins are divided, from a petrological point of view, into the following two types:

C-twins that include twins after the laws which are confined to, or are characteristic of, the volcanic and plutonic rocks.

A-twins that include twins after the laws which are commonly present in the igneous as well as in the metamorphic rocks.

(iii) The approximate frequencies of untwinned plagioclase and the above twin types in each rock can be estimated with the ordinary petrographic microscope, without the universal stage.

(iv) The plagioclase of volcanic rocks carries untwinned plagioclase, C-twins, and A-twins, C-twins being relatively abundant in the rocks with more calcic plagioclase.

(v) The features of plagioclase twinning of most plutonic rocks are fairly similar to those of the volcanic rocks.

(vi) The plagioclase of metamorphic rocks is mainly composed of untwinned plagioclase and A-twins, C-twins being absent or inconspicuous. The frequency of A-twins in these rocks depends on the average grain size of plagioclase in each rock.

(vii) The difference in plagioclase twinning between the igneous and metamorphic rocks may be attributed to differences in the mechanism of plagioclase formation in these rocks. The factor which controls the formation of C-twins seems to be related to the crystallization of plagioclase from a melt phase, the frequency of the development of this twin being controlled by the composition of the crystallizing plagioclase.

(viii) On the above interpretation as to the genesis of C-twins, one may be able to deduce the mechanism of plagioclase crystallization in the rocks formed near the boundary between the magmatic and metamorphic processes, and thus establish the mechanism of formation of the rocks themselves.

(ix) Granitic rocks are divided, with respect to the mode of plagioclase twinning, into the following two types:

I-granite, in which the mode of plagioclase twinning is igneous.

M-granite, in which the mode of plagioclase twinning is metamorphic. Most of the granitic rocks occurring as definite intrusive bodies are I-granites, while the granitic rocks intimately associated with gneissic rocks are mostly M-granites.

(x) It is suggested that I-granites are of magmatic origin, while M-granites are products of some metamorphic processes (granitization).

Manuscript received May 15, 1951.

NOTES AND NEWS

JAROSITE FROM THE CALIFORNIA TERTIARY

Louis I. Briggs, Jr., *University of Michigan, Ann Arbor, Michigan.*

Jarosite-bearing Tertiary sediments crop out along the west side of the San Joaquin Valley in the foothills of Diablo Range, about 10 miles south of Los Banos, California. The mineral has been observed microscopically in Paleocene siltstone of the Martinez formation, and in Eocene glauconitic and laminated sandstone and in diatomaceous shale in the lower portion of the Kreyenhagen formation. In all but the glauconitic sandstone, the grains of jarosite are so minute as to prevent positive identification by ordinary microscopic means; however, larger idiomorphic crystals intimately associated with glauconite yield grains sufficiently large to be identified with the petrographic microscope.

The glauconite-jarosite bed occurs in a basal pebble conglomerate that reaches a maximum thickness of 1–2 feet and is exposed for about one-eighth mile approximately 2½ miles southeast of Ortigalita Creek in Sec. 35, T. 11 S., R. 10 E., M.D.B. and M. Both to the north and to the south the bed is covered by Pleistocene terrace mantle and by minor soil creep from the overlying diatomaceous shale. Further southward along the strike of the beds, jarosite has not been observed in outcrops of similar strata. The pebble conglomerate disconformably overlies anauxitic quartzose sand and brown claystone of the Tesla(?) formation, and grades vertically through approximately 100 feet of greensands, quartzose sandstones, radiolarite, and cross-bedded sandstone and shale into the Kreyenhagen diatomite which in this area is about 700 feet in thickness. Efflorescent gypsum occurs abundantly as thin veins of selenite throughout the section.

Macroscopically, jarosite bears a close resemblance to "limonite" and is difficult to distinguish from limonitic or other ferruginous incrustations in the field. The glauconitic pebble conglomerate is colored a pale yellowish brown by jarosite which binds together the glauconite and other mineral constituents, lending a dull earthy appearance to the rock which in places has a slightly resinous luster, due most likely to patches of more coarsely crystalline jarosite. Nowhere is jarosite coarse enough to enable individual grains to be seen with the hand lens.

Petrography

Most of the jarosite in a thin section of the glauconitic sandstone occurs as drusy clusters, although in voids and in the argillaceous matrix individual grains reach a diameter of 0.01 to 0.05 mm. There is a strong tendency for the mineral to form aggregates of anhedral grains and even the larger and more euhedral grains are characteristically grouped in clusters (Pl. 1). In the rock section studied, jarosite comprises 30–40 per cent of the bulk, the remainder being made up largely of glauconite. Quartz, orthoclase, and irresolvable argillaceous matrix make up less than 15 per cent of the mineral grains.

Glauconite shows a considerable range of optical and textural properties. Whereas most of the grains appear to be granular aggregates of very small crystals, here and there are optically continuous grains with bent micaceous cleavage and characteristic ovate outline (Pl. 1, Fig. 1). The optic angle varies from 0° to 25° ±5°. Pleochroism was noted with X=pale yellowish green, Y and Z=olive-green, with $Z \geqq Y > X$. Upon weathering, glauconite assumes various shades of greenish brown, presumably due to the formation of ferric hydroxide. Most of the grains in the samples studied show some degree of weathering.

Of particular interest is the occurrence of jarosite within the glauconite, or drusy patches of jarosite enclosing scattered fragments of glauconite that are optically continuous. In fact all of the intermediate relationships between these two minerals may be observed in a single thin section. There can be little doubt that jarosite has replaced the glauconite.

Separation and Properties of Jarosite

A fair separation of jarosite from the other mineral constituents of the rock was made by disaggregation, sieving, and centrifuging the fraction finer than the 200-mesh Taylor sieve with bromoform (density 2.80). However, glauconite containing jarosite and pure jarosite could not be separated in this manner, nor could jarosite be further concentrated by its magnetic properties in the Frantz separator. Material thus obtained was used to determine the lower refractive index (N_e) which distinguishes potassium jarosite from natrojarosite and other members of the jarosite group. The optical properties are as follows:

$N_e=1.714\pm0.003$
$N_0>1.81$
Uniaxial—.(The typical division of the basal section into six biaxial segments was not observed).
X=very pale greenish yellow.
Z=deep golden yellow.
$Z>X$.
$N_0-N_e=0.1$ *ca.*, extreme birefringence.

Measurements of interfacial angles were made with use of the universal stage, giving angles of approximately 55° and 91° which agree closely with those recorded by Ford (1932, p. 769) for jarosite (*rr′* $(10\bar{1}1 \wedge \bar{1}101)$ $=90°45'$, *cr* $(0001 \wedge 10\bar{1}1 = 55°16')$.

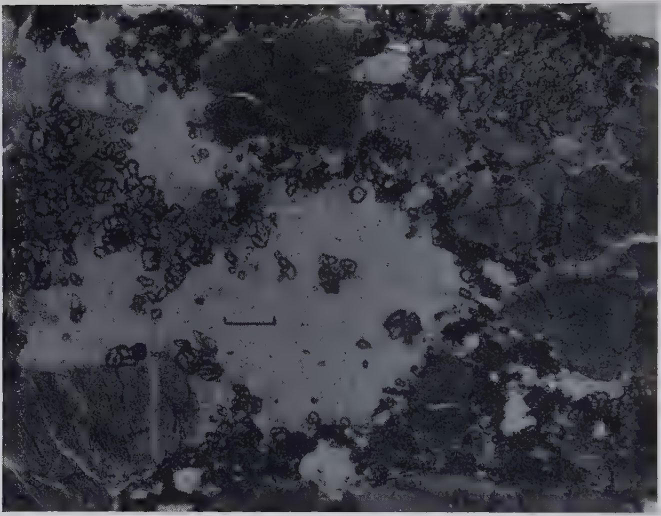

FIG. 1. Photomicrograph of jarosite-glauconite sandstone showing dark patches of anhedral jarosite and larger euhedral grains (with dark borders). Larger ovoid grains are glauconite which photographs in various shades of gray. Note the vermicular glauconite with strong cleavage in the lower portion of the photograph, and the mixture of jarosite and glauconite in the upper right. Distance between marks on the scale is one-tenth millimeter. Magnification 70×.

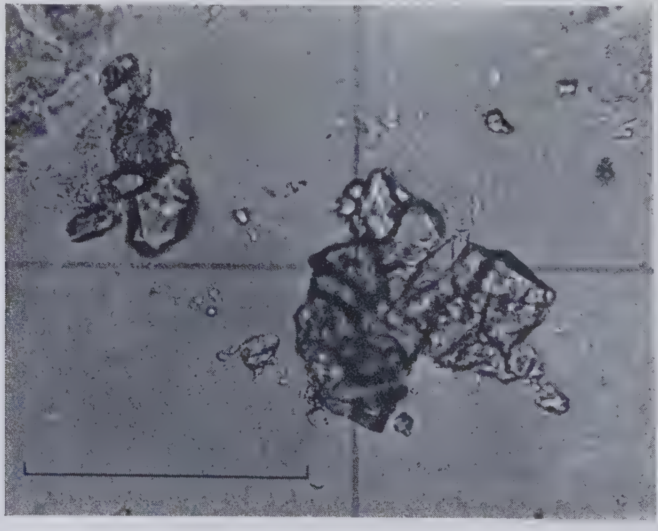

FIG. 2. Photomicrograph of the central portion of Fig. 1, much enlarged, showing facets on the jarosite crystals and the common occurrence of the mineral in clusters. Grains such as these were used to measure interfacial angles. Distance marks on the scale is one-tenth millimeter. Magnification 375×.

Photographs are published with permission of California Division of Mines, O. P. Jenkins, Chief.

One characteristic property of the minute grains is their symmetrical extinction observed on rhombohedral crystals which do not show the development of the basal pinacoid. The basal pinacoid is characteristic of larger grains, which indicates that rhombohedral faces are the first to develop and that subsequent growth of the crystal is more rapid along directions perpendicular to the *c*-axis, leading to the tabular form of the larger grains.

Origin

The intimate occurrence of jarosite with glauconite in a section of Tertiary sediments that is characterized by greensands leaves little doubt that jarosite is formed from glauconite.* The common association of efflorescent gypsum in this same stratigraphic section, in fact in the entire Cretaceous and Tertiary section, which in this area is over 40,000 feet in thickness, indicates a common genesis for both minerals. It is probable that reaction of sulfate-bearing interstratal solutions with glauconite has led to the formation of jarosite from glauconite-bearing sands and shales, and to the formation of gypsum from calcareous tests of micro-organisms contained in the Cretaceous and Tertiary shales. The sulfate ions very likely originated from the oxidation of pyrite such as was suggested for the Glenwood formation by Stanley A. Tyler (1936, p. 72). Cores from wells bored in the adjacent San Joaquin Valley contain considerable pyrite in the form of pyritized spots, foraminifera, and plant

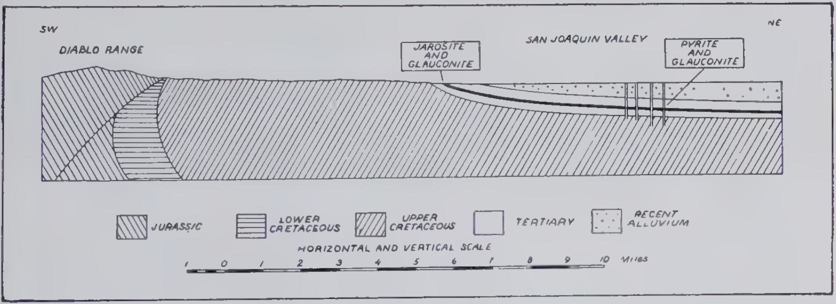

FIG. 1. Structure-section across the eastern foothill belt of Diablo Range and a part of the adjacent San Joaquin Valley. Distribution of the glauconite-rich Tertiary strata is shown by the heavy black line. Pyrite is found with glauconite in well borings beneath the San Joaquin Valley and jarosite is found with glauconite where the strata outcrop in the foothills.

---

* Stanley A. Tyler (1936, p. 59) described similar relations between glauconite and jarosite existing in the Glenwood formation overlying the St. Peter sandstone in Wisconsin.

remains, and in all records to which the writer has access the pyrite-bearing beds are interstratified with glauconite-bearing beds, indicating that glauconite and pyrite are stable in the buried sediments (Fig. 1). Pyrite has not been observed in the outcrop area. In all, over 60 thin sections and 20 heavy mineral separations of Cretaceous and Tertiary sediments were studied, and in none of the specimens is pyrite present. Furthermore, S. N. Daviess (1946) noted pyrite in heavy mineral assemblages from well cores in this area but did not observe jarosite, thus it is reasonable to assume that jarosite does not exist in the deeply buried sediments.

Conclusion

The formation of the hydrous sulfate of potassium and ferric iron, jarosite, in Tertiary sediments along the west side of the San Joaquin Valley is a near-surface diagenetic process involving the reaction of sulfate-bearing interstratal solutions with glauconite. Efflorescent gypsum in the same strata very likely is formed coeval with jarosite by reaction of these solutions with calcium carbonate tests of micro-organisms. There is reasonable assurance that the sulfate ions are released to the interstratal solutions by oxidation of pyrite, present in beds of the same formations beneath the San Joaquin Valley.

REFERENCES

Daviess, S. N., Mineralogy of late Upper Cretaceous, Paleocene, and Eocene sandstones of Los Banos district, west border of San Joaquin Valley, California: *Am. Assoc. Petroleum Geologists, Bull.*, **30,** 63–83 (1946).

Ford, W. E., A Textbook of Mineralogy (Dana) 4th ed., New York: John Wiley & Sons, Inc., (1932).

Tyler, Stanley A., Heavy minerals of the St. Peter sandstone in Wisconsin: *Jour. Sedimentary Petrology*, **6,** 55–84 (1936).

FLUID INCLUSIONS IN BERYL AND QUARTZ FROM PEGMATITES OF THE MIDDLETOWN DISTRICT, CONNECTICUT

Eugene N. Cameron, Robert B. Rowe, and Paul L. Weis,
University of Wisconsin, Madison, Wisconsin.

During the past year and one-half, the writers have studied fluid inclusions in quartz and beryl from 9 pegmatites of the Middletown district, Connecticut (Cameron and Shainin, 1947), in an attempt to determine the role of temperature in the formation of the pegmatites. The visual method, by which inclusions are observed under the microscope during heating, has been used exclusively in the study. Each temperature determination has been repeated at least once, as a precaution against leakage of the inclusions.

A number of sections of quartz from the Case pegmatites have been examined. Three types of fluid inclusions have been found in the mineral, as follows:

(1) Secondary inclusions situated along healed fracture planes. These are by far the most abundant type. The inclusions consist of a liquid phase plus a vapor phase that shrinks on heating and finally disappears. Four inclusions of this type in quartz from the Case No. 1 pegmatite gave temperatures of disappearance ranging from 316° C. to 343° C.

(2) Disseminated irregular inclusions. Most of these occur in the vicinity of healed fractures and are probably secondary. The type is divisible into two groups. One group consists of two-phase inclusions that behave like those of type (1) when heated. In 20 inclusions of this group in quartz from the core of the Case No. 2 pegmatite the vapor phase disappears at temperatures ranging from 199° C. to 292° C. The second group consists of inclusions in which first the vapor phase shrinks, then the liquid-vapor boundary fades and disappears. In 6 inclusions of this group in quartz from the core of the Case No. 2 pegmatite and in 1 inclusion in quartz from the wall zone, temperatures of boundary disappearance range from 320° C. to 390° C.

(3) Disseminated negative crystals, apparently primary. These contain a vapor phase and a liquid phase. When they are heated, first the vapor phase shrinks, then the liquid-vapor boundary fades and disappears. Temperatures of disappearance in 6 inclusions of this type from quartz of the core of the Case No. 2 pegmatite range from 293° C. to 347° C.

The number of inclusions for which data are given above is limited because most fluid inclusions in quartz fracture and leak before the temperatures of filling are reached.

Sections cut from specimens of quartz from the core of the Case No. 2 pegmatite, given by Cameron to Ingerson some years ago and studied by Ingerson (1947, p. 387) and Scott (1948, p. 650), were included in the study. Dr. Ingerson kindly returned the specimens for our use. He reported temperatures of disappearance of the vapor phase ranging from 153° C. to 165° C. Scott reported a value of 165° C. for a single specimen (46-C-3) run by the decrepitation method. We have been unable to duplicate the findings of these investigators. In a large number of sections of quartz cut from various specimens of the core, the only inclusions found that show disappearance of the vapor phase by shrinkage alone—type (1), and type (2) in part—are either definitely secondary or suspect of being secondary. Furthermore, temperatures of disappearance of the vapor phase range from 199° C. to 343° C. The significance of the temperature values obtained for the apparently primary inclusions of type (3) and for those of type (2) that behave similarly is uncertain.

More than 2,000 fluid inclusions in beryl crystals from the various pegmatites have been studied, and temperatures of disappearance of vapor phase or of phase boundary in 441 fluid inclusions have been determined. We have had little trouble with leakage of inclusions in beryl during heating. Fluid inclusions in this mineral are of 4 principal types:

(1) Disseminated negative crystals with long axes parallel to the *c*-axis of beryl.
(2) Disseminated tubular inclusions with long axes parallel to the *c*-axis of beryl.
(3) Disseminated rounded, elongate, or irregular inclusions, unoriented with respect to crystallographic elements.
(4) Rounded, elongate, or irregular inclusions and negative crystals arranged along planes or curving surfaces of random orientation. Intersections of planes or surfaces are common.

Inclusions of types (1) and (2) are apparently primary. The origin of inclusions of type (3) is uncertain. Inclusions of type (4) are definitely secondary.

According to their behavior when heated, inclusions of types (1) and (2) are divisible into three groups, as follows:

Group A—Fluid inclusions having a vapor phase that shrinks on heating and finally disappears. Only beryl from the Selden east pegmatite contains inclusions of this group. The vapor phase disappears in various inclusions at temperatures ranging from 210° C. to 353° C.

Group B—Fluid inclusions in which the vapor phase expands on heating and finally occupies the entire cavity. Temperatures of disappearance of the liquid phase range from 305° C. to 401° C. Inclusions of this group occur in 4 of the pegmatites studied.

Group C—Fluid inclusions consisting of 3 phases (liquid-liquid-vapor) at room temperatures. At or somewhat below 31° C., one liquid phase disappears; this phase is probably liquid carbon dioxide. With further heating the vapor phase shrinks and finally disappears in turn, at temperatures ranging from 230° C. to 455° C. All inclusions of types (1) and (2) found in beryl crystals from the Case pegmatites are of this type. We are therefore unable to check the value of 175° C. determined by Ingerson (1947, p. 387) from a single inclusion in a beryl crystal from the Case No. 2 pegmatite.

The behavior of one inclusion of the negative crystal type in a crystal from the Bordonaro south pegmatite suggests that there may be additional group of inclusions in beryl. When this inclusion is heated, the vapor-liquid boundary remains unchanged in position but fades and finally disappears at 335° C. Four irregular inclusions arranged along a plane in a beryl crystal from the Case No. 1 pegmatite behave similarly. Temperatures of disappearance for these inclusions range from 311° C. to 316° C.

Curves obtained by plotting temperature against volume of liquid for the inclusions of group *A* correspond closely to calculated curves for hypothetical inclusions consisting of pure water. As the influence of composition on the vapor-liquid volume ratio cannot be predicted from available data, this correspondence does not prove that inclusions of group *A* approach pure water in composition, but comparable curves for the inclusions of group *C* differ markedly from those for pure water. An attempt to determine molar concentrations by measuring freezing points of the liquid phases is being made.

The following conclusions are drawn from the results of the study to date:

(1) Quartz from the Case pegmatites is unsatisfactory for temperature studies by fluid inclusion methods. Most of the inclusions are secondary; others are suspect of being secondary. Inclusions that appear to be primary are few, and their significance in terms of temperatures of crystal formation is in doubt. The majority of the inclusions in quartz fracture and leak at temperatures below the true temperatures of cavity filling or disappearance of the liquid-vapor phase boundary. The source of the low values obtained by Scott by the decrepitation method is uncertain. The value may represent the temperature of bursting of the definitely secondary inclusions. If so, the inclusions must have burst at temperatures below the true temperatures of filling, as indeed would be expected from the present study. The same reasoning would hold if the values represent bursting of one or both types of disseminated inclusions. Correspondence between Dr. Ingerson and the writers has not as yet indicated a satisfactory explanation of the discrepancy between his results and ours. It may be, however, that the differences are related to the fact that the vapor bubbles are very difficult to see in the final stages of shrinkage. This caused difficulties in the early stages of the present investigation, but ultimately we found that satisfactory observations could be made and duplicated by different observers if the upper surfaces of the crystal plates studied were given a very high polish. Considerable adjustment of the illumination system was also necessary.

(2) Even if the pressure at time of crystal formation is known, temperatures at which the vapor phase disappears in fluid inclusions in beryl cannot be taken to indicate the temperatures of crystal formation until more is known of the compositions of the fluid inclusions. The behavior of the inclusions through a broad range of temperature must be determined as a clue to composition. Preliminary tests indicate that the lower limit of this range is well below 0° C.

(3) The use of fluid inclusions in pegmatite minerals for determining temperatures of formation requires full knowledge of the kinds of inclusions present and their behavior when heated. It seems apparent that decrepitation curves of these minerals cannot be interpreted satisfactorily on the basis of microscopic inspection of inclusions at room temperatures.

(4) The physical characteristics of fluid inclusions in quartz are difficult to determine because the inclusions are minute. In beryl crystals studied, all inclusions that appear to be primary consist of materials that are highly mobile at room temperatures and are evidently of low viscosity. This generalization holds for beryl from border zones and wall zones as well as for beryl from inner zones and replacement bodies. None of the cavities occupied by the inclusions contains solids. None shows linings that would indicate that material other than beryl has been precipitated on the walls during cooling of the inclusions since their formation. If the inclusions are primary and are true samples of the mother liquors from which beryl crystallized, then (1) the mother liquors had the physical characteristics of hydrothermal solutions, not magmas, and (2) the mother liquors of crystals formed in border zones did not contain all the constituents necessary for the quartz, feldspars, and micas

> that formed subsequently in the inner zones of the pegmatites. A search for conclusive evidence of the origin of the inclusions is now needed, for if inclusions of types (1) and (2) are truly primary, and if current theory of the origin of fluid inclusions is valid, the pegmatites formed in open systems, not in closed or restricted (Cameron, Jahns, McNair, and Page, 1949, pp. 99–105) systems. We suggest, however, that even if the inclusions are ultimately proved to be primary, the assumptions underlying current theory of liquid inclusions should be reviewed, and they should be tested by laboratory studies of liquid inclusions in crystals precipitated from polycomponent solutions. Both the development and the composition of the inclusions should be investigated.

The present investigation has been carried on as a project of the Wisconsin Alumni Research Foundation. We gratefully acknowledge this support. We also wish to express our thanks to Dr. E. Ingerson for useful comments.

References

Cameron, E. N., Jahns, R. H., McNair, A. H., and Page, L. R. (1949), The internal structure of granitic pegmatites: *Econ. Geol., Mon.* **2,** 115 pp.

Cameron, E. N., and Shainin, V. E. (1947), The beryl resources of Connecticut: *Econ. Geol.,* **42,** 353–367.

Ingerson, E. (1947), Liquid inclusions in geologic thermometry: *Am. Mineral.,* **32,** 375–389.

Scott, H. S. (1948), The decrepitation method applied to minerals with fluid inclusions: *Econ. Geol.,* **43,** 637–654.

APPARATUS FOR THE SEPARATION OF MINERAL GRAINS

F. E. Senftle, *Department of Metallurgy, Massachusetts Institute of Technology, Cambridge, Massachusetts.*

It is often necessary to separate a large number of microscopic mineral grains from an assemblage of various mineral grains. For example, if one desires a sample of a very pure mineral, it is often necessary to separate the pure mineral grain by grain from the gangue-locked grains. The usual method of picking individual grains with a stylus and tweezer is laborious and time-consuming, especially when a large number of grains is required. The apparatus to be described was constructed to facilitate and speed up the picking method.

For the most efficient use of a grain segregating apparatus, a concentrated sample of the desired mineral should be used. Thus, a rough purification of the mineral should be made in the conventional manner with an isodynamic separator, a superpanner, or heavy liquid separation. The mineral should then be screened as closely as possible. In this work 65 to 100 mesh was used.

The apparatus consists of three parts; namely, the distribution drum, the turntable and air ejector (see Fig. 1) and the vacuum picker (see

Fig. 2). The mineral concentrate is charged into the distribution drum which is mounted on a revolving shaft. The mineral is admitted to the drum through a cork plugged hole in the side of the drum. On the opposite side of the drum is a 3/8″ hole covered with a thin piece of aluminum foil cemented to the wall of the drum. The foil in turn is punctured with a small hole about the average size of the mesh being separated. The exit hole was made in the foil rather than directly in the side of the drum for two reasons: (1) the wall is thick relative to the size of the particles and such a hole acts like a tube which is easily clogged, and (2) the foil facilitates the changing of the hole size if a different size mesh is to be separated. The number of grains spilled out onto the revolving turntable directly below on each revolution of the drum is controlled by the size of the small hole in the foil. The most convenient size is found by trial and error starting with a small hole and enlarging it until the desired distribution is obtained.

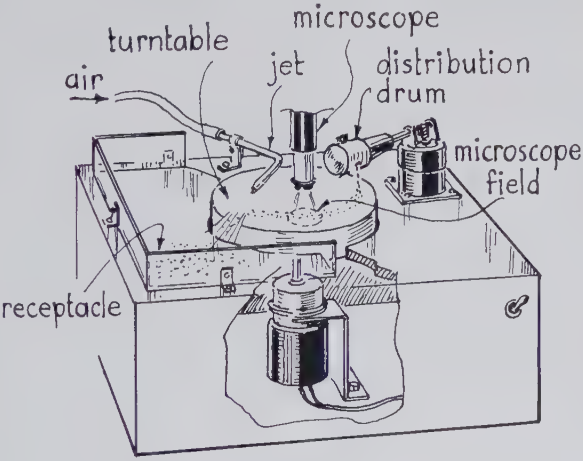

Fig. 1

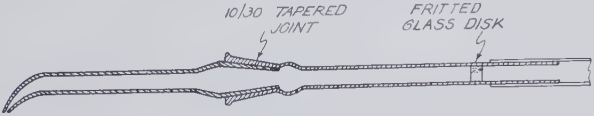

Fig. 2

The turntable on which the grains fall is a 3″ diameter stamped aluminum "can cover" mounted on a slowly revolving shaft. It carries the particles into the field of the microscope where the desired grains are picked. The undesired grains (locked grains, gangue, etc.,) are allowed to remain on the turntable. As they are carried in front of the ejector, an air jet blows them into the discard receptacle. White or black paper is glued to the top of the turntable to facilitate identification of the desired grains.

As the assemblage of grains is brought into the field of the microscope, the operator picks the desired grains with the vacuum picker shown in the figure. This consists of a glass tube drawn out to a fine opening at one end and connected to a water filter pump at the other end. Close to the vacuum end of the glass tube is a sintered glass disk. As the grains are sucked up, they collect in the tube just in front of this disk. To remove the grains, the tube is made in two parts connected by a ground glass joint secured with small springs (not shown in diagram).

The apparatus is built on a $5'' \times 6'' \times 9''$ metal box. The turntable motor is geared to revolve at $3\frac{1}{2}$ turns per minute at 110 volts, and its speed is further reduced to about $\frac{1}{4}$ turns per minute by reducing the voltage with a Variac control. The distribution drum motor is also geared down and controlled by a Variac. Its speed will vary with the size of hole used. In this case 100 to 200 turns per minute was found to be a convenient speed. The discard receptacle is made from a plastic box cover cut to fit close to the turntable. It might be pointed out that the distribution drum should not be made of plastic material. The electrostatic charges built up on such a drum tend to clog the orifice restricting the flow of particles.

Where this type of work is to be conducted over an extended period of time, eye strain on the operator may be reduced by projecting the field on a small screen with a prism. To do this, however, requires stronger illumination than can be obtained with an ordinary microscope lamp.

The author wishes to thank Mr. Leonard Nanis and M. D. Fuerstenau for drawing the sketches. This apparatus was built in the Richards Mineral Engineering Laboratory at the Massachusetts Institute of Technology and was sponsored by the Research Division of the Atomic Energy Commission.

UNIT CELL OF SCHAIRERITE

C. W. Wolfe and Alice Caras, *Boston University, Boston, Mass.*

Schairerite ($Na_2SO_4 \cdot Na(F_{.814}Cl_{.186})$) was discovered in the Searles Lake complex of salts by Foshag and described by him in 1931. The mineral occurs with a pronounced trigonal habit with the suggestion of rhombohedral symmetry. Artificial crystals of the same substance had previously been synthesized by Schairer (1930) of the Geophysical Laboratory for whom the mineral was named. Dr. Clifford Frondel of Harvard in a paper on *Habit Variations of Sodium Fluoride* (1940) gave x-ray data obtained from a natural crystal of schairerite. In this paper he suggested that the elements he obtained "gave a hexagonal cell inconsistent with the morphology." He suggested a rhombohedral interpretation with a tripling of his value for c_0.

Crystals of the natural mineral came to the attention of the senior author, and it was decided to investigate the discrepancy between the morphological and x-ray values. Results of that investigation follow.

Morphology.—Foshag noted four forms: $c\{0001\}$, $m\{10\bar{1}0\}$, $r\{10\bar{1}1\}$, and $e\{01\bar{1}2\}$. The authors examined six crystals and did not observe any additional forms. It should be noted, however, that although the forms r and e apparently show a rhombohedral development which conforms to the rhombohedral centering rule of $h+i+l=3n$, the development of the prism $\{10\bar{1}0\}$ is not at all typically rhombohedral. The typical and expectable prism in rhombohedral minerals is $\{11\bar{2}0\}$. On morphological grounds alone, then, a rhombohedral symmetry for schairerite is to be questioned. A trigonal symmetry, however, is obvious. Reproductions of Foshag's figures 3 and 4 are shown, Figures 1 and 2, to demonstrate the apparently non-rhombohedral symmetry of the mineral. Foshag gives 2.764 as an average value for c/a from 24 measurements of r faces; from 8 measurements of e faces he obtained 2.749. Our best average value is 2.752. Foshag gives as his preferred value 2.7634 which is not appreciably different.

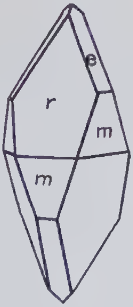

FIG. 1. Schairerite. (Figure 3 of Foshag.)

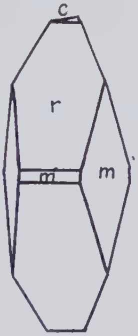

FIG. 2. Schairerite. (Figure 4 of Foshag.)

X-Ray Data.—Rotation, 0, 1st, and 7th layer line photographs were taken about the c axis. There was no hint in the rotation picture of the possible tripling of the c axis which was suggested by Dr. Frondel. Since c_0 was of the order of 19kX units and since Cu radiation was used, there was doubt in the authors' minds that the 0 or 2nd layer line spots could be screened adequately while taking the 1st layer line. For this reason, a

7th layer line picture was obtained upon which any rhombohedral distribution of lattice planes could be noted. None was observed. Photographs about the c axis gave the following data:

Non-rhombohedral symmetry
No systematic omissions
$c_0 = 19$ kX ca.
$a_0 = 7.05 \pm 0.02$ kX units
$m_0 = 12.22 \pm 0.03$ kX units

Since Frondel had given a_0 equal to 12.12 and c_0 equal to 19.19, it seemed desirable to check the chosen a_0 by rotations around the a and m axes. Rotation and 0-layer line photographs were taken about each of these axes and the results showed unequivocally that Frondel's a_0 was actually m_0 of the lattice. A value for c_0 was obtained from the 0-layer line picture about the m axis $[10\bar{1}0]$. Interpretation of these pictures gives the following data:

Non-rhombohedral symmetry (all orders of (0001) were present, not just $3n$ orders).
$c_0 = 19.33$ kX units.

Crystal class.—The trigonal symmetry of the crystals restricts the crystal class to the following:

$$3,\ \bar{3},\ 3m,\ 32,\ \bar{3}2/m,\ \bar{6},\ \bar{6}m2$$

An examination of the crystals on our own part and of those drawn by Foshag seems to indicate that four of these may be eliminated for the following reasons:

Class 3 is not proper since there is no center of symmetry in that class and a center of symmetry seems to be present on most crystals. Foshag's figure 4 (our figure 2), however, does not indicate a center of symmetry. The major part of the evidence indicates, however, a higher symmetry operation than is present in class 3.

Class $3m$ is unlikely because it does not account for the typical symmetrical relationship of the bottom faces to the top faces, or of the generally equal development of the six faces of $\{10\bar{1}0\}$.

Class $\bar{6}$ is eliminated because of the presence of equal development of six faces of the prism $\{10\bar{1}0\}$ and because there is no hint of an horizontal plane of symmetry on most crystals.

Class $\bar{6}m2$ is eliminated because of the absence of a horizontal symmetry plane on the crystals.

X-ray Weissenberg layer line photographs of class $\bar{3}$ minerals would not show planes of symmetry, but on the 0 and 7th layer line pictures around [0001], symmetry planes are noted in each 60° position; therefore, class $\bar{3}$ is eliminated as a possibility.

The trigonal trapezohedral class 3 2 and the hexagonal scalenohedral class $\bar{3}\ 2/m$ remain as possibilities, and these cannot be distinguished on the basis of x-rays. The distinction between these classes must be based on morphology, and morphological data is inadequate for the determination. A piezoelectric determination might also serve to establish the 3 2 symmetry, but equipment for this test is not available to the authors.

Space Group.—No systematic omissions were noted for any of the planes of reflection. If the symmetry class be 3 2 the space group would be $C312$; if it is $\bar{3}\ 2/m$ the space group would be $C\bar{3}1m$.

Cell Contents.—If we assume the composition of the schairerite to be $Na_2SO_4 \cdot Na(F_{.814}Cl_{.186})$ as given by Foshag's analysis and accept Foshag's specific gravity of 2.612, the contents of the unit cell may be established, using our cell volume of 832.0 kX^3. We find that there would be 7 of the simplest molecules in the unit cell. Frondel obtained 21, but his cell volume is approximately 3 times ours because he used m_0 for a_0. The cell contents, then, are $Na_{14}(SO_4)_7Na_7(F_{5.70}Cl_{1.30})$. Foshag has indicated the probable isomorphous relationship of the fluorine-chlorine in the composition, and the non-rational quantities of these elements in the unit cell bear out his conclusion.

The calculated specific gravity obtained from this cell is 2.60 which is in close agreement with the 2.612 specific gravity obtained in heavy liquids by Foshag. We made a specific gravity determination by using 10 small crystals on the Berman Balance and obtained 2.63. Foshag's measurement is in closer agreement with the calculated value.

Conclusions.

Lattice Mode: Hexagonal—P (not rhombohedral).
Crystal class: 3 2 or $\bar{3}\ 2/m$.
Space Group: $C\ 312$ or $C\ \bar{3}1m$.
Lattice periods: a_0 7.05, c_0 19.33. $c_0/a_0=2.742$.
Cell contents: $7[Na_2SO_4 \cdot Na(F \cdot Cl)]$.
Specific gravity: 2.60 calc.; 2.612, 2.63 meas.
Morphological linear ratio:
  $c=2.7634$, Foshag
  $c=2.752$, Wolfe and Caras

References

Foshag, W. F., *Am. Mineral.*, **16**, 133 (1931).
Frondel, C., *Am. Mineral.*, **25**, 352 (1940).
Foote, H. W., and Schairer, J. F., *Jour. Am. Chem. Soc.*, **52**, 4202 (1930).

A NEW DUMORTIERITE LOCALITY FROM MONTANA

Charles E. Graham and Forbes Robertson*

The mineral dumortierite, a boron-aluminum-silicate, is reported for the first time in Montana. It is found in a foliated pegmatite in the Ruby Range, in secs. 3 and 4, T. 7 S., R. 6 W., about 14 miles east of Dillon, Montana, as shown on the index map.

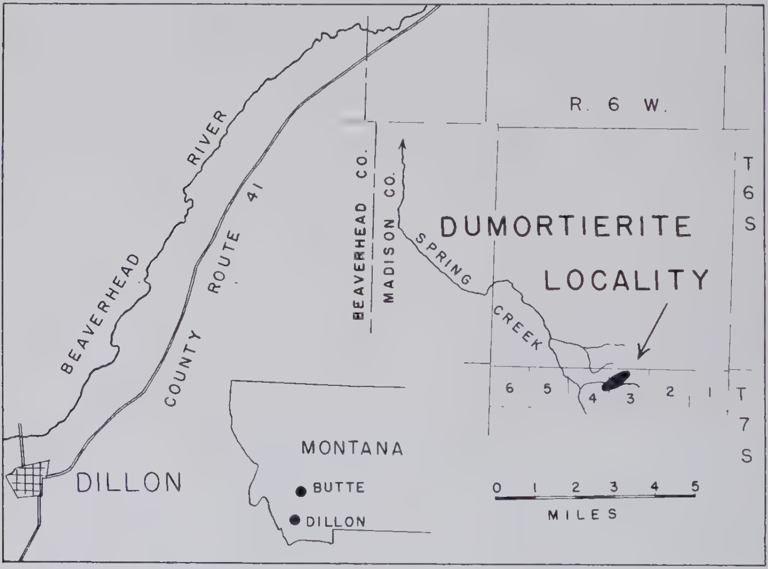

Fig. 1

The pegmatite occurs in the pre-Cambrian Pony series of schists and gneisses, and lies parallel to the foliation planes in the metamorphic rocks. It can be traced along the strike, intermittently, for more than 2500 feet in a N. 50°–65° E. direction, and has a maximum width of about 60 feet. The pegmatite is composed of microcline-microperthite, quartz, oligoclase, and muscovite. Black tourmaline and the royal blue dumortierite are found in quartz-rich pods or irregular vein-like bodies within the pegmatite. The boron minerals are sporadically distributed at several points along the strike and comprise several per cent of the rock, locally.

The physical properties of the Ruby Range dumortierite agree closely with previously published descriptions. They are as follows: crystals acicular to fine columnar with prominent longitudinal striations; twinning on {110} with *c* the axis of rotation; distinct {100} cleavage; longitudinal and transverse partings, the basal parting making an angle with {001} of about 10° ± 6°; hardness 7; specific gravity about 3.25; infusible with loss of color on ignition; insoluble in acids.

---

* University of Iowa, Iowa City, Iowa, and Montana School of Mines, Butte, Montana.

The optical properties differ in some respects from those previously published. These properties are: optic plane is parallel to (010); X = c; twinning on {110} with the angle between adjacent optic planes 61° to 64°; $2V = 56°$; dispersion rather weak $v > r$; $n_\alpha = 1.661 \pm .001$, $n_\beta = 1.678 \pm .001$, $n_\gamma = 1.683$ (calculated); $n_\gamma - n_\alpha = .022$; strongly pleochroic, in thin section X = light steel blue, Y = Z = colorless; in fine grains X = brilliant blue, Y = Z = colorless to very faint yellow. Inclusions are very few including: rectangular colorless, minute irregular opaque, and very small dumortierite grains.

Qualitative spectrographic analysis indicates silicon, aluminum, and boron as the essential constituents in the silicate mineral. The boron doublet 2496.8, 2497.7 is conspicuous on the film. Titanium is present in an amount which suggests a minor essential element as is the case in the Nevada, California, and Washington (1, 2, 3) dumortierites. The titanium lines checked include 5036.5, 5025.6, 5014.2, 4991.1, and 4870.1. Copper is present in trace amounts, with lines 3273.9 and 3247.5 visible. Iron is a very minor impurity and may originate in the opaque inclusions. Other rock-forming constituents are absent.

Other minerals found with the blue dumortierite include a green variety of dumortierite which is strongly pleochroic in fine grains with X = brilliant apple green, blue-green, or yellow green, Y = Z = colorless. It is a conspicuous minor mineral which is intimately associated with the blue variety. The refringence is somewhat greater than the blue dumortierite, whereas 2V is smaller. Several other pleochroic minerals which are thought to be rather rare species of boron silicates have been recognized but not positively identified.

ACKNOWLEDGMENTS AND REFERENCES

Qualitative spectrographic analysis by Wilbur O. Aikin, Montana School of Mines, Butte, Montana.

1. PECK, A. B., Dumortierite as a commercial mineral: *Am. Mineral.*, **11**, 98 (1926).
2. SCHALLER, W. T., Dumortierite: *Am. Jour. Sci.*, **19**, 221 (1905).
3. SCHALLER, W. T., Dumortierite: *U. S. Geol. Sur., Bull.* **262**, 117 (1905).

UNIT CELL AND SPACE GROUP OF GLAUCOCHROITE

J. H. O'MARA, *Department of Mineralogy, Harvard University, Cambridge, Mass.*

Glaucochroite, $CaMnSiO_4$, is a rare member of the olivine group first described by Penfield and Warren[1] from the Parker shaft at Franklin, New Jersey. The morphology and optical properties were later described by Palache,[2] who also cited two other analyses.

A Weissenberg *x*-ray study has been made of the crystals measured by Palache, using both copper and iron radiation. The space group, unit cell content, axial ratios and specific gravity are:

Space group: *Pbnm* (V_h^{16}) $a_0=4.92\pm0.03$ Å
Unit cell content: $Ca_4Mn_4Si_4O_{16}$ $b_0=11.19\pm0.02$
Sp. G. $=3.465$ (calc.); $c_0=6.51\pm0.02$
3.407 (Penfield, meas.)
$a_0:b_0:c_0=0.440:1:0.582$
$a:b:c=0.4409:1:0.5808$ (Palache, morph.)

SOME MEASUREMENTS ON MINERALS OF THE PYRITE GROUP

ROBERT B. GORDON, *Yale University, New Haven, Connecticut.*

X-ray measurements

Since two measurements of a_0 for pyrite from Leadville, Colorado, have already been published, pyrite from this locality was used in the present experiments. Peacock and Smith (1) found $a_0=5.4079\pm.0005$ Å using $\lambda=1.93239$ kX for iron $K\alpha_1$ radiation, and Kerr, Holmes, and Knox (2) reported $a_0=5.40667\pm.00007$ Å. Although the latter paper does not give the wavelength of *x*-rays on which the determination of a_0 is based, it seems likely that kX units were used. When these values are converted to Å, the agreement with the new determination here reported is very satisfactory, as shown in the table.

The lattice constants reported here were determined from *x*-ray diffraction patterns produced in a symmetrical focusing back reflection camera of 10 cm. diameter, with unfiltered iron radiation. The lines due to $K\beta$ radiation were too weak to be measured accurately. Unequivocal indexing of the back reflection film was not practicable when *x*-rays from a copper target were used for the exposure.

The values of a_0 were computed by the method of least squares, according to Cohen's (3) method for the improvement of lattice constants.

---

[1] Penfield, S. L., and Warren, C. H.: *Zeit. Krist.,* **32,** 231–234 (1900).

[2] Palache, Charles: *U. S. Geol. Survey, Prof. Paper* **180,** 79–80 (1935).

The experimental errors indicated are the probable errors computed from residuals.

The temperatures given are the average temperatures of the metal case of the camera during the course of the exposures. The Philips precision camera receives considerable heat from the electric motor mounted in its base. It is consequently necessary to allow the entire apparatus to reach a steady operating temperature before beginning an exposure. The variation during an exposure never exceeded ±0.5° C.

Summary of X-ray Results

	Peacock and Smith (1)	Kerr, Holmes, and Knox (2)	Gordon ($t=29°$ C., $\lambda\text{FeK}\alpha_1 = 1.93597$ Å)
Pyrite, Leadville, Colorado (Brush Min. Coll., No. 5818)	$a_0 = 5.4182 \pm .0005$ Å†	$5.41759 \pm .00007$ Å‡	$5.4179 \pm .0003$ Å
Sperrylite* (Brush Min. Coll., No. 2952)			$5.9680 \pm .0003$ Å
Hauerite, Radduse, Sicily (Brush Min. Coll., No. 2821)			$6.1008 \pm .0001$ Å

* Locality uncertain, presumably Ontario.

† Converted fron kX units by factor, 1.00185 computed using authors' λ.

‡ Converted fron kX units by factor, 1.00202.

Optical Measurements

The index of refraction of a prism of the same hauerite was measured on a spectrometer by the method of normal incidence, the transmitted signal being observed with a Bausch and Lomb infrared image converter mounted on the spectrometer telescope. The wavelength corresponding to the greatest spectral sensitivity of the converter was estimated to be 9100 Å by measuring the index of a glass prism of known dispersion with the converter on the telescope. The refractive index of hauerite is $n = 2.58 \pm 0.02$ for the wavelength used. Two other measurements of this index have been published: Dana's *System of Mineralogy* (4) gives $n = 2.69 \pm 0.01$ for the lithium red line and R. Bailly (5) has published the value $n = 2.634$ for "infrared light."

Acknowledgment

The work here reported was done in the Mineralogical laboratories of the Department of Geology, Yale University, under the supervision of Professor Horace Winchell.

References

1. *Univ. of Toronto Studies, Geological Series* No. **46,** 107 (1941).
2. *Am. Mineral.,* **30,** 498 (1945).
3. *Rev. Sci. Inst.,* **6,** 68 (1935); *ibid.,* **7,** 155 (1936). See also Jette and Foote, *J. Chem. Phys.,* **3,** 605 (1935).
4. Dana's *System of Mineralogy,* 7th Edition, New York (**1944**).
5. *Bull. Soc. Fr. Min.,* **70,** 117 (1947).

BOOK REVIEWS

COLLOIDAL CHEMISTRY OF THE SILICATE MINERALS, by C. Edmund Marshall, Professor of Soils, University of Missouri, price, $5.80. This publication comprises Volume 1 of a series of monographs prepared under the auspices of the American Society of Agronomy.

The mode of approach used by Dr. Marshall in planning this volume may be illustrated by quotations from the preface. He says: "I have deliberately chosen to restrict this work in the main, to evidence obtained from the study of reasonably pure materials; well aware that by so doing, diverse and important applications have been relegated to the background. In the present state of our knowledge of the colloidal minerals it is in my opinion, more important to clarify the fundamentals than to describe technical details of application.

"In so far as I have been able to judge, this field has been free alike from competitive overeagerness and sterile controversy. Mineralogists, colloid chemists, soil scientists and ceramists have all contributed."

Thus the volume, although prepared under the direction of those interested in soils, has no narrow appeal, and should interest a wide circle of those concerned with the colloidal properties of minerals. Of course this interest centers largely around clay minerals, but this is because these are the typical colloidal minerals, and not because the author is interested in these alone. Throughout the paper he aims to present the basic science of the problems involved. This is the reason for confining the consideration largely to pure minerals, and to the reviewer this seems a sound approach.

Chapter 1 on "Historical Outline" should interest all mineralogists, not alone those interested in colloidal materials, for it shows what a fundamental role in the development of this complex problem has been played by mineralogists, and mineralogical techniques. Here the mineralogist will meet many old friends.

Chapters 2 to 6 discuss the structures of the various groups of silicate minerals. This section should appeal to all those who desire to become acquainted with the laws governing the atomic arrangements in crystals. Chapter 7 deals with "the sizes and shapes of clay particles," and presents the results of studies by means of the electron microscope. Chapter 8 deals with "the optical properties of clay aggregates and suspension." Chapters 9 to 14 turn to the more abstruse properties of colloidal materials, Chapter 9 on "Adsorption by the Clays and Its Consequences"; and Chapter 10 on "Clay Acids and Their Titration Curves." Chapter 11 deals with "Ionic Exchange Reactions of the Clays." This is a valuable treatment of this very widely important property of clay materials. Chapter 12 is on "Electrokinetic Properties of the Clays"; Chapter 13 on "The Mechanical Properties of Clay Suspensions, Soils and Pastes"; and 14 on "The Properties of Clay Aggregates and Films."

Each chapter is followed by a well selected list of references, ranging up to about 40 entries. In this synthesis comprising many lines of work Professor Marshall has been very modest in presenting his own important contributions. The writing is clear and concise; the book is well printed on good paper, and is a credit to the author and the publisher.

Clarence S. Ross,
U. S. Geological Survey, Washington, D. C.

X-RAY IDENTIFICATION AND CRYSTAL STRUCTURE OF CLAY MINERALS, edited by G. W. Brindley. Published by Clay Minerals Group of the Mineralogical Society, London, 1951, 345 pages. $6.00. Copies in the U.S.A. from R. E. Grim, Geology Dept., Univ. Illinois, Urbana, Illinois.

Information, within the scope of the title, on clay minerals and several related or associated mineral groups is presented in fourteen articles prepared chiefly by English authors. G. W. Brindley, who has concerned himself much with the subject within recent years, is responsible for three of these dealing with experimental methods, diffraction from randomly displaced layers, and the kaolin minerals. The last two are treated very thoroughly as a central part of the general subject. The first is necessarily abbreviated and is probably included since it could not be logically omitted. Brindley is co-author on two other articles dealing with chlorites and the interpretation of diffraction patterns. A considerable amount of original work is presented for the first time in the treatment of chlorites which closely parallel the micas in their structural disorders. The weakness of this article as well as the one by R. E. Grim, W. F. Bradley, and G. Brown on "The Mica Clay Minerals" is that adequate information is lacking on variations in chemical composition, which, of course, is outside the province of the authors.

D. M. C. MacEwan, of the Rothamsted organization, prepared an article dealing with the montmorillonite minerals and was co-author with G. Brown of "*X*-ray diffraction by structures with random interstratification." Both articles are very thorough but the latter is of particular value for its many figures showing intensities of *x*-ray scattering from various averaged combinations of silicate layers as encountered in mixed layer minerals.

More than sixty tables, many of them several pages in width, chiefly summarizing diffraction data are perhaps of greatest value since the original literature is spread so widely as to hinder ready reference. Here too, a considerable part of the data is original. There are many illustrations serving to describe the structures discussed and the points raised. The reader should not be lulled into placing too great value on the *x*-ray method for qualitative and quantitative work since neither ideal of a completely oriented nor disoriented specimen can be realized for powder diffraction work. The diffraction method fails with those finely divided materials in shales and soils that so often are mixtures of several clay minerals including mixed layer minerals. The tables of diffraction data, nevertheless, are a necessary guide.

As the reviewer and the dispassionate, I hope, originator of much that is described here I can perhaps best serve my reader by an excursion into the personal. Many obscure beauties of structural crystallography were first met in the clays to be described and seemingly lost again. The authors have found most of these and have treated them with insight not to be found in a dashed off book. I would quibble as to whether they fully appreciate the evidence for a few layer displacements in dickite, pyrophyllite, and talc; that kaolinite can be demonstrated by powder diffraction methods alone to have an ordered triclinic form; and with other points here and there, but these are minor. The subject is not closed and this summary should aid in the future development.

Sterling B. Hendricks,
Plant Industry Station, Beltsville, Maryland

EINFÜHRUNG IN DIE GESTEINSKUNDE, by H. Leitmeier, Springer-Verlag, Vienna, 1950. viii+275 pages, 100 text figures, DM 18.50.

It has been more than 20 years since a general elementary textbook of petrology appeared in German, the last ones being the 1923 revision of Rosenbusch's *Elemente der Gesteinslehre* by Osann and Rinne's *Gesteinskunde* (1928). Leitmeier's *Einführung in die Gesteinskunde* was written to serve as an up-to-date substitute for the out-of-print *Elemente*. It was deliberately made much shorter (275 pages as against 779 pages for the 1923 edition of *Elemente der Gesteinslehre*) in part to produce a textbook that students can more readily afford and in part to appeal to a wider audience; it is intended for geographers, and all other naturalists who are interested in knowing more of the building stones of the Earth's crust, as well as for petrologists, mineralogists, and geologists.

It is more the descriptive detail and numbers of examples that have been curtailed than the scope of the treatment. For example, there are approximately the same number of index entries (mostly rock names) in the book under review and the 1923 edition of the *Elemente*, but there are some 1550 chemical analyses of igneous rocks and minerals from igneous rocks given in the latter as against only 80 in the former.

In a general introductory section Leitmeier discusses briefly (6 pages) the methods of petrology, field methods, optical methods, and quantitative analysis (chemical and mineralogical). The second part of the introduction gives a 10 page tabular summary and discussion of the crystallographic and optical characteristics of the important groups of rock-forming minerals. Nine common accessory minerals are described briefly.

In the main part of the book 111 pages are devoted to igneous rocks, 49 pages to sedimentary rocks, and 84 pages to metamorphic rocks. Mylonites are discussed briefly in a separate section of 3 pages at the end of the text.

The section on igneous rocks leads off with a short discussion of the structure and composition of the earth. This is followed by a treatise on the formation of igneous rocks in which differentiation, assimilation, anatexis (palingenesis), and granitization are discussed. In the treatment of differentiation a very clear and concise description of the derivation and use of "Niggli-numbers" is given. Granitization is given more attention than the other topics because of the recent emphasis in the literature. Many recent books, papers and developments are cited. The author recognizes various degrees and types of granitization but describes them objectively and leaves to the reader the choice of what and how much he will accept. There is a 2 page outline of the relation of igneous rocks to orogenesis, followed by a 10 page discussion of order of crystallization and structures and textures of igneous rocks.

The classification used for igneous rocks is essentially that of Rosenbusch, but the order of treatment is different. Instead of discussing all plutonic rocks, then dike rocks, then extrusive rocks, as Rosenbusch does, Leitmeier describes together all of the rocks with the same chemical characteristics. For example, trachyte, syenite and syenitic dike rocks are treated in that order instead of being widely separated in the text. The classical order of treatment followed by most textbooks of petrology is from silica-rich to silica-poor, i.e., granite, syenite, diorite, gabbro, peridotite. Leitmeier departs from this sequence by discussing basalt and related rocks first because "basaltic" magma is supposed to be the material from which all other igneous rocks are derived directly by differentiation or indirectly by assimilation and subsequent differentiation, weathering and eventual granitization, etc. These relations are shown in detail in a diagram on page 40, modified after Cloos and Rittmann. After the section devoted to basalt, gabbro and related rocks the following groups are treated in the order listed: pyroxenite, hornblendite, periodotite, anorthosite, alkalic basic rocks, diorite, monzonite, nepheline syenite, syenite, quartz diorite, and granite, each with the equivalent hypabyssal and extrusive rocks where known.

The sections on sedimentary and metamorphic rocks follow Rosenbusch in general in classification and manner of presentation, but both sections have been brought up to date and take into account modern workers and their ideas. For example, Sander's ideas concerning development and interpretation of *s*-planes and related preferred orientation of mineral grains in rocks play an important part in the section on metamorphic rocks.

It appears to the reviewer that the author has done an excellent job of what he set out to do. The book is nicely illustrated with photomicrographs of thin sections and well chosen pictures of hand specimens and field occurrences of the various types of rocks. There are no diagrams of artificial systems and no systematic discussion of the physical chemistry of igneous rocks, but these things are hardly to be expected in an elementary textbook of this nature. The style is pleasing and the German easy to read. The book should be very good for students in non-German countries to learn German and petrology simultaneously, as well as appealing to a wide audience among German-speaking students and scientists.

Earl Ingerson,
U. S. Geological Survey, Washington, D. C.

DIE SILICATISCHEN TONMINERALE, by K. Jasmund. Monograph #60 "Angewandte Chemie" and "Chemie—Ingenieur-Technik." Published by Chemie, Bergstrasse, Weinheim, Germany, 1951. 142 pages, 40 figures and 67 tables, price 15.80 DM.

This small monograph is an excellent treatise of what is known about the silicates which make up most of the clays. The author has made a thorough search of the literature on the subject as is attested by the 298 references which even include many as late as 1950. The work is in two parts. The first deals with the following general subjects: mineralogical composition, occurrence and separation of the minerals, methods of investigation, structures of the layer silicates, syntheses of some, swelling, plasticity and viscosity, base exchange and thixotropy. The second part takes up the minerals by special groups. One hundred pages are filled with a wealth of information in which very little has been overlooked. While great stress has been put on the properties depending on structures, optical properties are also given in detail. It is highly satisfying that the author has been able to integrate the great many facts and ideas. He has succeeded in giving each investigator due credit for his contributions. In doing so he seems to avoid bringing forth ideas of his own on the subject, which is to be regretted.

Ion exchange (base exchange) is discussed in greater detail than in the usual mineralogical treatises as the author has made use of numerous references of soil chemists. Those referring to the exchange of phosphate ions were new to the reviewer. The author does not favor the new nomenclature for halloysite (endellite) and metahalloysite (halloysite), and retains the original meanings. While glauconite and vermiculite are not strictly clay minerals, they are discussed in detail. On the other hand, chlorites are only mentioned in connection with hydromicas.

Very few typographical errors were seen. On page 99 in the formula of sauconite Mg should read Zn. The arrangement and printing are a credit to the publishers. The paper stock is of fair quality. The monograph should be very useful to mineralogists and soil chemists.

John W. Gruner,
University of Minnesota, Minneapolis, Minnesota

OPTICAL CRYSTALLOGRAPHY, by Ernest E. Wahlstrom. Second edition (1951), John Wiley and Sons, Inc., vii+247 pp.

The addition of several new three-dimensional drawings in this edition has raised even higher the standard of textbook illustration set by the first edition. This excellence alone makes the book a valuable contribution. It goes beyond the basic requirements of students of crystal optics by emphasizing several of the light surfaces which are only of historical significance and by devoting considerable space to such topics as conical refraction. On the other hand, it falls short of giving a complete and accurate presentation of optical theory.

The discussion of crossed axial dispersion in brookite and especially the addition of Fig. 4 makes the treatment of this subject less adequate than that in the first edition. A brief chapter on the universal stage added to this edition will suffice to introduce the basic concept of the utility of this instrument to the student.

C. B. Slawson,
University of Michigan, Ann Arbor, Michigan

NEW MINERAL NAMES

Kobeite

Jitsutaro Takubo, Yasuo Ukai, and Taneo Minato, Studies on the minerals containing rare elements. (II) A new mineral, "kobeite" found at Shiraishi, Kobe-mura, Kyoto Prefecture, Japan: *J. Geol. Soc. Japan,* **56,** No. 663, 509–513 (1950). Abstracted from a translation by Shigeo Ofuji, edited by Miss Rachel Barker, U. S. Geological Survey, Tokyo.

Chemical Properties: Two analyses were made on material separated from parisite with a needle and further purified by floating off material with specific gravity less than 3.

	1	*2*
CaO	1.15	1.23
MgO	0.53	1.28
MnO	0.35	0.84
FeO	0.61	0.62
Fe_2O_3	9.67	12.93
Al_2O_3	2.69	0.34
Ce_2O_3	0.90	0.58
Ce group oxides	0.05	1.63
Y group oxides	23.91	22.21
SiO_2	2.29	3.83
TiO_2	33.03	34.72
$Nb_2O_5+Ta_2O_5$	5.45	4.84
ThO_2	1.19	0.82
U_3O_8	12.64	9.95
PbO	—	0.13
H_2O^+	3.19	3.75
H_2O^-	0.92	0.44
Sum	98.57	100.14
Analyst	Taneo Yasuo	J. Takubo

This gives very nearly $AB_2(O, OH)_6$ where A=Y, U, etc., B=Ti, Nb, etc., like the euxenite-polycrase and the blomstrandine-priorite series.

Physical Properties: In radiated crystals and parallel growths, color black, luster vitreous. Brittle, optically isotropic, brown in thin plates. Metamict and remains so (microscope and *x*-ray study) when heated at 900° C. for 30 minutes in an electric furnace. Strongly radioactive.

Occurrence: In a pegmatite associated with parisite, zircon, monazite, tscheffkinite, xenotime, bitotite, albite, smoky and white quartz, and muscovite.

Name: For the locality.

Discussion: Differentiated by the authors from polycrase and blomstrandine by the low $Nb_2O_5+Ta_2O_5$ content. Presumably a variety, but needs further study.

Michael Fleischer

Magniophilite

A. A. Beus, Magniophilite and mangankoninckite, two new minerals from pegmatites: *Doklady Akad. Nauk S.S.S.R.,* **73,** 1267–1279 (1950).

The name magniophilite is given to a salmon-pink mineral, occurring in prismatic crystals associated with triphylite in microcline-muscovite pegmatite at Kyrk-Bulaka, Turkestan Ridge. Analysis gave: FeO 16.95, Fe_2O_3 none, MnO 30.77, CaO 0.54, MgO 9.50, P_2O_5 42.53, H_2O_+ 0.42; sum 100.71%, corresponding to $(Mn, Fe, Mg)_3(PO_4)_2$ with Mn:Fe:Mg=434:236:235. Optically positive with $\alpha=1.695$, $\beta=1.706$, $\gamma=1.712$, all ±.002; $2V=45-48°$. *X*-ray powder data (12 lines) are given.

Discussion: An unnecessary name for magnesian graftonite. The indices of refraction given correspond to an optically negative mineral with high 2V.

M. F.

Mangankoninckite

A. A. Beus, *loc. cit.*

Pinkish violet to blue fine-grained material in the oxidized part of the pegmatite contained FeO none, Fe_2O_3 33.62, Mn_2O_3 2.72, P_2O_5 31.44, H_2O_- 7.98, H_2O_+ 24.13; sum 99.89%, corresponding to $(Fe, Mn)PO_4\cdot 3H_2O$. G.=2.65, $n=1.68$–1.70.

Discussion: An unnecessary name for a manganian variety. The validity of koninckite is questionable; likely it is strengite or phosphosiderite.

M. F.

Perrierite

Stefano Bonatti and Glauco Gottardi, Perrierite, nuovo minerale ritrovato nella sabbia di nettuno (Roma). *Rend. acad. nazl. Lincei, Classe sci. fis., mat. e nat.*, Ser. 8, 9, No. 6, 361–368 (1950).

The mineral was found as grains and crystals up to 0.2 mm. in the tuffaceous sands of Nettuno. It resembles epidote in habit. It is rare, perhaps 0.1%, but is easily recognized by its marked pleochroism. The crystals are monoclinic, prismatic, with $a:b:c=2.047:1:2.380$, β 113°28′. Fifteen forms were recognized. Frequently twined on (100). No cleavage was noted; fracture uneven to conchoidal. Biaxial, neg., $2V_x$ very small, with $nX=1.90$–1.95, $nZ=2.02$–2.06; absorption strong $Z>Y>>>X$; Z opaque to deep brown, Y opaque to rose-violet, X yellow; $Z=b$, $X\wedge a+24°$; $2V_x$ very small. Color black to brownish, luster resinous; streak brown. G.=4.3, hardness=$5\frac{1}{2}$. Analysis of a sample 95% pure, containing zircon, monazite, spinel, and with inclusions believed to be apatite gave: SiO_2 18.21, TiO_2 20.71, P_2O_5 2.07, FeO 5.47, MgO 0.92, CaO 3.85, rare earths 43.45, ThO_2 4.60, Na_2O 1.00, H_2O none; sum 100.28%. This gives $SiO_2:TiO_2=1:1$, but a formula can not be computed, as the atomic weight of the rare earths was not determined. The mineral dissolves in hot, concentrated H_2SO_4. The Nettuno sands were derived from the weathering of tuffs and contain pyroxene, ilmenite, garnet, and magnetite. Further work is in progress. The name is for the Italian mineralogist, Carlo Perrier.

Discussion: Bonatti and Gottardi point out that perrierite has a composition close to that of chevkinite (tacheffkinite), which they consider to be a non-crystalline mineral. However, the literature contains optical and goniometric and *x*-ray data on chevkinite. The physical and optical properties of perrierite fall in the range listed for chevkinite and many interfacial angles of perrierite are close to some given for chevkinite, although the orientations adopted are apparently different. No evidence is presented that the supposed new mineral perrierite differs from tscheffkinite.

M. F.

Nickel Cabrerite

Cobalt Cabrerite

Heinz Meixner, Über Cabrerit. *Neues Jahrb. Mineral.*, Monatsh. 1950, 169–174.

Heinz Meixner, Kobalt cabrerit, ein neues Mineral aus der Magnesitlagerstatte auf der Millstatter Alpe bei Radenthein, Karnten. *Neues Jahrb. Mineral.*, Monatsh. 1951, 17–19.

The name cabrerite was given in 1868 by Dana to material described by Ferber in 1863 and which corresponded to annabergite containing 9.3% MgO. In 1937, Barth showed that some "cabrerite" had the optical properties of annabergite. In the first paper cited above, Meixner shows that material from near Friesach, Carinthia, has $\beta = 1.630$, $\gamma = 1.657$, and gave tests for Ni, Mg, As, and H_2O (Co not mentioned—M.F.), hence is a member of the solid solution series $(Ni, Mg)_3(AsO_4)_2 \cdot 8\ H_2O$, with Ni:Mg about 2:1. In the second paper, Meixner describes incrustations on magnesite from near Radenthein, Carinthia, with $\beta = 1.625$, $\gamma = 1.657$, which gave tests for Co and As (Ni not mentioned—M.F.). This corresponds to a member of the erythrite-hoernesite series with a composition approximately $Co_{1.8}Mg_{1.2}(AsO_4)_2 \cdot 8\ H_2O$. The name cobalt cabrerite is suggested for this material and nickel cabrerite for the member of the solid solution series annabergite-hoernesite.

DISCUSSION: These are unnecessary names for magnesian erythrite and magnesian annabergite.

M. F.

DISCREDITED MINERALS

Eschwegeite(=tantalian polycrase)

ELYSIARIO TAVORA, Eschwegeita e euxenita. *Anais acad. brasileira ciencias*, **23,** 119–128 (1951).

Eschwegeite from the type locality, Rio Dôce, Minas Gerais, Brazil, was metamict, but gave a sharp *x*-ray powder pattern after being heated to 1,000°. The data were indexed and correspond to an orthorhombic cell with $a_0 = 5.516$, $b_0 = 14.550$, $c_0 = 5.154$ Å, in good agreement with available data on the euxenite-polycrase series. From the original analysis, eschwegeite is a tantalian polycrase.

M. F.

Harttite (=calcian svanbergite)

ELYSIARIO TAVORA, Constantes reticulares da harttita. *Anais acad. brasileira ciencias*, **23,** 129–134 (1951).

X-ray study of material from the type locality, São Jośe River, Lençois, Bahia, Brazil, showed it to be a member of the alunite-beaudantite group, with lattice constants intermediate between those of woodhouseite and svanbergite. The original analysis corresponds to a calcian svanbergite.

M. F.

inest 3 Dimensional Image Quality
. . . Wider Fields Than Ever Before

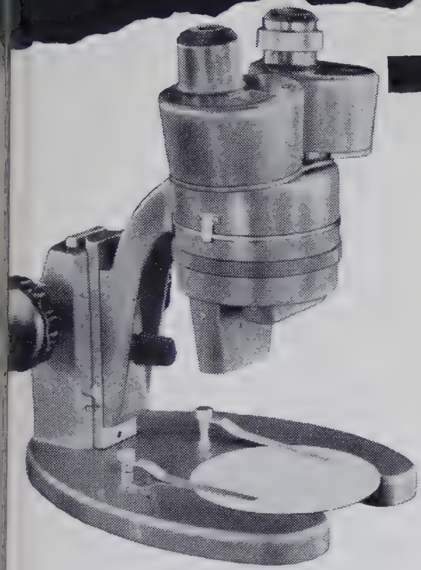

FOR FIELD USE

- Conveniently portable . . . lightweight but sturdy
- Shockproof, dustproof optical system
- Magnifications 10X and 20X (Other magnifications available)
- Modern stand design, balanced for stability and steadiness
- Portable Illuminator (Optional)

Plus WIDEST FIELDS

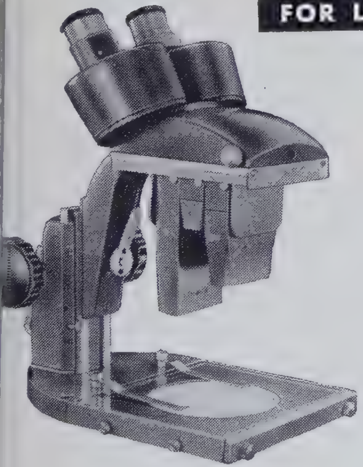

FOR LABORATORY USE

- The finest optics ever produced for wide field work
- Wider range of magnifications—6.6X to 45X (Higher magnifications available)
- Inclined eyepieces for comfortable examination
- Patented drift-free focusing . . . Extra-long focusing range
- Wide adaptability to specific applications in science and industry

Plus WIDEST FIELDS

WRITE For complete information and demonstration to Bausch & Lomb Optical Co., 676-11 St. Paul St., Rochester 2, N.Y.

Bausch & Lomb *Stereoscopic* Wide Field Microscopes

- STANDARD STRAIN-FREE OBJECTIVES AND EYEPIECES
- SIMPLE GRADUATED ROTATABLE STAGE
- PINHOLE OR TELESCOPIC EYEPIECE FOR VIEWING INTERFERENCE FIGURES
- BUILT-IN ILLUMINATION WITH DISC DIAPHRAGM APERTURE CONTROL

MEET THE NEW POLARIZING MICROSCOPE

Everyone Can Afford

CRYSTALLOGRAPHERS, chemists, petrologists . . . here is the laboratory and teaching instrument you have been looking for. It's the AO Spencer P45 Microscope, suitable for powers up to 430X, numeral apertures up to 0.66. The built-in polarizer and removable body tube analyzer are of *precision* optical-quality polaroid. All standard AO compensators are accommodated.

Although simplified in construction and operation, the P45 retains highest-quality AO Spencer optical and mechanical features throughout. See it at your first opportunity. You'll be amazed at the price—a fraction of the amount you would expect to pay. For further information, write Dept. Y7.

American Optical
COMPANY
INSTRUMENT DIVISION • BUFFALO 15, NEW YORK

- Designed for the examination of polished, opaque specimens in polarized, reflected light
- Focusing stage with rack and pinion motion
- Special prism eliminating elliptical polarization
- *Coated* optics and prisms
- Interchangeable tube
- Long working distance

Leitz Microscope MOP

Polarizing microscope arrangement for observation in reflected polarized light.

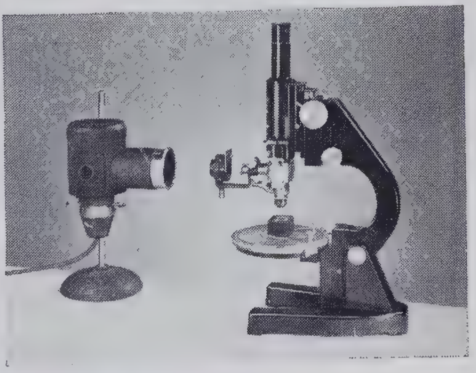

Leitz

Polarizing

ORE MICROSCOPE

For information, see your Leitz franchised dealer, or write to Dept. A

E. LEITZ, Inc., 304 Hudson Street, New York 13, N. Y.

LEITZ MICROSCOPES • SCIENTIFIC INSTRUMENTS • BINOCULARS
LEICA CAMERAS AND ACCESSORIES

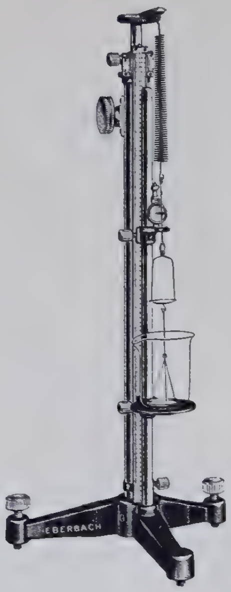

KRAUS JOLLY BALANCE

For Speedier Specific Gravities

This professional model is mentioned in *Mineralogy* by Kraus, Hunt and Ramsdell, in *Dana's Manual of Mineralogy* by Hurlbut and *Elements of Mineralogy* by Winchell.

The Kraus Jolly balance simplifies the determination of specific gravity; only two readings and a division are necessary; older forms of the balance require more extensive computation. The balance is especially well adapted for the rapid and accurate determination of specific gravity of solids, such as minerals, rocks, coal, precious stones, etc.

Send for our bulletin.

SCIENTIFIC
INSTRUMENTS
& APPARATUS
Eberbach CORPORATION
ANN ARBOR, MICH.
ESTABLISHED 1843

W. HAROLD TOMLINSON
Petrographic Laboratory
260 N. ROLLING RD., SPRINGFIELD, PA.
ROCK SECTIONS **ORIENTATED MINERAL SECTIONS**

CRYSTALLOGRAPHY

Specializing in choice crystals, singles, groups, from world wide sources. Catalog free.

V. D. HILL
Complete Gem & Mineral Establishment
Route 7-F, Box 188, Salem, Oregon

Cargille

HEAVY LIQUIDS

For the Determination of Specific Gravity of Minerals, Gems and Other Substances

Range of Specific Gravity:
1.2 to 7.5

New Liquids Cover the Range up to Specific Gravity 7.5

Write for Leaflet HL-AS

R. P. Cargille

118 Liberty Street
New York 6, N.Y.

MINERALS UNLIMITED

•

Suppliers of high quality minerals to students and research organizations. Catalogues available on request.

Our firm is interested in obtaining unusual massive or crystallized minerals in quantity, as well as single examples of fine crystallization, collections being of particular interest. Either purchase or exchange is welcome.

•

MINERALS UNLIMITED
1724 University Avenue Berkeley 3, California, U.S.A.

INDEX MEDIA

LIQUID IMMERSION MEDIA—Original series, colorless, odorless, stable, exact specified indices, range Nd 1.41 to 1.65, steps of .01, in twenty-five 1-ounce applicator vials, with cabinet $27.50

Set of thirty-eight Immersion Media Nd 1.41 to 1.78 in steps of .01, in ⅛ fl. oz. each, applicator vials with cabinet $35.00

J. T. Rooney, Chemist, P.O. Box 358, Buffalo, N.Y.
"Supplying dependable index media to petrographers for more than 25 years"

Princeton

UNIVERSITY PRESS

A NEW LABORATORY TOOL

Tables for Microscopic Identification of Ore Minerals

By W. UYTENBOGAARDT,
University of Stockholm

- In the tables of this practical laboratory handbook, minerals are listed in order of increasing hardness. The columns of tables are: 1. Name; 2. Chemical composition; 3. Crystal system; 4. Talmage hardness; 5. Reflectivity values; 6. Color, reflection pleochroism and tint; 7. Etch tests; 8. Miscellaneous (polishing features, twinning, cleavage, references, etc.) *$5.00*

At your bookstore,
PRINCETON UNIVERSITY PRESS

The 200 page Author-Subject

INDEX TO VOLUMES 21-30, 1936-1945, of

THE AMERICAN MINERALOGIST

by

Earl Ingerson, Geophysical Laboratory

and

Michael Fleischer, U. S. Geological Survey

is now available

The price is $2.00 to members and subscribers and $3.00 to non-members. The Treasurer will be glad to receive your order now. Address, Dr. Earl Ingerson, U. S. Geological Survey, Washington 25, D.C.

COOKE POLARIZING MICROSCOPES

The polarizing microscopes made by Cooke Troughton and Simms, Ltd., may be said to be the most modern in design of any of this type now on the market. This is true largely because fullest recognition was given to the qualities and advantages of Polaroid screen.

Many workers in the field have long been aware of the advantages accruing from the use of a full-size condenser with a large polarizer. Utilizing Polaroid screen, carefully selected, Cooke now supplies this, providing better optical performance and eliminating the need for swing-out condensers for use with high and low power objectives. Use of Polaroid also does away with the need of collimating lenses for the analyzer, required by the construction of the Nicol prism.

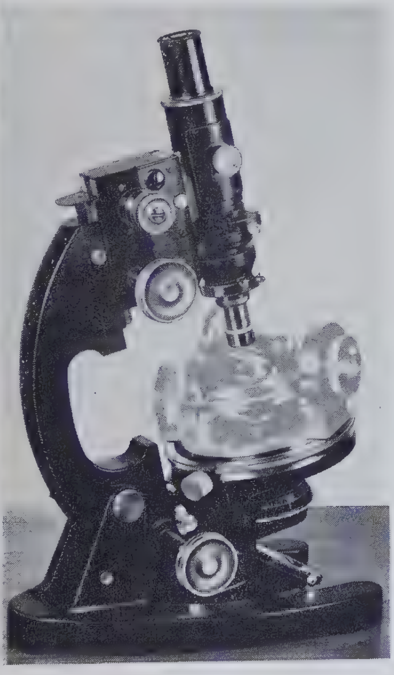

The Cooke Bertrand lens is of patented trip-in design with no need to refocus the objective to form an image on the Bertrand diaphragm.

These and other improvements are fully described in the complete catalog on these instruments which will gladly be sent on application. Two of the more popular instruments are described in the following pages.

It remains here to call attention to the comparatively low prices at which these instruments are now being sold. No even partially comparable instruments sell for as low a price.

American Agents

THE R. Y. FERNER COMPANY, INC.

110 Pleasant Street, Malden 48, Massachusetts

COOKE RESEARCH POLARIZING MICROSCOPE

M7110

TUBE Large or normal size body tube, depending on size of eyepieces required.

Bertrand Lens of trip-in type.

Polaroid analyzer and glass compensator in sliding mount.

Slot for compensators.

Two way, spring-opposed centering adjustment.

Quick-change objective mount or revolving nose-piece.

STAGE Circular, 120 mm. dia., graduated, plain bearing, rotating, with clamp to motion.

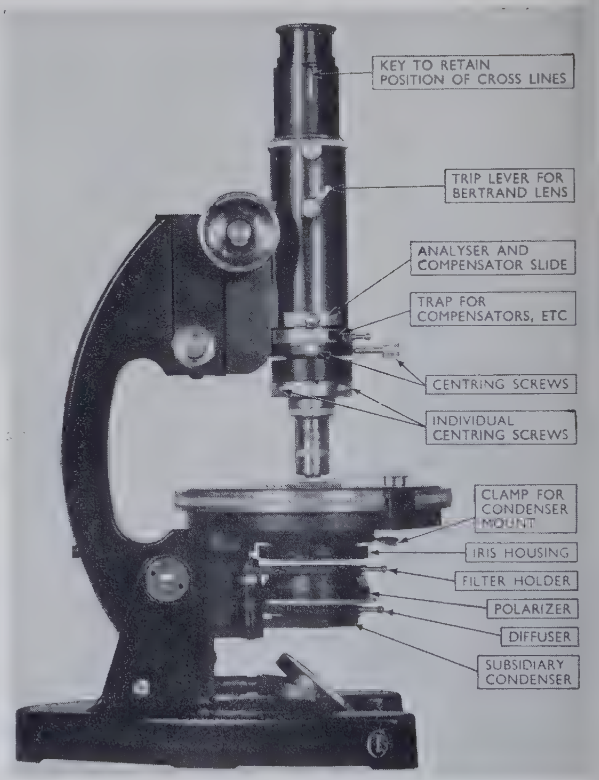
KEY TO RETAIN POSITION OF CROSS LINES
TRIP LEVER FOR BERTRAND LENS
ANALYSER AND COMPENSATOR SLIDE
TRAP FOR COMPENSATORS, ETC
CENTRING SCREWS
INDIVIDUAL CENTRING SCREWS
CLAMP FOR CONDENSER MOUNT
IRIS HOUSING
FILTER HOLDER
POLARIZER
DIFFUSER
SUBSIDIARY CONDENSER

SUBSTAGE Substage with Abbe type condenser, iris diaphragm, swing-out filter holder, rotatable graduated polarizer in swing-out mount, swing-out filter holder, auxiliary lens for very low powers, plane and concave mirror.

Optical and mechanical accessories listed on following page.

PRICE, without eyepieces and objectives, F.O.B. Boston **$387.35**

THE R. Y. FERNER COMPANY, INC.

110 Pleasant Street, Malden 48, Massachusetts

(Sold in the United States with service and replacement stock facilities maintained.)

Send for complete brochure on microscopes and accessories.

COOKE UNIVERSAL POLARIZING MICROSCOPE

M7250

(Monocular and Binocular Bodies)

TUBE Interchangeable monocular (with Bertrand Lens) and binocular bodies. The binocular is offered for all polarizing microscope uses not requiring a Bertrand Lens. On dovetail slide allowing positioning up to two inches above normal.

STAND Much heavier construction than M7110 with patented ball bearing fine adjustment of unusual accuracy and freedom of movement.

STAGE Ball bearing. Rack and pinion vertical movement of 42mm, increased to 75mm on removal of substage. Stage on dovetail slide allowing interchange of stages of different types, or use without stage.

SUBSTAGE As described on preceding page except that it is provided with vertical motion and is removable as a unit when necessary to accommodate large specimens. 1.4 N.A. aplanatic condenser supplied.

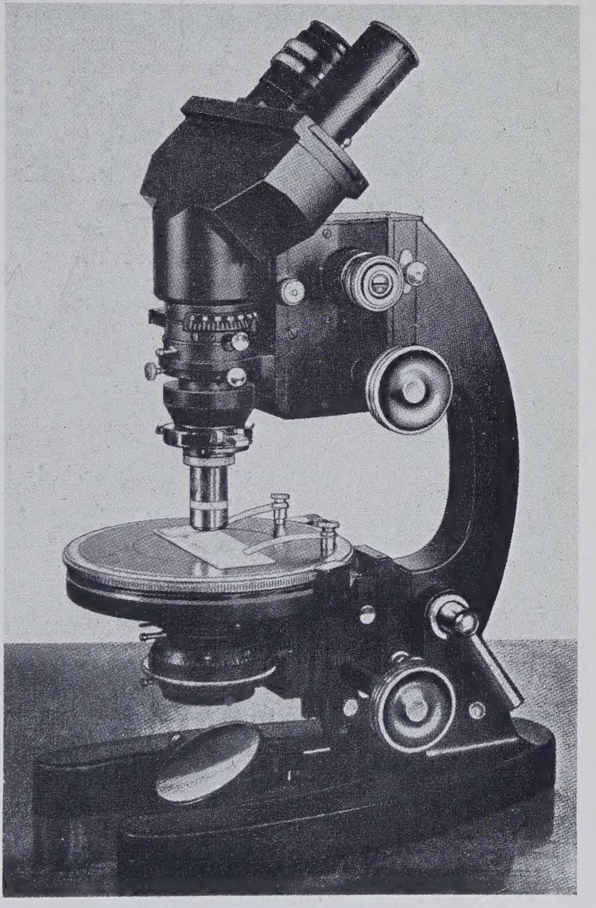

Optical and mechanical accessories listed on following page.

PRICE, without eyepieces and objectives, F.O.B. Boston ***$962.50***

THE R. Y. FERNER COMPANY, INC.
110 Pleasant Street, Malden 48, Massachusetts

(Sold in the United States with service and replacement stock facilities maintained.)

Send for our complete brochure on microscopes and accessories.

COOKE POLARIZING MICROSCOPE ACCESSORIES

(A selected list—complete listing in catalog available)

OBJECTIVES

M7801	33mm	N.A. 0.1	$17.05
M7806	25mm	N.A. 0.15	$18.70
M7811	16mm	N.A. 0.28	$18.75
M7818	8mm	N.A. 0.45	$26.40
M7820 **	4mm	N.A. 0.85	$48.40
M7821 *	4mm	N.A. 0.65	$33.00
M7822 **	4mm	N.A. 0.65	$33.00
M7823 *	4mm	N.A. 0.85	$41.25
M7831	1.8mm	N.A. 1.30	$65.45

* For use with covered specimens
** For use with uncovered specimens

EYEPIECES

(Focusing with crosslines)

M7508	7X	Normal dia.	$11.55	
M7516	10X	Normal dia.	$11.55	
M7506	7X	Large Field	$19.25	
M7511	10X	Large Field	$25.30	
M7509	7X	Normal dia.	(paired)	$18.15
M7517	10X	Normal dia.	(paired)	$18.15

(Latter two for use in binocular body instruments)

WEDGES

M7585	Quartz, 6 orders	$25.30
M7590	As above, graduated	$37.95
M7586	Quartz sensitive tint	$9.35
M7587	Mica ¼ wave plate	$7.15

MECHANICAL ACCESSORIES

M7306	Rotation movement to analyzer	$23.10
M7734	Attachable graduated mechanical stage	$70.95

We also supply for polarizing work a variety of:

Condensers
Slotted objectives
Other wedges
Incident Light Equipment
Dick and Wright Type Slotted Ocular
Micrometer Eyepieces
Attachable Polarizing Units
Superstages with vertical adjustment
Photomicrographic Equipment
Light Sources
Dark Ground Equipment

THE R. Y. FERNER COMPANY, INC.
110 Pleasant Street, Malden 48, Massachusetts

(Sold in the United States with service and replacement stock facilities maintained.)

Welcome News!

Collectors of fluorescent minerals are highly enthused with the recent startling fluorescent minerals to come from Franklin, N.J., long noted for the brilliant red and green calcites and willemites and other rare minerals. Now we are offering WOLLASTONITE with its bright orange fluorescence, BARITE with its peculiar grayish-blue fluorescence and NORBERGITE with its yellow fluorescence. These are three new and exciting colors you can add to your fluorescent collections.

ORANGE WOLLASTONITE

It is a pleasure to offer at moderate prices, the new highly fluorescent orange WOLLASTONITE associated with pink calcite. WOLLASTONITE is a calcium metasilicate and occurs abundantly as a contact mineral in crystalline limestones. However, very little has been found that fluoresces and we believe that this lot is some of the most brilliant WOLLASTONITE ever discovered. The mineral received its name after the English chemist, W. H. Wollaston. This material we offer cannot be readily distinguished from the calcite that it is associated with but upon exposure under a short wave MINERALIGHT or other short wave lamps will fluoresce a brilliant orange and the calcite will fluoresce a pale pink color. We recommend it highly to be one of the best and rare Franklin fluorescent minerals.

Specimens with numerous irregular masses of WOLLASTONITE in calcite may be purchased for 1½" 75¢ and $1.00; 2" $1.50 and $2.00; 2" x 3" $2.50 and $3.00; 3" $3.50 and $4.00; 3" x 4" $5.00, $6.00 and $7.50. A limited number of larger specimens are available at comparatively higher prices.

GRAYISH-BLUE BARITE

BARITE, a barium sulphate is usually not a fluorescent mineral but a new find at Franklin, N.J., is highly fluorescent and is attractive and will command front space in your fluorescent cabinet. The grayish-blue spots numerously scattered in pink fluorescent calcite are not only a new combination of colors under the short wave MINERALIGHT and other short wave lamps but is also a very desirable one.

Richly spotted specimens may be had for 1½" 50¢; 2" $1.00; 2" x 3" $1.50 and $2.00; 3" $2.50; 3" x 4" $3.00 and $4.00.

PALE YELLOW NORBERGITE

NORBERGITE is a basic fluosilicate of magnesium occurring in metamorphosed dolomitic limestones. This is another showy Franklin, N.J., fluorescent mineral that should be included in every fluorescent collection. NORBERGITE fluoresces a delicate pale yellow color and occurs as small irregular masses nicely grouped together in limestone. It fluoresces under short wave MINERALIGHTS and other short wave lamps.

Desirable specimens may be purchased for 1½" 50¢; 2" $1.00; 2" x 3" $1.50 and $2.00; 3" $2.50; 3" x 4" $3.00 and $4.00. A few larger specimens are in stock.

Prices quoted do not include postage and insurance charges.
Please include enough to cover the recent increase in postal rates.

SCHORTMANN'S MINERALS

6 McKinley Avenue **Easthampton, Massachusetts**

We carry a complete line of fluorescent minerals, MINERALIGHTS, etc. Write for circulars.

[illegible] 10 1951

From the Sulphate Deposits of Chile

BANDYLITE. Blue xls and groups, showing superficial alteration, on rock: 2 x 2″, $2.00, $2.50; 3 x 4″, $3.50, $4.00; 4 x 5″, $5.00

BOTRYOGEN. Orange-red xline with copiapite, etc.: 2 x 3″, $1.50; 3 x 4″, $3.00. With pickeringite: 2 x 2″ to 2 x 3″, $1.50, $2.00; 3 x 4″, $2.50, $3.00

CHENEVIXITE. Xline green: 3½ x 4½″, $7.50

COPIAPITE. Olive yellow with coquimbite: 3 x 3½″, $2.50; 4½ x 4½″, $4.00; 5½ x 5½″, $5.00. Xline yellow: 2 x 3″, $1.50; 3 x 4″, $3.00; 4 x 5″, $4.00

COQUIMBITE. Massive, amethystine color: 2 x 3″, $2.00; 2½ x 3½″, $2.50

FERRINATRITE. Fibrous with other sulfates: 3 x 4″, $2.50, $3.00; 3½ x 4″, $3.50

FIBROFERRITE. Xline gray, 1½ x 2″, $1.50; 2 x 3″, $3.00; 2½ x 3½″, $3.50

JAROSITE. Massive brown: 3 x 4″, $2.50

KROEHNKITE. Xline and partly xled with tamarugite: 2 x 2 to 2 x 3″, $1.00, $1.50

LEIGHTONITE. Light blue xled on rock: 2 x 3″, $2.00; 5 x 5½″, $6.00

METAVOLTINE. Greenish brown with ferrinatrite, etc.: 2 x 3″, $2.00, $2.50; 3 x 4″, $3.50; 3 x 5″, $4.00, $4.50

NATROCHALCITE. Green xled on rock: 2 x 2″, $1.00; 2 x 3″, $2.00; 3 x 4″, $2.50; 3½ x 4½″, $4.00

NATROJAROSITE. Brown xled, xline and massive with metavoltine, etc.: 3 x 4″, $3.00; 4 x 6½″, $4.50

ROEMERITE. Brown massive: 2 x 3″, $1.50; 3 x 4″, $2.50. Massive with coquimbite: 1½ x 4″, $1.00; 3 x 4″, $3.50

SIDERONATRITE. Yellow fibrous with other sulfates: 2 x 2″, $1.50; 2 x 3″, $2.50; 3 x 4″, $3.50

TAMARUGITE. Xline: 2 x 3″, $1.00; 3 x 4″, $2.00; 4 x 6″, $3.50

ITACOLUMITE—FLEXIBLE SANDSTONE

A new shipment of this amazing sandstone has just arrived from the Jind State, Punjab Province, India. All of the slabs possess a remarkable degree of flexibility: 8 x 2 x ¾″, $3.00; 12 x 2½ x ⅞″, $5.00; 10 x 2½ x ⅞″, $4.00; 15 x 5 x 1⅛″, $6.50.

LATEST CATALOGS AND PRICE LIST ISSUED

GEOLOGICAL MATERIALS CATALOG. ***A complete listing of Ward's well-known mineral, rock, and fossil collections; of minerals in bulk; and of the finest available color slides and models. Write for Catalog 513a.***

Ward's 1951 CATALOG OF FINE MINERALS. ***Comprising the outstanding offering of one-of-a-kind specimens, including meteorites. Free on request. . . . In writing please specify Catalog FM-4a.***

WARD'S *NATURAL SCIENCE ESTABLISHMENT, INC.*
3000 RIDGE ROAD EAST · ROCHESTER 9, N.Y.

GEORGE BANTA PUBLISHING COMPANY, MENASHA, WISCONSIN